UNIVERSITÁ DEGLI STUDI DELL' INSUBRIA

Dipartimento di Scienza ed Alta Tecnologia

ETHYLENE OR PROPYLENE BASED COPOLYMERS WITH HIGHER 1-OLEFINS BY METALLOCENE CATALYSTS: CORRELATION BETWEEN MICROSTRUCTURE AND PROPERTIES

Corso di Dottorato XXVIII Ciclo in Scienze Chimiche

Ph. D. dissertation of

Dott. LUIGI FANTAUZZI

Tutor: Dott. Simona Losio

Co-Tutor: Dott. Carlo Lucarelli

Index

Preface

   Polymers are one of the modern world's most intriguing and versatile materials, able to assume a near-infinite variety of shapes and properties that permeate almost every aspect of our lives as consumers. The commutative nature of plastic materials is not only a function of their melt-processing capabilities, but also a reflection of the wide variety of possible microstructures that each polymer chain (or distribution of chains) can assume as a unique fingerprint of the polymerization mechanism.

Among the different polymer categories, polyolefins are nowadays commodities. Their industrial production, which is more than 100 Mt/yr, continues to grow exponentially and it is reported that it will increase to about 170 Mt/yr by 2018.[1] There is thus the risk that also the research on polyolefins could be considered sort of "commodity research", that proposes poor novelty. Already in 2007, V. Busico, wrote as follows: "Linear polyolefins are 50-year-old, which seems to be enough for most opinion makers to decide that they are ''mature'' products…This mood has progressively permeated even the chemical community…In reality, catalytic olefin polymerization is still progressing fast, and is possibly at the verge of a new accelerating cycle".[2] Indeed, in recent years the vitality of the research in the polyolefin field has been demonstrated. For example, again V. Busico in "Ziegler-Natta catalysis: Forever young" discusses the future of polyolefin-based materials and the opportunities for further research and development in Ziegler-Natta catalysis.[3] The statement is that "thorough control of polymer microstructure and architecture ensured by modern olefin polymerization catalysts and processes warrants further progress in fundamental and applied research for many years to come". Moreover, L. Resconi in "Heterogeneous Ziegler-Natta, metallocene, and post-metallocene catalysis: Successes and challenges in industrial application" states that "The success of polyolefins is governed to a large extent by the development of robust and versatile catalysts offering excellent morphology control. … metallocene and the other "single-site" catalysts enable an unprecedented fine-tuning of chain microstructure by ligand design".[4] In the same paper it is also reported that "special emphasis is placed on the influence of catalyst type on polymer structure characteristics … and, ultimately, on the end-use properties of polyolefin". It is in particular interesting the statement that "it is the excellent balance among price, performance and processability that will further strengthen the position of polyolefins as a dominant class of materials in the polymer industry." It is thus clear that novel research on polyolefins is indeed performed. To use the above reported words, "the influence of catalyst type on polymer structure characteristics" plays a key role.

   Today, the development of a new polyolefinic material requires a keen understanding of how to manipulate the most intimate features of the polymer chains (e.g. tacticity, branching, comonomer content, comonomer sequence distribution, block length, regioerrors, molecular weight,) in order to obtain the desiderable physical properties and performance. Thus it is strictly

necessary a good understanding of fundamental microstructural structure-properties relationships both from the synthetic perspective (relationships between polymerization catalyst ligand/active site structure, polymerization mechanism and chain microstructure) and the performance perspective (relationships between chain microstructure, phase behaviour, and bulk properties). Thus, it is possible to conclude that there is much room for "further progress in fundamental and applied research" and I hope with this PhD thesis to show that further progress has been made in this research field to achieve new frontiers for such "dominant class of materials".

1.

Introduction

1.1   Polyolefins: a brief history

Low density polyethylene (LDPE), a polyethylene with a high branching extent, is the first example of polyolefin to be largely manufactured since the 1930. It is generated by a high-pressure free radical initiated polymerization: at temperatures around 200 °C and pressures well above 1000 bar, traces of oxygen initiated the free radical ethylene polymerization.[5] Due to intra- and intermolecular chain transfer reactions, short and long alkyl branches are formed, thus accounting for reduced density and reduced melting temperature with respect to linear polyethylene.

Several groups came very close to the discovery of catalysts for low pressure ethylene polymerization but the breakthroughs occurred during the early 1950's in the laboratory of Karl Ziegler. He introduced a new type of catalysts,[6-9] based on zirconium or group 4-6 transition metal compounds and aluminium alkyls, which were very effective in producing polyethylene in high yield at low pressure. High- density polyethylene (HDPE), a polyethylene with a negligible degree of branching along the chain backbone, was thus produced under close to ambient conditions. HDPEs exhibit higher crystallinity, melting point and density with respect to LDPEs. Later on, introduction of comonomers such as 1-butene, 1-hexene, and 1-octene lead to the synthesis of linear low density polyethylene (LLDPE), which has much better mechanical performances, but cannot be processed as easily as LDPEs. In the mid-1980s, incorporation of a high level of 1-olefin comonomers into the polymer backbone lead to ultra-low-density polyethylene (ULDPE) and very-low-density polyethylene (VLDPE).

On March 11, 1954 the group of Giulio Natta at the Milan Polytechnic succeeded to polymerize propylene using Ziegler's catalyst system to produce a tacky solid. The polypropylene obtained was composed of different diastereoisomers with very different physical properties by extraction using boiling solvents. Three fractions were obtained: the amorphous and sticky diethyl ether soluble fraction, the crystalline heptane insoluble fraction with a melting temperature above 160 °C and a less regular benzene insoluble fraction with a melting temperature ranging from 144 to 151 °C. Natta applied X-ray crystal structure analysis to identify the stereochemistry of polypropylene and distinguished between highly crystalline isotactic, syndiotactic and amorphous atactic polypropylene. His concept of stereoisomers is displayed in Figures 1.1 and 1.2.
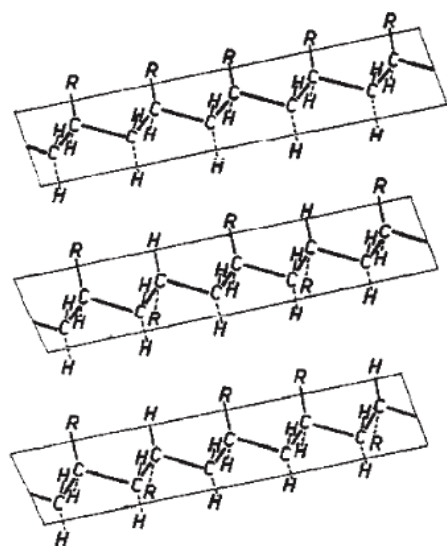
Figure 1.1 Polypropylene stereoisomers as proposed by Natta: isotactic, syndiotactic and atactic.[10]

Right-handed Threefold Helix
of Isotactic Polypropylene

Right-handed Helix of Syndiotactic Polypropylene
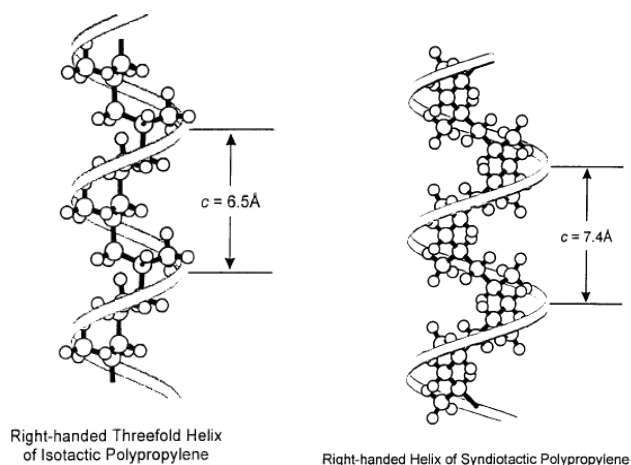
Figure 1.2 Model of the helical chain of isotactic and syndiotactic polypropylene in the crystalline state.[11]

Ziegler and Natta shared the Noble prize in Chemistry in 1963 for their eminent achievements. Natta's new concept of polymer stereoregularity in conjunction with transition metal catalyzed stereospecific had a great impact on polymer science and technology[12] and in 1957 Montecatini Company started the industrial production of polypropylene at its Ferrara plant.[13]

During the first three decades, most research on stereospecific 1-olefin polymerization was focused on heterogeneous catalysts until the discovery of new activators during the 1970's and novel single site catalysts during the 1980's expanded the frontiers of polyolefin technology well beyond traditional titanium based heterogeneous catalysts and changed the landscape of olefin polymerization.

In 1980, Professor Sinn and Kaminsky discovered the activation effect exerted by methylaluminoxane (MAO) on metallocenic catalysts,[14] producing completely atactic poly(propylene). Metallocene-based catalysts will be treated more extensively in the following

chapters. The discovery of MAO activators has led to the development of new homogeneous catalysts for olefin polymerization.

Since the 1980's the performance of metallocene-based catalyst systems was improved to produce on an industrial scale isotactic, syndiotactic, and stereoblock poly(propylene)s.[15] In the early 1990's supported single site metallocenes catalysts were introduced to enable gas phase polymerization.[16] Also ethylene/1-olefin copolymers with high 1-olefin content, cycloolefin copolymers, syndiotactic polystyrene, and long-chain branched ethylene copolymers became available.

Recently, the potential of the late transition metal complexes of Ni, Pd, Co and Fe was recognized. Recent advances and new concepts of non-metallocene catalysts for olefin polymerization were summarized in comprehensive reviews by Gibson.[17,18]

1.1.1 Polyolefins industry

Polyolefins represent today approximately half of the global volume of polymers: low density polyethylene (LDPE), linear low density polyethylene (LLDPE) and high density polyethylene (HDPE) and polypropylene (PP) account for more than 47% (11.2 million tonnes) of Western Europe's total consumption of 24.1 million tonnes of plastics each year.[19]

They are not only the polymers with the highest production volume, but they also show an unbroken production increase. The production requires only easily available and nontoxic monomers and proceeds with almost no losses or side reactions. After their end of use, polyolefins could be recycled mechanically or by incineration that did not result in any toxic discharges.

Polyolefins industry is based mainly on heterogeneous catalysts which have become highly selective and efficient. Classical Ziegler-Natta catalysts are heterogeneous and the polymerization takes place on dislocations and edges of $TiCl_3$ crystals.[14] Polymerization at the active site is influenced by the electronic and steric environment of the crystal lattice. Consequently they produce polyolefins that reflect the complex organometallic nature of catalyst with different types of active sites and a broad molecular weight distribution.[20] Another possibility is represented by chromium oxides-based catalysts, *e.g.* Cr on silica (Phillips catalyst) which polymerize ethylene to give high-molecular-weight rigid polymethylene-type polymers, but are inactive towards propylene. Heterogeneous titanium-based Ziegler-Natta catalysts, on the other hand, are more versatile. They are able to polymerize propylene with a very high degree of stereoselectivity and catalyze the copolymerisation of ethylene with higher 1-olefins such as 1-hexene, important for the production of flexible, non-brittle polymers for use in films and packaging. Although these are successful processes which give rise to a wide range of polymer products, the diversity of active sites in heterogeneous catalysts leads to an uneven degree of comonomer incorporation with a high incorporation rate in short chains and little incorporation in the high molecular-weight fraction, a drawback that homogeneous catalysis offers particular promise to overcome.

In the early nineties, the development of heterogeneous catalysts was growing so rapidly that few major advances were still expected. But in these years the homogeneous metallocene-based technology took place, giving rise to a new era in the field of catalytic olefin polymerization. Such

a catalysis led to a higher comonomer incorporation along with narrower comonomer distribution. These features ensures better physical properties, such as impact resistance, sealing capabilities, optical properties, elasticity, and dispersability to the new materials. Moreover, the metallocene catalysts allowed to obtain increased activity in gas and solution-phase processes, mainly for high volume commodity products.

Since the pioneering days of Ziegler and Natta, the successfully development of the catalysts is reflected by a steady increase of catalyst activities well beyond 1000 kg per gram of transition metal to less than 1 ppm transition metal left in the polymer. With further increases of catalyst activity the amount of residual transition metal is approaching 0 ppm.

1.2 Homogeneous catalysts

1.2.1 Metallocene catalysts

The structure of metallocenes, which are also called "*sandwich compounds*" because the π-bonded metal atom is situated between two aromatic ring systems, was uncovered by Fischer and Wilkinson, for this awarded the Nobel Prize in 1973.[21-23] However, their early catalysts, based on Cp_2MtX_2/$AlRCl_2$ or $AlCl_3$ (Cp = cyclopentadienyl, Mt = transition metal, R = alkyl) exhibited a low activity in ethylene polymerization and failed to homopolymerize higher 1-olefins.

In 1977, the group of Sinn and Kaminsky[14] found that methylalumoxane (MAO, $(-AlMe-O-)_n$ with n = 5–20) is a cocatalyst able to activate group 4 metallocenes (and a large number of other transition metal complexes, too) toward the homo and copolymerization of any 1-olefins, enhancing the catalyst activity by a factor of 10000. The discovery of MAO paved the way for the development of many new families of highly active so-called single center catalysts with well-defined molecular architectures and give clear correlations between catalyst structure, polymer microstructural features, and ensuing properties.

A further milestone was reached when Britzinger and co-workers synthetized the chiral bridged metallocenes, the so-called "*ansa*" metallocenes, in 1982,[24] providing the solid scientific base for the discovery of the homogeneous stereospecific 1-olefin polymerization. The main feature of these catalysts was that the cyclopentadienyl ligands were connected to a bridge and this made the overall molecule more rigid. Indeed, they realized that metallocenes need to retain their configuration stability to achieve stereospecific polymerization.[25] Furthermore, Ewen[26] for the first time showed from a mixture of *rac*- and *meso*-ethylenbis(indenyl)titanium dichloride $[Ti\{(\eta^5-C_9H_6)_2C_2H_4\}Cl_2]$ complexes that only the steric rigid racemic form yields *isotactic* polypropylene (*i*PP) while the achiral meso form produces low molecular weight *atactic* polypropylene (*a*PP). Highly stereoregular materials were obtained with analogous homogeneous metallocenes.[27] However, the titanocene was unstable at room temperature and gave polypropylene polymerizations with low activity and low stereoselectivity (71% of isotactic triad for *i*PP).
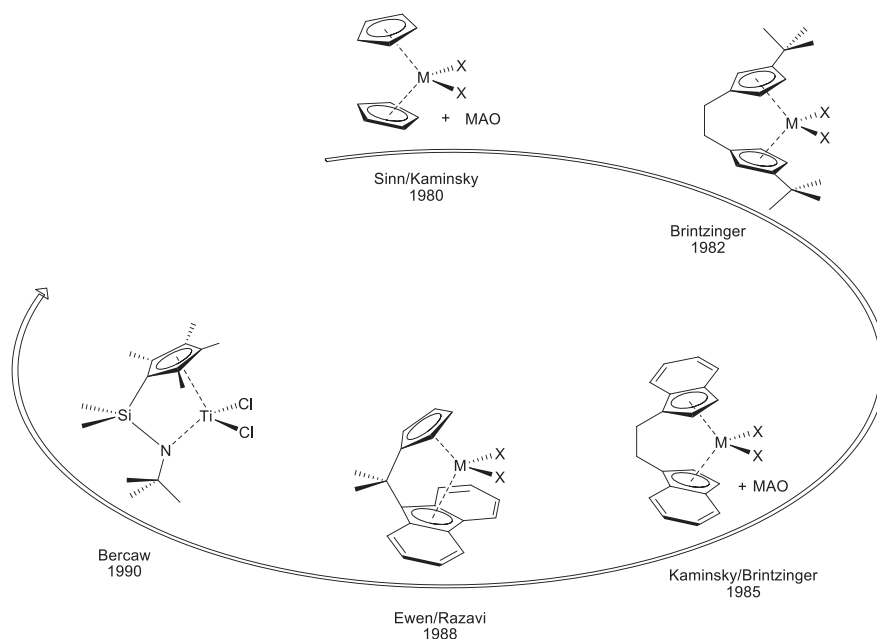
Figure 1.3 Evolution in metallocene research.

Shortly after this disclosure, Kaminsky and Brintzinger reported that a similar C_2 symmetric zirconocene complex produced *i*PP with high yields. After this discovery, several metallocenes as well as new families of catalysts were developed (Figure 1.3): a huge number of different ligand structures have been synthetized, the effect of the substituent on the properties of the ensuing polymers and on the activity of the catalysts is now mastered to a high level. As far as the transition metal is concerned, Zr is the most active. The prototype of this class of metallocenes and the best studied is Brintzinger's *rac*-C_2H_4(1-Ind)$_2$ZrCl$_2$.

Modification of the catalysts by variation of the ligands surrounding the active centre permitted a correlation of catalyst structure with catalytic activity and stereospecificity and, apart from *i*-PP and *a*-PP polypropylene, the *syndiotactic* (*s*-PP) as well as the *stereoblock*-PP were industrially produced (Figure 1.4).[15]
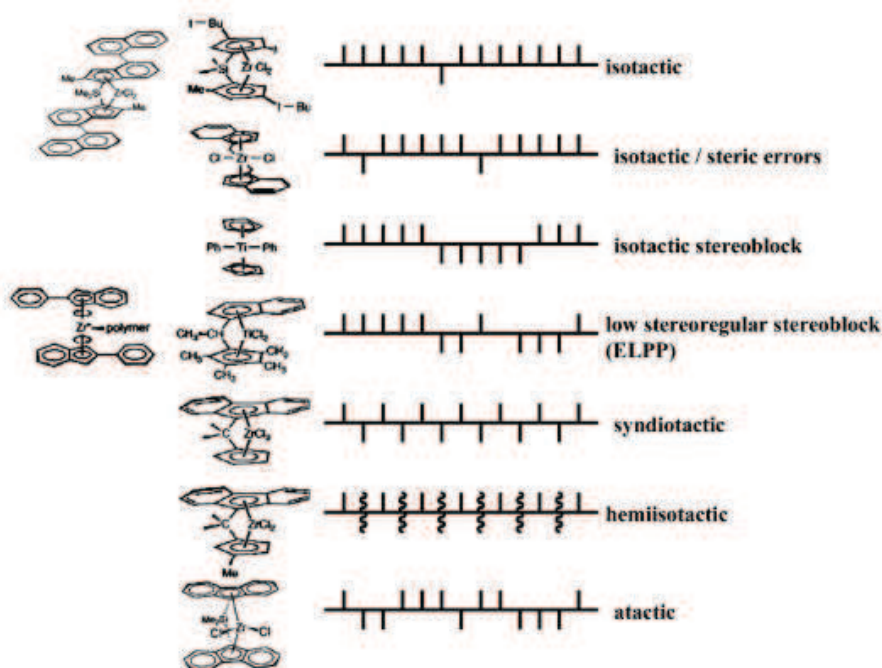
**Figure 1.4** Correlations between polypropylene architectures and metallocene catalyst structures.[10]

In the early 1990s there was great interest for a novel class of group IV metal complexes, become known as "Constrained Geometry (CGC)" catalysts reported by both Dow Chemical and Exxon Chemical Company (Figure 1.3). The terminology "Constrained Geometry" refers to the ligand bite angle (N-Ti-Cp centroid angle) that is smaller than the analogous angle in metallocene systems (Cp-Ti-Cp centroid angle). From the definition point of view, CGC is not a metallocene but rather a half sandwich Cp or substituted Cp complex. However, CGCs are often referred to as "metallocenes".

A peculiar characteristic of CGCs is that they are quite aselective catalysts; only a few of them are able to produce stereoregular polypropylenes. In particular CGCs based on fluorenyl-amido structures give *syndiotactic* or *isotactic* polypropylene as a function of the activator. The substitution of a cyclopentadienyl moiety of a linked bis(cyclopentadienyl) ligand by the 3-electron-donating *tert*-butylamido group resulted in a ligand system with many key advantages:[28] i) higher reactivity toward α-olefin substrates, ii) favoured incorporation of sterically hindered monomers into the polyolefin chain, iii) higher thermal stability of alkyl and dialkyl CGCs when compared to related metallocenes that permitted higher polymerization temperature. CGCs were found to be superior catalysts for the production of ethylene/styrene copolymers, and allowed even copolymerization of cyclic olefins such as norbornene.[28] Starting from the original $[Ti(\eta^5:\eta^1-C_5Me_4SiMe_2NCMe_3)Cl_2]$ a large number of modification of the catalyst by variation of the ligands and of the dimethylsilyl bridging unit were reported, and several new families of polymers were thus developed.

1.2.2 Cocatalyst: MAO

The cocatalyst is a crucial part of the two-component Ziegler-Natta catalytic system and its development played a decisive part in the homogeneous polymerization revolution. Nowadays, methylaluminoxane is the most widely used activator for the largest number of metallocenes and other soluble complexes.

It is an oligomeric compound of general formula $[Al(Me)O]_n$ obtained by the controlled hydrolysis of trimethylaluminum ($AlMe_3$) and typically having n = 5 – 20. Although extensive researches were carried out in both academia and industry, the exact composition and structure of MAO is far from being known.[29] By element analysis, cryoscopic and NMR measurements, and decomposition with HCl, it was found that MAO is a mixture of different compounds including residual coordinated $AlMe_3$, possibly AlO_3 units, oligomers, and some ring structure (Figure 1.5).
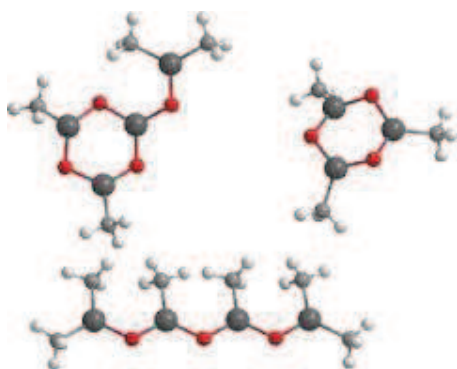
Figure 1.5 Unit structures of cyclic and linear MAO: *big balls* aluminium, s*mall balls* oxygen and methyl groups.[30]

As the aluminium atoms in the unit structures of MAO are coordinatively unsaturated, the units join together to form clusters and cages. They have molecular weights from 1200 to 1600 g/mol (as measured by cryoscopy in benzene) and are soluble in hydrocarbons, especially in aromatic solvents. A probably association of two linear unit structure and a cage structure of four $[Al_4O_3Me_6]$ units are shown in Figure 1.6 and Figure 1.7, respectively.
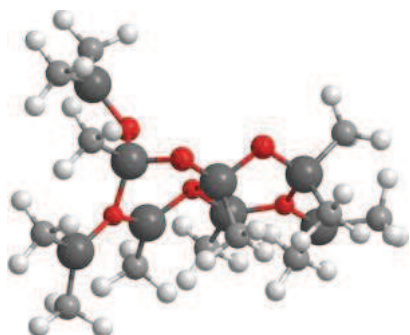
Figure 1.6 MAO association of two linear unit structures; *big balls* aluminium, *small balls* oxygen and methyl groups.[30]

Figure 1.7 MAO cage formed by four linear unit structures.[30]

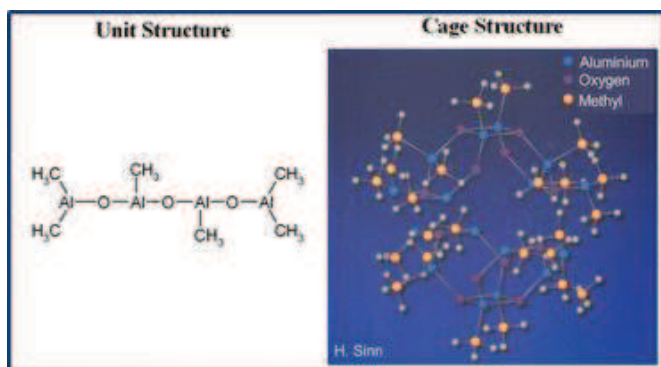The compound dissolves readily in hydrocarbons such as toluene where, due to the facile ligand exchange in aluminium complexes, it establishes complex solution equilibria. Samples are usually rich in methyl groups and in commercial MAO samples as much as 30–40% of $AlMe_3$ may be present. The free trimethylaluminum directly influences the polymerizations: activity and molar masses decrease when $AlMe_3$/MAO increase. Though the high volatility of trimethylaluminum, not all free $AlMe_3$ can be removed and even after drying *in vacuo* MAO contains typically 3-4 % free A_2Me_6.[31]

The true active species in metallocene/MAO systems are metallocene alkyl cations: cationic d^0 14-electron complexes of the type $[L_nMR]^+$ (with M a metal of group IV), bearing a weakly non-coordinating anion which is complexed by the cage-like MAO molecule.[32] The formation of the catalytically active complex involves a series of reactions: i) a rapid ligand exchange reaction with the metallocene dichloride that forms a metallocene methyl and a dimethylaluminum compounds; ii) the formation of a bulky cocatalyst anion and a metallocene cation with a weak back donation due to the abstraction of Cl^- or CH_3^- from the metallocene compound by an Al-center in MAO, (Scheme 1.1). The polymerization than occurs by the coordination and subsequent insertion of the olefin into the transition metal-carbon bond of $[L_nM-CH_2R]^+$. It is generally assumed that the lower the ion interactions, the higher the catalyst activity.

Bulky ligands at the transition metal can produce metallocene monomethyl cations which dissociate more easily from the MAO anion. As a consequence, the activity can be increased by factors of 5 or 6.[33] The high excess of MAO is required to provide sufficiently bulky MAO cages. The cocatalyst has to be employed usually at [Al]/[M] ratios of 10^3–10^4/l, so that in such catalysts the cost of MAO by far outstrips that of the metallocene complex. Moreover, there are possible additional roles for MAO that explain the large amount required for high activity and selectivity: i) it scavenges the impurities from the reaction medium such as water and oxygen; ii) prevents deactivation of the catalyst by bimolecular processes between two metallocenes through either reductive elimination of polymer chains or oxidative coupling forming hydrocarbon bridges between two transition metal atoms, iii) the coordination of MAO to some metallocenes can lead to improved stereochemical control of catalysts.[34]
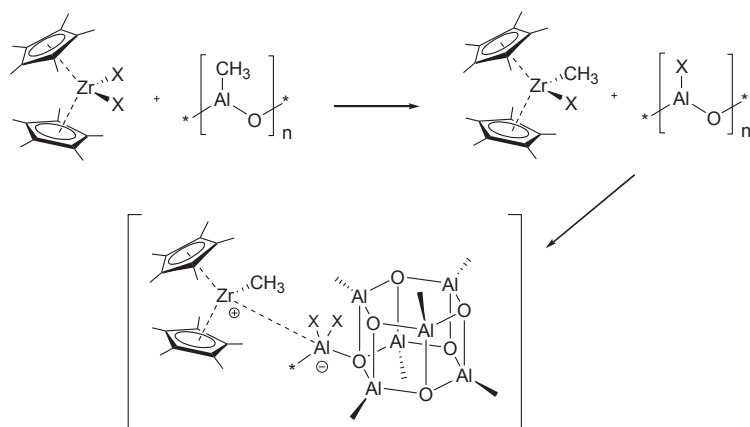
Scheme 1.1 Activation pathway of metallocenes by the Lewis acid cocatalyst methylaluminoxane (MAO) yielding a MAO-cage stabilizing an activated metallocene complex.[35]

The main limitation to the commercialization of metallocene catalysts is the need for large amounts of the expensive MAO, hence there is a large interest to find alternative activators. Marks[36,37] and others[38-41] developed other bulky and weakly coordinating cocatalysts such as tris(pentafluorophenyl)borane or organic salts of the non-coordinating tetrakis(pentafluorophenyl)borate $[(C_6F_5)_4B]^-$, and aluminum fluorides. Such cocatalysts require a metallocene/cocatalyst ratio of 1:1 is used, but only if a high excess of an aluminum alkyl as scavenger is present. Details of the polymerization using other cocatalysts are described by Shiono.[42] The major disadvantages of this class of cocatalysts are their sensitiveness to decomposition, their high price, and the incorporation of fluorine into the polymer which can cause problems when polyolefins are thermally decomposed.

1.2.3 Polymerization mechanism

Homogeneous metallocene based catalysts are amenable for mechanistic studies of Ziegler-Natta polymerization. Compared to conventional heterogeneous systems in which a variety of active centres with different structures and activities usually coexists, homogeneous catalysts give very uniform catalytically active sites which possess controlled, well-defined ligand environments. Therefore the polymerization processes in homogeneous systems are often more simple, and kinetic and mechanistic analyses are greatly simplified.

As already pointed out, several investigations gave evidences that the active polymerization species is a ion pair $[L_nMR]^+[X]^-$ (M = Ti, Zr, Hf) formed by metallocene alkyl cations, that is cationic d^0 14-electron complexes and an anionic methylalumoxane (or another weakly bonding anionic counterion such as borates or boranes).[43] In MAO-activated catalyst systems, alkyl zirconocenium cations are likewise thought to be present, presumably in weakly bound inner-sphere ion pairs with anions of the type MeMAO$^-$.[44,45] These anions, still only vaguely characterized as large agglomerates,[46] are assumed to be formed from MAO by uptake of a methyl anion from the alkyl zirconocene precursor. In equilibrium with these inner-sphere ion pairs A, outer-sphere ion pairs B (Figure 1.8) are observed in MAO-activated pre-catalyst systems[45,46-48]

that contain a heterobinuclear cationic AlMe$_3$ adduct,[49] presumably together with MeMAO¯ as counter-anion.

A : R = methyl
A': R = polymeryl

B : R = methyl
B': R = polymeryl
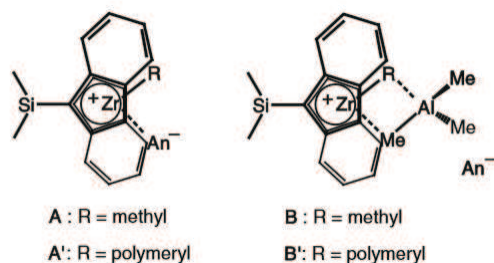
Figure 1.8 Inner-sphere ion **A**, containing a methyl zirconocenium cation and outer-sphere ion pairs **B**, containing a heterobinuclear AlMe$_3$ adduct of the latter, together with a weakly coordinating anion An¯, such as MeMAO¯, MeB(C$_6$F$_5$)$_3$¯ or B(C$_6$F$_5$)$_4$¯, observed in *ansa*-zircocene system activated with MAO, B(C$_6$F$_5$)$_3$, Ph$_3$CB(C$_6$F$_5$)$_4$, respectively.[44,45,50] The corresponding species **A'** and **B'** with R= polymeryl, observed in active catalyst system in presence of olefin.[51,52]

The electronically unsaturated cationic alkyl metallocenes exhibit a strong tendency to coordinate with the weak Lewis base olefin molecules. A study based on molecular orbital (MO) theory indicated that once an olefin coordinated to the metallocene alkyl, the insertion of the olefin into the alkyl—metal bond would proceed rapidly. The driving force for the insertion is the energy gain on converting a π bond into a σ bond, with energy release of about 20 Kcal/mol.[53]

Amongst the various developed models and reaction mechanisms, Cossee and Arlman's comprehensive monometallic mechanism catalysis is generally accepted (Scheme 1.2) and their mechanism further supported by molecular orbital calculations.[54] The mechanism assumes that the catalytically active centre incorporates both the growing chain (GC) and a vacant coordination site that allows π-coordination of the incoming monomer (Scheme 1,2, Step I). Subsequently, in a concerted rearrangement via a four centred transition state (Step II), the insertion by a *cis* opening of the olefin double bond occurs with the simultaneous GC migration to the olefin ligand; at the same time a new free coordination site is generated, providing the conditions for the next propagation step.
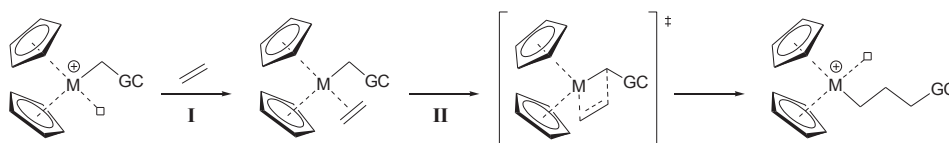
Scheme 1.2 Two-step mechanism of olefin polymerization: **I**) olefin coordination to a vacant site; **II**) alkyl migration of the π-coordinated growing chain (GC) to the π-coordinated olefin.[54]

There are different elements of chirality in the stereospecific homogeneous polymerization. First of all, the coordination of a prochiral olefin, such as propylene, gives rise to non-superimposable coordinations, as sketched in Figure 1.9.

si-coordinated
propene

re-coordinated
propene
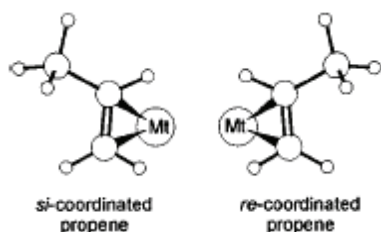
Figure 1.9 Non-superimposable coordinations obtained by coordination of a prochiral olefin such as propylene to metal center.

The configuration of the tertiary carbon atom of the growing polymer chain nearest to the metal atom is the second element of chirality. In fact, a new stereogenic center is formed in the growing chain at each propylene insertion (Scheme 1.3).
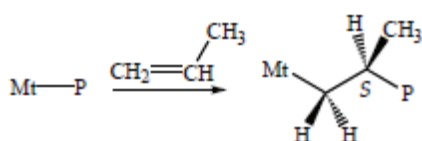
Scheme 1.3 A new stereogenic center is formed at every insertion of a prochiral olefin such as propylene, into the metal-growing chain bond.

The third element of chirality is the chirality of the catalytic site, which, can be of two different kinds: (i) the chirality arising from coordinated ligands, other than the alkene monomer and the growing chain; (ii) an intrinsic chirality at the central metal atom. Examples of the two kinds of chirality are reported in Figure 1.10.
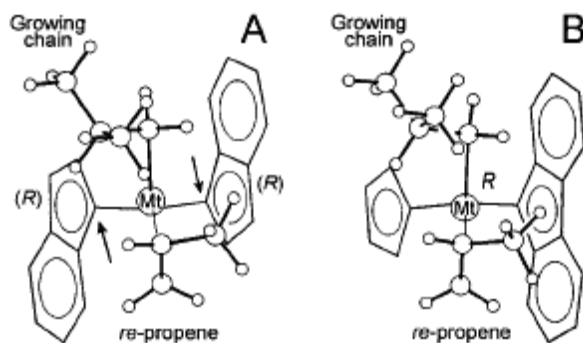
Figure 1.10 A: model comprising a $Me_2C(1\text{-Ind})_2$ ligand, a propylene molecule *re*-coordinated and an isobutyl group (simulating a growing chain). The chirality of coordination of the bridged π-ligand is (R,R), labelled according to the absolute configurations of the bridgehead carbon atoms marked by arrows. **B**: model comprising a $Me_2C(Cp)(9\text{-Flu})$ ligand, a propylene molecule *re*-coordinated and an isobutyl group. No chirality of coordination of the bridged π-ligand exists, while *R* is the chirality at the metal atom.[35]

Since 1-olefins are prochiral, in principle they can coordinate and insert into a transition metal-carbon bond in four different ways (Figure 1.11).
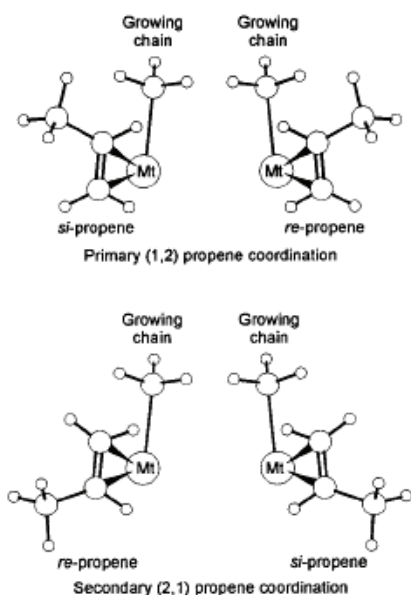
Figure 1.11 Four possible insertion modes of a prochiral olefin such as propylene, into the Mt-growing chain (simulated by a methyl group) bond.[35]

Whether the olefin insertion is primary or secondary defines the regiochemistry of insertion, while the choice of the olefin defines the stereochemistry of each insertion. When the addition of the 1-olefin occurs with the formation of a metal-CH_2 bond, the insertion is called primary (or 1,2) while when the addition occurs with the formation of a metal-CH bond, the insertion is secondary (or 2,1). The insertion of an 1-olefin into a metal-carbon bond is mostly primary. One of the features of most isospecific metallocene catalysts is their generally lower regioselectivity when compared to heterogeneous Z-N catalysts: indeed, despite the fact that primary propylene insertion is clearly favored by electronic factors, isolated secondary propylene units are often detectable in isotactic polypropylene samples and their presence is the signature of a metallocene catalyst.

Since every propylene insertion creates a new stereogenic center, the catalyst stereoselectivity (and the stereoregularity or tacticity of the polymer) is determined by the stereochemical relationship(s) between the stereogenic carbon atoms in the polymer chain.

Multiple insertions of the same enantioface produce a polymer chain with chiral centers of the same configuration, i.e., an *isotactic* polymer (A in Figure 1.12). Multiple insertions of alternating enantiofaces produce a polymer chain with chiral centers of alternating configuration, i.e. a *syndiotactic* polymer (B in Figure 1.12). Random enantioface insertions produce a polymer chain with no configurational regularity, i.e. an *atactic* polymer (C in Figure 1.12).
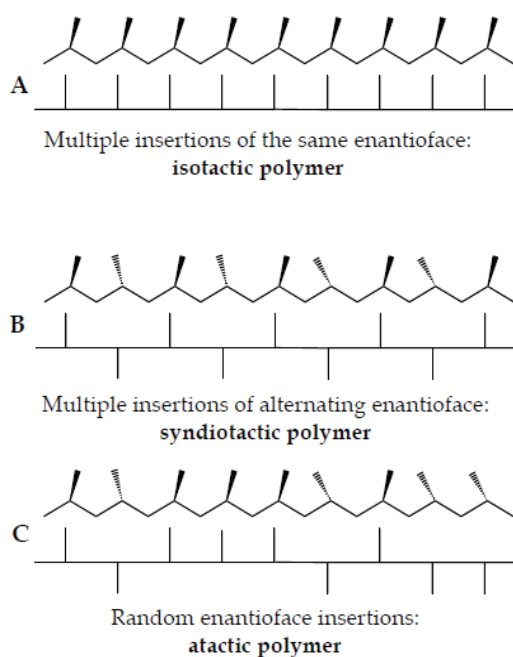
Figure 1.12 Chain segments shown in their trans-planar and modified Fisher projections.

There are two possible mechanisms of stereocontrol in primary insertion: the *enantiomorphic site control* and the *chain-end control*. In the enantiomorphic site control, the chiral induction comes from the asymmetry of the reaction site sources. It is the chirality relationship of the two coordination sites of the catalytic complex that determines the stereochemistry of the polymer. In the chain-end control, the chiral induction comes from the last formed stereogenic unit (Figure 1.13).
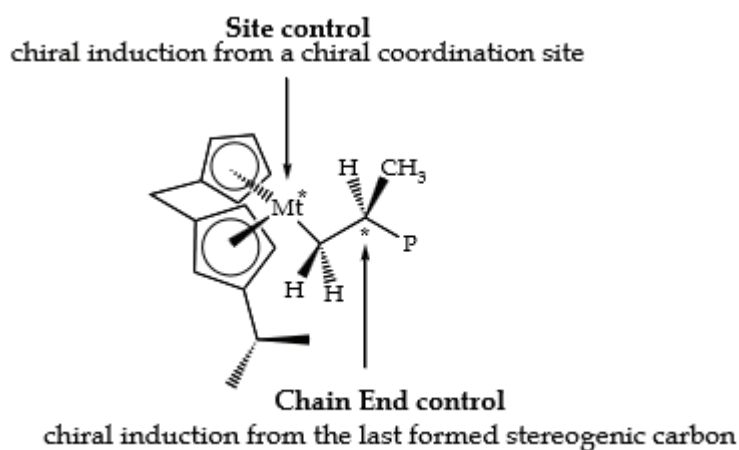
Figure 1.13 Chiral induction could come from Site control or Chain End control.

Chain termination occurs typically via β-hydrogen elimination pathways, a process that is about three orders of magnitude slower than the insertion step, and that produces a terminal olefin function at the end of the polymer chain.[55] In addition, also intermolecular reactions with

monomers,[56] cocatalysts,[57] chain transfer agents[58] or poisons[59] or quenchers can occur by different mechanisms (Scheme 1.4).
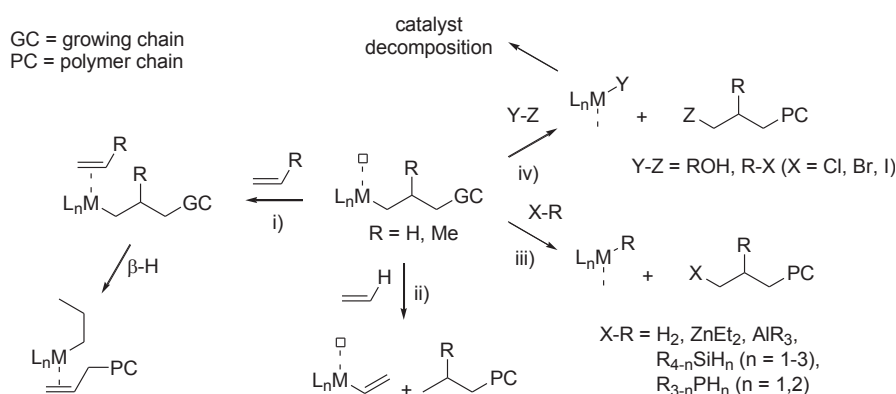
Scheme 1.4 Common Intermolecular chain termination pathways in polyethylene and polypropylene synthesis: i) β-H transfer to monomer and chain release; ii) C-H bond activation and transfer from monomer to chain; iii) metathesis with cocatalysts or chain transfer agents; iv) poisoning and catalyst decomposition.

Besides terminations, which release the polymer chain and often form still active species, there are deactivation reactions which induce a decay of polymerization activity along the reaction time by decreasing the number of active sites. In MAO-catalyzed polymerization a typical deactivation is the α-H transfer to MAO which leads to methane and a bimetallic μ-alkyl-bridged species catalytically inactive.[60]

For olefin polymerization, the relative rates of chain propagation and termination reactions determine the polymer chain length (M_w), which influence many important polyolefin properties and the molar mass distribution (M_w/M_n), which represents the degree of homogeneity of the lengths of polymer chains.[61]

1.3 Ziegler-Natta catalysts for 1-olefins copolymerization

Conventional Ziegler-Natta catalysts are involved in many successful processes which give rise to a wide range of polymer products.

However, in the field of copolymers, they show some drawbacks. Indeed, these catalysts have a variety of active sites for polymerization being multi-sited. Thus, they yield copolymers with broad molecular weights and comonomers distributions; beside this, they are capable of producing a narrow range of copolymer structures.

Metallocenes, and more in general, homogenous catalysts, permit to overcome some of these obstacles. It is in fact possible to refine, and even to design, the structure of polymers. Stereoselective catalytic sites can homopolymerize and copolymerize many monomers in an exact manner. Polymer molecular weight and molecular weight distribution, comonomer distribution

and content, and tacticity can be independently controlled. And with well-characterized molecular structures, catalyst composition and geometry can be varied systematically to produce extremely uniform homo- or copolymers "programmed" with the desired physical properties.[62]

1.3.1. General introduction on copolymerization

When a polymeric chain is formed by two different kinds of monomers it is referred to as a copolymer.

Copolymerization allows various monomers to be combined in such a way so as to provide materials with different and sometimes unique properties.

On the basis of the microstructure and the macromolecular chain geometry we can distinguish *alternating copolymers*, where the monomers alternate themselves along the chain (1), *random (*or *statistical) copolymers*, where the two monomers A and B are present without order in the chain (2), *block copolymers*, where to a sequence of the monomer B succeeds one of the other monomer A (3), and *graft copolymers*, where from a main chain formed by only one monomer lateral chains formed only by the second monomer start (4). Their structures are shown in Figure 1.14.
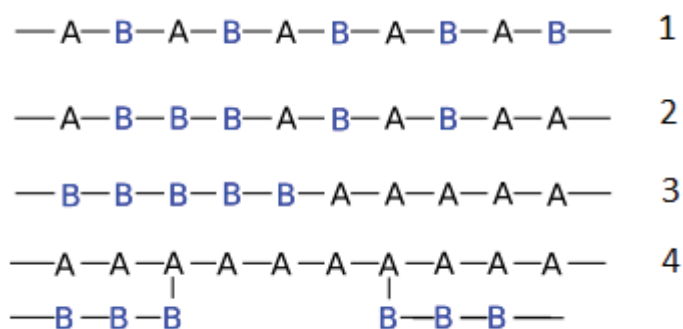
Figure 1.14 1) alternating copolymer, **2)** random copolymer, **3)** block copolymer and **4)** graft copolymer chain.

The four copolymer classes present great differences in their chemical and physical properties, whereas inside each class the properties depend on the ratio between the two comonomers and from the microstructure.

1.3.1.1 Copolymerization equation and statistical analysis

Addition copolymerization, as homopolymerization, involves three main steps: initiation, termination and propagation. The last step is the one giving copolymerization its special character. For polymerization of two different monomers, A and B respectively, there are four possible propagation reactions:

$$\text{\textasciitilde\textasciitilde A* + A} \xrightarrow{k_{11}} \text{\textasciitilde\textasciitilde A*}$$

$$\text{\textasciitilde\textasciitilde A* + B} \xrightarrow{k_{12}} \text{\textasciitilde\textasciitilde B*}$$

$$\text{\textasciitilde\textasciitilde B* + A} \xrightarrow{k_{21}} \text{\textasciitilde\textasciitilde A*}$$

$$\text{\textasciitilde\textasciitilde B* + B} \xrightarrow{k_{22}} \text{\textasciitilde\textasciitilde B*}$$
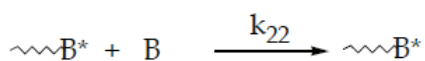
where A* and B* are the propagating species and *kij* are the kinetic constants relative to the sum of monomer *j* to the growing chain with a last *i* unit.

If as in this case, the rate of addition of monomers depends only upon the nature of the species at the end of the growing chain we speak of *terminal model* (or *first-order Markov statistical model*).[63]

Considering the terminal model, the reactivity ratios r_1 (for monomer A) and r_2 (for monomer B), defined to as:

$r_1 = k_{11} / k_{12}$ and $r_2 = k_{22} / k_{21}$

express the growing chain tendency to sum the same monomer of the chain end rather than the other monomer. In practice, they are a kind of measure of the probability to have along the chain an AA sequence rather than an AB sequence. For example, if r_1 is $>> 1$ (that is, $k_{11} >> k_{12}$) the copolymer will be formed by sequences in which to an A unit succeeds another A unit.

From the reactivity ratios and the kinetics equations relevant to the two comonomers consumption it is possible to derive the *copolymerization equation*:

$$n = x \frac{r_1 x + 1}{x + r_2}$$

where *n* is the instantaneous ratio of the molar concentration of the two monomers in the copolymer and *x* is the monomer feed ratio. With this equation it is possible to know the right instantaneous composition of the copolymer being produced from a certain feed mixture. If we wish to know the mole fraction of each monomer in the copolymer, we can use a rearrangement

of the above equation, introducing the mole fractions of the two monomers in feed, f_1 and f_2, and the corresponding mole fractions of the monomers in the copolymer, F_1 and F_2:

$$F_1 = \frac{r_1 f_1^2 + f_1 f_2}{r_1 f_1^2 + 2 f_1 f_2 + r_2 f_2^2}$$

We could distinguish some different limiting copolymerizations categories, on the basis of the reactivity ratios product ($r_1 r_2$).

$r_1 r_2 = 1$: truly random copolymer. This situation is called an ideal copolymerization. The real ideal copolymerization is when $r_1 = r_2 = 1$, the two monomers show the same reactivity towards the two different growing species; in this case the copolymer composition is always the same of the feed composition. When instead $r_1 < 1$ and $r_2 > 1$, or opposite, the copolymer composition becomes richer in the more active monomer.

$r_1 r_2 < 1$: alternating copolymer. this is the most frequent case, with both reactivity ratios smaller than 1. Each active center prefers to add to the other monomer, so that in the chain there are only short sequences of A or B and there is a tendency to produce an alternating copolymer. The limit situation occurs when $r_1 = r_2 = 0$: then the growing chain of type 1 never wants to add to itself ($k_{11} = 0$), and the same happens for the type 2 ($k_{22} = 0$); and a perfectly alternating copolymer is produced until one of the monomers is used up (at this point the reaction stops).

$r_1 r_2 > 1$: block copolymer. In this case each growing chain prefers to add the same monomer, so in the chain there are long sequences of at least one comonomer.
If there is a dependence on the character of the last two inserted units in the growing chain we refer to the *penultimate model* (or *second-order Markov statistical model*).[63]
As a consequence of the adoption of the 2nd order Markovian model, the following reactivity ratios are derived:

$r_{11} = k_{111}/k_{112}$
$r_{21} = k_{211}/k_{212}$
$r_{22} = k_{222}/k_{221}$
$r_{12} = k_{122}/k_{121}$

where k_{ijk} is the rate constant of the reaction for the addition of the comonomer k to a growing chain bearing the comonomers i and j as the penultimate and the ultimate inserted units, respectively. An analogous index can be derived from the second-order Markov model: comonomer distribution index (CDI),[33] given by the following equation:

$CDI = (r_{11}{}^2 r_{22}{}^2 r_{12} \, r_{21})^{1/3}$

The r_1r_2 and CDI values have the same meaning: a high CDI value indicates the presence of relatively long sequences of comonomers.

To apply a copolymer description of this kind we have to suppose that all the macromolecular chains have the same composition. Actually it has been experimentally observed that copolymers obtained with Ziegler-Natta catalysts could be separated in several fractions, in which the composition is more or less different from the average.[64] Since the compositional heterogeneity is observed also operating in kinetically controlled conditions, it could be due to the presence of different active species in the system. This is true especially for the heterogeneous systems, but it could occur also in metallocenic catalysts.[65] In the latter case the interactions catalyst–cocatalyst have been demonstrated important in the production of different active species.

On the basis of Ziegler Natta polymerization mechanism, comonomers reactivity in the copolymerization could depend on both steric and electronic factors. Indeed, it has been established that the relative reactivity k_{1i}/k_{11} of a certain monomer M_i compared with the standard monomer M_1 = propylene changes in the following order:

ethylene > propylene > 1-butene > 1-pentene > 1-hexene… etc

and decreases increasing the steric hindrance of the alkyl substituent on the 1-olefin. This implies that very blocked substituents present at the last inserted monomeric unit decrease the copolymerization speed.

1.4   Non-conventional comonomers

ISMAC research group has a long tradition in the study of ethylene and propylene based copolymers and in the determination of the copolymer microstructure.

The copolymer properties depend in many parameters, such as the comonomer content, the distribution of the comonomers along the polymer chain and also the chain stereoregularity, which are determined by the structure of the catalyst precursor.

The ^{13}C NMR spectroscopy is the most powerful analytical tool to study the structure of (co)polymers and allows researchers to obtain information on the comonomer sequences, short-chain and long-chain branch distributions, and quantitative analyses of the composition.[66,67] Moreover, it is important for the development of models describing polymerization mechanisms and for the structure–property relationships.

Since the discovery by Kaminsky, Sinn and Ewen of polymerizations catalyzed by metallocene catalysts with high activity and stereoselectivity, several reports have been published dealing with ethylene and propylene copolymerizations with linear 1-olefins (e.g. 1-butene, 1-hexene and 1-octene).[68] In more recent years, and as a consequence of the discovery of novel metallocene and post-metallocene complexes capable of incorporating bulky comonomers at unprecedented amounts, new attention was centered in 1-olefin copolymerization with non traditional and/or sterically hindered comonomers.

Indeed, in the past very little interest has been shown in copolymers with odd-numbered 1-olefins such as 1-pentene, 4-methyl-1-pentene,1-heptene, and 1-nonene. This is due to the fact that the world's 1-olefin market is saturated with even-numbered monomers while South Africa has a monopoly on odd-numbered monomers from Sasol's Fischer-Tropsch processes.[69] With such a process, an olefin source alternative to oil is becoming more market friendlier as the energy demand increases and oil is becoming less affordable. The route to olefins is shorter and a complex mixture of hydrocarbon rich in olefin is obtained. Therefore the Fischer–Tropsch process is viewed as a sound solution for the oil crisis and a resource for comonomers with potential application. Among the obtained odd-numbered monomers, *1-pentene* is often used to engineer a host of specific characteristics such as strength, thinness, elasticity and puncture resistance in products ranging from dense and durable plastic for wire coatings, automotive interiors, raincoats to low-density, high-quality shopping bags, cling-wrap film and myriad related consumer plastics.[70]

Moreover, a promising family of sterically hindered monomers is represented by branched α-olefins, like *4-methyl-1-pentene* (4M1P).[71] The synthesis of copolymers with variable content of 4-methyl-1-pentene which offers a larger specific volume due to its branching, is expected to be a feasible route for tuning the diffusion properties of materials for gas separating applications (e.g. membranes and hollow fibres) and/or for permeable films destined to particular packaging requirements.

1.4.1 4-methyl-1-pentene based copolymers

1.4.1.1 Ethylene/4-methyl-1-pentene copolymers

In the last decade, ethylene/4-methyl-1-pentene copolymers have been carefully analyzed as regards their chemical distribution and thermal properties.

Ethylene/4-methyl-1pentene copolymers have been synthetized with several C_2-symmetric metallocenes catalysts and with the classical Constrained Geometry Catalyst CGC (Figure 1.15a). The selected organometallic complexes were endowed with different stereospecific ability, as shown by data on polypropylene (PP) microstructure, given in Table 1.1. Isotacticity index, expressed through the % of the fully isotactic *mmmm* pentads, and regioregularity index, indicated with the amount of 2,1 inserted propylene units, show that *rac*-Et(Ind)$_2$ZrCl$_2$ (EBI) (Figure 1.15b) and *rac*-Et(IndH$_4$)$_2$ZrCl$_2$ (EBTHI) (Figure 1.15c) are moderately isospecific, whereas *rac*-CH$_2$(3-^{t}BuInd)$_2$ZrCl$_2$, TBI, (Figure 1.15e) and *rac*-Me$_2$Si(2-Me-4PhInd)$_2$ZrCl$_2$, MPHI (Figure 1.15e) are able to prepare a highly regio- and stereoregular PP.[35] CGC gives rise to an essentially atactic regioirregular polypropylene.
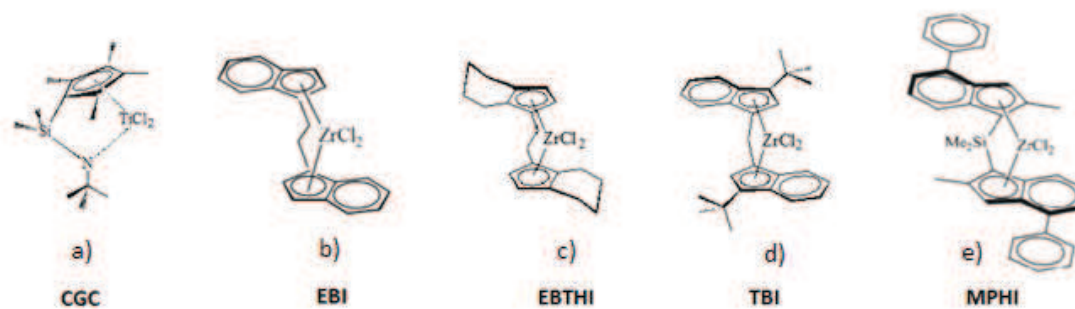
Figure 1.15 Structure of the catalysts: (a) CGC, (b) EBI, (c) EBTHI, (d) TBI and (e) MPHI.

Table 1.1 Isotacticy index and regioregularity index of C_2 symmetric isospecific catalysts.[35]

Catalyst	I.I.[a] (mmmm%)	Regioregularity index (%)
EBI	87.4	0.6
EBTHI	91.5	1.0
TBI	97.0	0.0
MPHI	99.5	0.5

[a] I.I.: isotactic index

Table 1.2 reports all the details of ethylene/4-methyl-1-pentene assignments according to reference 99.

Table 1.2 Chemical shift assignments for ethylene/4-methyl-1-pentene copolymer.

Chemical Structure	Carbon	Sequence	Chemical Shift
CH$_2$ (sc)	methylene	PP<u>P</u>PZ EP<u>P</u>PE PP<u>P</u>EZ EP<u>P</u>EZ E<u>P</u>E	43.67 43.60 43.12 43.05 42.50
(C$_4$H$_9$)(C$_4$H$_9$)(C$_4$H$_9$)(C$_4$H$_9$) chain...* ...chain	S$_{\alpha\alpha}$	PPPPPP PPPPPZ EPPPPE	40.03 40.43 40.22
(C$_4$H$_9$)(C$_4$H$_9$)(C$_4$H$_9$) chain...* ...chain		PPPPEZ EPPPEZ	39.73 39.66
(C$_4$H$_9$)(C$_4$H$_9$) chain...* ...chain		EPPE	38.87
(C$_4$H$_9$) chain...* ...chain	T$_{\delta\delta}$	EEPEE	33.62

Structure	Carbon	Sequence	Shift
chain—⟋⟍⟋(C_4H_9)—*—⟍⟋(C_4H_9)—chain	$S_{\alpha\gamma}$	EPEPZ	33.56 - 32.65
chain—⟋(C_4H_9)—⟍(C_4H_9)—*—⟋⟍(C_4H_9)—(C_4H_9)—chain		PPEPP	28.44 - 28.17
chain—⟋(C_4H_9)—*—⟍⟋⟍⟋—chain	$S_{\alpha\delta^+}$	PEE	32.54
chain—⟋⟍(C_4H_9)—*—(C_4H_9)—⟍⟋—chain	$T_{\beta\delta}$	↑ EPPZ	31.29
chain—⟋(C_4H_9)—(C_4H_9)—*—(C_4H_9)—chain	$T_{\beta\beta}$	EPPPE PPPPZ	29.42 - 29.04
chain—⟋(C_4H_9)—⟍⟋—*—⟍(C_4H_9)—chain	$S_{\gamma\gamma}$	PEEP	28.65
chain—⟋(C_4H_9)—⟍⟋—*—⟍⟋—chain	$S_{\gamma\delta}$	PEEE	28.23
chain—⟋⟍⟋—*—⟍⟋—chain	$S_{\delta\delta}$	EEEE	27.73
chain—⟋(C_4H_9)—*—⟍⟋⟍—chain	$S_{\beta\delta}$	PEE	24.81
chain—⟋(C_4H_9)—⟍(C_4H_9)—*—(C_4H_9)—chain	$S_{\beta\beta}$	PPEPZ	24.57
chain—⟋⟍(C_4H_9)—*—(C_4H_9)—⟍⟋—chain		EPEPE	21.80
CH (sc)	methine	EP<u>P</u>E EP<u>P</u>EZ PP<u>P</u>EZ PP<u>P</u>PZ EP<u>P</u>PE	23.75 23.69 23.64 23.57 23.52
CH$_3$ (sc)	methyl	EP<u>P</u>PE PP<u>P</u>PZ EP<u>P</u>^{i}EZ PP<u>P</u>^{i}EZ E<u>P</u>E PP<u>P</u>^{e}EZ EP<u>P</u>^{e}EZ	21.42 21.40 21.40 21.30 21.18 21.08 21.06

E = ethylene, P = 4-methyl-1-pentene, Z means ethylene or 4-methyl-1-pentene in all pair of sequences which are indistinguishable.

Blocky copolymers were prepared with all of the metallocenes, however longer sequences of comonomers were present in E/Y copolymer chains obtained with TBI and EBTHI rather than with EBI and MPHI. E/Y copolymers from MPHI were characterized by the presence of (very) short ethylene and 4-methyl-1-pentene sequences randomly distributed along the polymer chain. Copolymers from TBI showed ethylene-rich sequences alternating with 4-methyl-1-pentene-rich sequences, with a minor amount of isolated ethylene units distributed in the 1-olefin sequence. Long ethylene sequences with isolated comonomer unit were substantially absent with TBI catalyst.

Recently, living copolymerization of ethylene with 4-methyl-1-pentene by an α-diimine Ni(II) complex (Figure 1.16) and (diethylaluminium chloride) Et_2AlCl as activator was reported by Ricci *et al.*[72] and such a living nature of copolymerization was exploited to prepare poly(E-*co*-4M1P)-*block*-poly(1-hexene) with low polydispersity index ($M_w/M_n \sim 1.20$) and qualitatively good elastomeric properties.

Figure 1.16 Ni(II) complex [ArN=C(CH₃)-(CH₃)C=NAr]NiBr₂   (Ar=2,6-(ⁱ-Pr)₂C₆H₃).

The investigation of the microstructure of copolymers prepared with Nickel complex in Figure 1.6 and MAO or Et_2AlCl as cocatalyst , reported by Losio *et al.*,[73] showed a complex copolymer chain architecture. The resonance assignments has been correlated with the chain-walking mechanism: branching analysis showed that the total amount of 2,1 insertion of the comonomer, followed by backward migration of the nickel active species along the polymer chain, is higher than that of 1,2 inserted comonomer units.

1.4.1.2 Propylene/4-methyl-1-pentene copolymers

In the last years Losio and coworkers reported the complete and detailed signal assignments of the complex spectra of propylene/4-methyl-1-pentene (P/Y) copolymers[74] from C_2-symmetric metallocene catalysts, *rac*-Et(IndH₄)₂ZrCl₂, EBTHI and *rac*-H₂C-(3 ᵗBuInd)₂ZrCl₂, TBI (Figure 1.17).
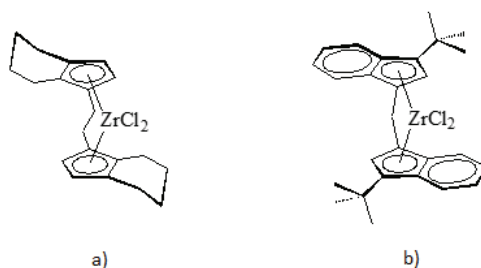
Figure 1.17 C_2-symmetric metallocenes catalysts: (a) EBTH), (b) TBI.

The general structure and carbon numbering of an isotactic propylene/4-methyl-1-pentene copolymer chain are sketched in Scheme 1.5.
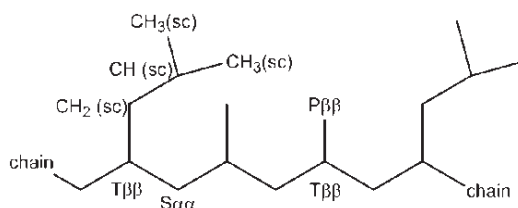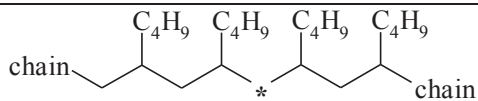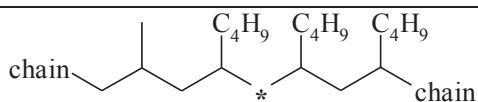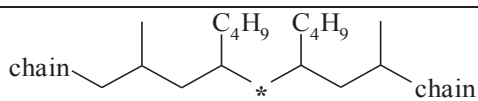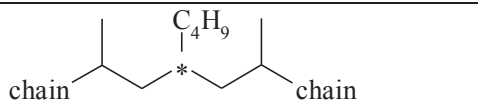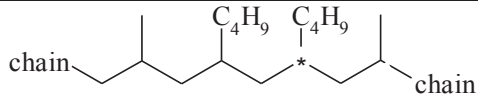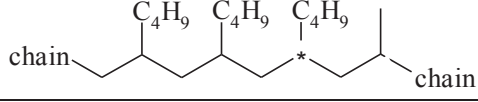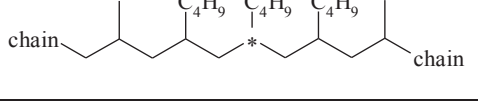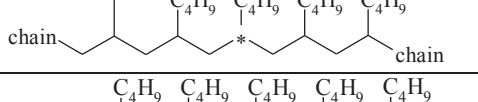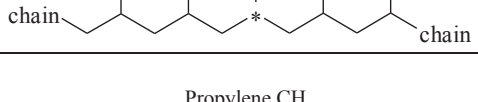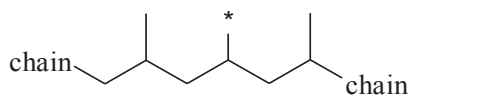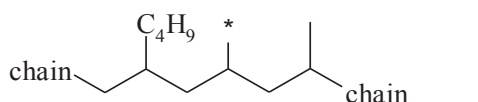
Scheme 1.5 Structure and carbon numbering of propylene/4-methyl-1-pentene copolymer.

The carbons were labelled according to the nomenclature first defined by Carman[75] and modified by Dorman[76] and Randall,[77] where P, S, and T refer to the primary (methyl), secondary (methylene), and tertiary (methine) carbons of the main chain, respectively. Methylene carbons along the backbone were identified by a pair of Greek letters to indicate the distance to branches in either directions. Methyl, methylene, and methine carbons in the side chain were designated by the symbols $CH_3(sc)$, $CH_2(sc)$, and $CH(sc)$.

Table 1.3 reports all the details of propylene/4-methyl-1-pentene assignments. The first column lists the molecular structure that includes the carbon being assigned, labelled as "*", the second column the kind of assigned carbon, and the third one the sequences whose center unit contains the assigned carbon. The fourth and fifth columns list the corresponding compositional or steric sequences. Finally, in the last column, the chemical shifts are reported.

Table 1.3 Chemical shift assignments for propylene/4-methyl-1-pentene copolymer.[74]

Chemical Structure	Carbon		Compositional Sequence	Steric Sequence	Chemical Shift (ppm)
		PP	YP<u>P</u>Y		45.05−44.97
			PP<u>P</u>Y		44.48
			PP<u>P</u>P	*mmmmrrm*	44.58
				mmrrm	44.24
				mmmmmmm	44.10
	$S_{\alpha\alpha}$	PY	YP<u>Y</u>Y+YP<u>Y</u>P		42.49−42.28
			PP<u>Y</u>P+PP<u>Y</u>Y		41.90

Structure	Group		(underlined)	tacticity	Value
C_4H_9 C_4H_9 C_4H_9 C_4H_9 chain ... * ... chain	YY		Y<u>Y</u>YY		40.05
C_4H_9 C_4H_9 C_4H_9 chain ... * ... chain			P<u>YY</u>Z		39.90
C_4H_9 C_4H_9 chain ... * ... chain					
CH₂ (sc)	methylene	PYP			44.20
		PYY			43.89
		YYY	P<u>YYY</u>Z		43.75
			Y<u>YYY</u>Y		43.65
C_4H_9 chain ... * ... chain	T_ββ	PYP	<u>PYP</u>		29.34
C_4H_9 C_4H_9 chain ... * ... chain		YYP	P<u>PYY</u>Z		29.29
C_4H_9 C_4H_9 C_4H_9 chain ... * ... chain			Y<u>PYY</u>Z		29.11
C_4H_9 C_4H_9 C_4H_9 chain ... * ... chain		YYY	P<u>YYY</u>P		29.03
C_4H_9 C_4H_9 C_4H_9 C_4H_9 chain ... * ... chain			P<u>YYY</u>Y		28.93
C_4H_9 C_4H_9 C_4H_9 C_4H_9 C_4H_9 chain ... * ... chain			Y<u>YYY</u>Y		28.85
Propylene CH	T_ββ	P	P		26.49−25.87
CH (sc)	methine	Y	Y		23.50
CH₃ (sc)	methyl	Y	PY^{l}Y		21.51
			Y<u>YYY</u>Y		21.44
			PYP		21.24
			PY^{h}Y		21.10
chain ... * ... chain	P_ββ	PPP	P<u>PPP</u>P	*mmmm*	19.68
				mmmr	19.40
				mmrr	18.87
				mrrm	17.64
			Y<u>PPP</u>Z		19.59
C_4H_9 * chain ... chain		PPY	P<u>PPY</u>P		19.55
			Y<u>YPP</u>Z		19.43–19.40
			P<u>YPY</u>Z		19.31

chain $\diagdown$ C_4H_9 $*$ C_4H_9 chain		YPY	Y<u>YPY</u>Z	19.11

P = propylene, P = 4-methyl-1-pentene, Z means propylene or 4-methyl-1-pentene in all pair of sequences which are indistinguishable.

In figure 1.18 the ^{13}C NMR spectra of a series of P/4M1P copolymers, from EBTHI catalyst, at increasing comonomer content are reported along with those of the two homopolymers, taken as references. Due to the low molecular weights produced by the catalyst, there are several signals (from now on starred in the spectra along with the resonances attributed to the regioirregularities) belonging to a variety of chain-end groups. Specifically, in the spectrum of polypropylene (Figure 1.18a), the quite intense signals of saturated *n*-propyl (12.42, 18.02, 18.70, 28.28 and 37.46 ppm) and unsaturated vinylidene (20.53 ppm) chain-end groups are indicated, along with the signals due to 1,3 enchainments (18.76, 25.39, 28.58 and 35.16 ppm).[78-80]
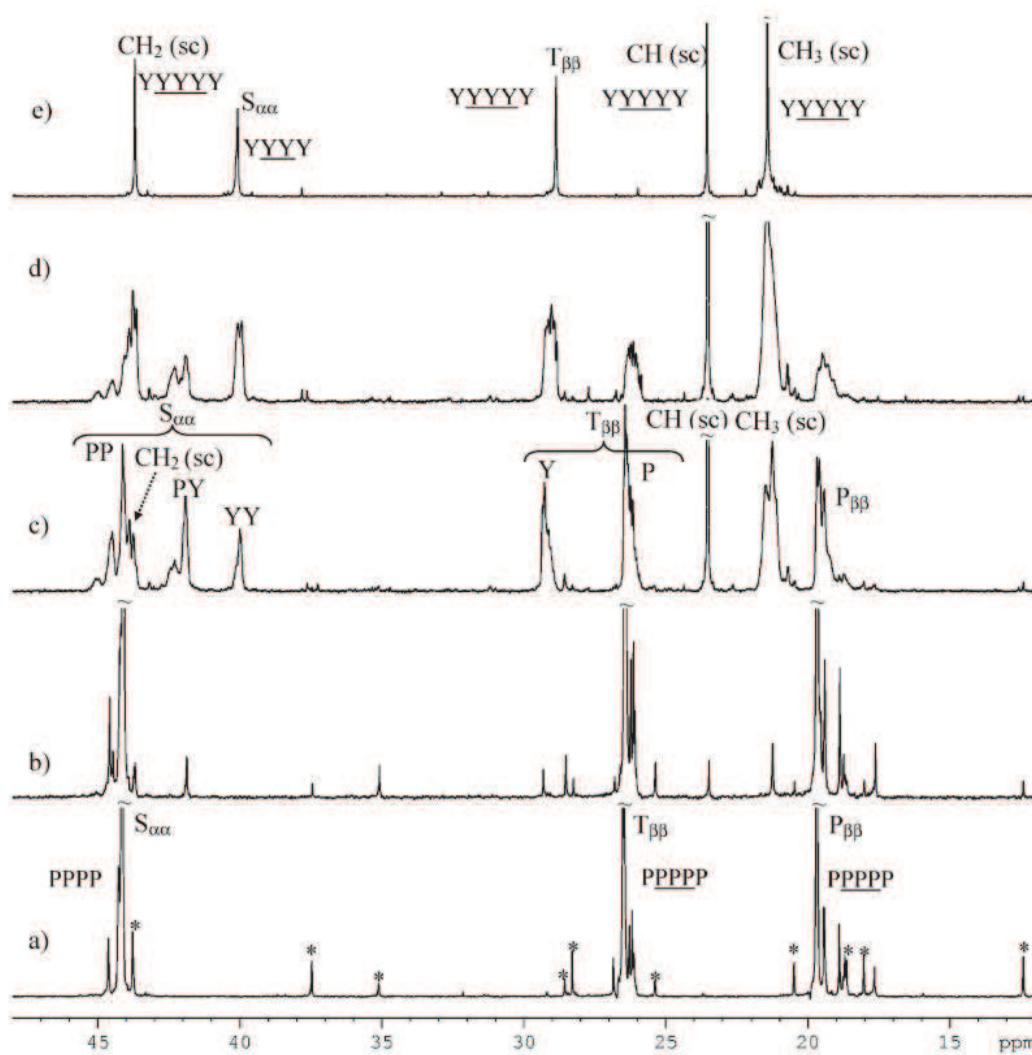
Figure 1.18 ^{13}C NMR spectra of P/4M1P copolymers from EBTHI at different comonomer content: (b) 1.88 mol%, (c) 35.88 mol%, and (d) 60.75 mol%. The spectra of the P (a) and 4M1P (e) homopolymers are reported as points of reference. Chain-end groups and regioirregularities are starred in spectrum a.[74]

1.4.1.3 4-methyl-1-pentene polymorphism

1.4.1.3.1 Poly(4-methyl-1-pentene)

Several studies have been conducted about structural properties of homo- and copolymers of 4-methyl-1-pentene. Isotactic poly(4-methyl-1-pentene), *i*P(4M1P), exhibits a polymorphic behavior which is even more complex than that of *i*PP. It has been established that, at least, five different crystalline forms, namely Form I, Form II, Form III, Form IV and Form V (Figure 1.19), exist. So far, the crystalline structure of the different polymorphs has been completely solved only for Form I, II and III.

Form I

Form I is the most common and stable crystal structure and is typically found in melt crystallized samples and in fibers. This structure can also be obtained by crystallization from solution in solvents such as *n*-alkanes with carbon atom numbers higher than 9.

This form is characterized by chains in 7_2 helical conformation packed in a tetragonal unit cell with axes $a = 18.66$ Å, $c = 13.80$ Å.[81-83]

Form II

Form II of isotactic poly(4-methyl-1-pentene) can be obtained from i) dilute xylene solutions by isothermal crystallization at 20°C or ii) tetramethyltin solution by crystallization. Takayanagi *et al.*,[84] from X-ray diffraction patterns on single-crystals, propose a tetragonal unit cell with axes $a = 19.16$ Å and $c = 7.12$ Å and chains in the 4_1 helical conformation. The chains are in a 4_1 helical conformation and are packed in a monoclinic unit cell with axes $a = 10.49$ Å, $b = 18.89$ Å, $c = 7.13$ Å, and $\gamma = 113.7°$, as reported by De Rosa[83] and Ruan *et al.*[85]

Form III

This modification results by crystallizing the polymer from dilute solutions in xylene by isothermal crystallization at 65 °C[84] and in decalin.[86] It is also obtained in linear and branched alkanes, as well as in carbon tetrachloride and cycloalkanes.[87,88]

The crystal structure of Form III has been determined and refined by Corradini *et al.*: chains in 4_1 helical conformation packed in a tetragonal unit cell with axes $a = 19.46$ Å, $c = 7.02$ Å.[89,90]

Form IV

Form IV can be obtained by annealing Form I above 200°C under high pressure (4500 atm)[91] or from cyclopentane solution.[92]

A 3_1 helical conformation of the chains and a hexagonal unit cell with axes $a = 22.17$ Å, $c = 6.5$ Å has been proposed for this polymorph. Form IV can be transformed into Form I by annealing at 130 °C.[83, 92-93]

Form V

The last modification is obtained by crystallization from concentrated cyclohexane gels and by crystallization from cyclohexane/carbon tetrachloride solutions.[83,94] Form V transforms into Form I by annealing at ≈ 90 °C.

No information on the crystal structure of Form V is yet available.
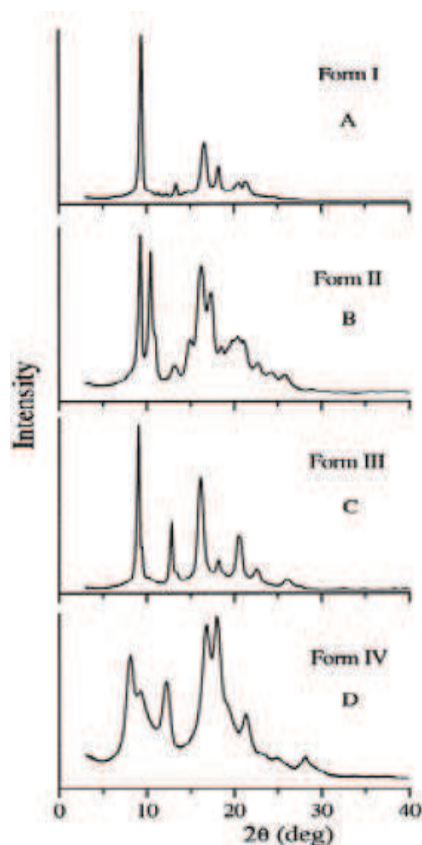
Figure 1.19 WAXD spectra of Form I-IV iP(4M1P) polymorphs.[83]

1.4.1.3.2   4-methyl-1-pentene based copolymers

Losio *et al.*[95] studied effect of ethylene comonomer on iP(4M1P) polymorphism on a series of ethylene/4-methyl-1-pentene copolymers from C_2-symmetric metallocene catalyst at increasing 4-methyl-1-pentene content; as abovementioned isotactic poly(4-methyl-1-pentene) is known to give rise to a rich polymorphism and the tetragonal form I, directly obtained by cooling from the molten state, is the most stable polymorph.
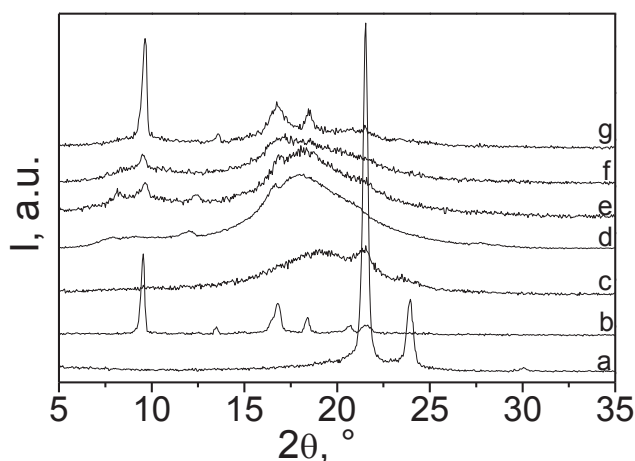
Figure 1.20 WAXD patterns of a selection of E/Y copolymers: (a) polyethylene and (b) poly(4-methyl-1-pentene) homopolymers. The mol % of Y are as follows: (c) 18.4; (d) 45.8; (e) 54.4; (f) 69.8; (g) 84.6. The curves are shifted vertically for sake of clarity.[95]

In Figure 1.20 the reflections featuring this polymorph, at $2\theta = 9.80$, 16.50, and 18.35°, are present in the WAXD pattern of the homopolymer as well as of the copolymer containing *ca.* 15 mol % of ethylene: see traces b and g, respectively. In the sample containing ca. 30 mol % of ethylene units, the reflections of form I are also present, specifically the peak at $2\theta = 9.80°$, corresponding to the (007) plane, is the only one clearly distinguishable in trace f. Beside this reflection, two other peaks at $2\theta = 8.05$ and 12.25° emerge from the broad amorphous halo in trace e, referring to the copolymer with about equimolar content.

According to literature, these new reflections are indicative of the presence of crystals in form IV.[91,92] The presence of these new reflections suggests that increasing amount of ethylene units in the copolymers favors the formation of this polymorph, either by acting as "solvent molecules" for the Y blocks or, by shortening the length of isotactic sequences, in analogy with the role of defective units in the development of α and γ polymorphs of isotactic polypropylene.

For the copolymer containing about 45 mol % of Y only reflections typical of form IV are detectable in the WAXD spectrum (trace d). The occurrence of detectable crystalline reflections of Y crystals even in this sample, which according to the statistical calculations contains no more than 10% of relatively long Y sequences, is likely due to the inclusion in the crystal lattice of isolated ethylene units, thus increasing the number and the length of actually crystallizable sequences.

Recently, Canetti *et al.*[96] reported on the diffractograms of pure polyethylene and some ethylene/4-methyl-1-pentene copolymers from the Ti(IV) diisopropoxy complex bearing a dianionic [O- ,S,O-] bis(phenolato) ligand, in combination with methylalumoxane, as catalyst system. The WAXD profiles showed, for polyethylene, the typical peaks of the orthorhombic cell of polyethylene. The relative intensity of the peaks reduced with increasing the branched comonomer content, indicating a progressive decrease of the crystallinity due to the increased number of non-crystallizable branches. The amorphous halo centered around 19.5 of $2\theta°$ becomes progressively evident enhancing the comonomer content in the copolymer. The WAXD profile of a copolymer with 20.3 mol% of 4M1P showed a prominent amorphous halo and a small crystalline diffraction at about 21 $2\theta°$. The expansion of the cell increases slightly at increasing comonomer content probably due to the strain that the branches n the interphase cause to the

crystallites. In fact, only small size branches like methyls can be incorporated in the crystalline lattice and have a large effect on the cell dimension.

One of the targets of this PhD thesis is to continue the structural studies, in order to gain information on copolymers' crystallization, in particular for what regards propylene/4-methyl-1-pentene copolymers.

1.5   1-pentene based copolymer

1.5.1. Ethylene/1-pentene copolymers

In the last years, odd branched 1-olefins based copolymers have been extensively studied concerning their microstructures by ^{13}C NMR and also their properties.[63,68c,d,e,73,95,97-104] While propylene/1-pentene copolymers have been prepared and their microstructural characterizations have been performed,[68d,74,98,102] there are only a few works on ethylene/1-pentene copolymers.

To date, the ^{13}C NMR assignment of the spectra of ethylene/1-pentene copolymers relies on few works: the former by Galland, where only one composition of this kind of copolymer (6.51 mol% of inserted comonomer), obtained with the catalytic system *rac*-Et[Ind]$_2$ZrCl$_2$/MAO, was analyzed and the latter by Nomura with nonbridged half-titanocenes.[100,105]

Luruli described the results of the copolymerization of ethylene with 1-pentene, utilizing a zirconoxycarbene complex as catalyst precursor (Figure 1.21).[104]

The copolymers synthesized with [(CO)$_5$W=C(Me)OZr(Cp)$_2$Cl] had higher average molecular weights and broader polydispersities compared to those produced with Cp$_2$ZrCl$_2$, more like a Ziegler-Natta catalyst type. The results obtained indicate that carbene ligand plays a role at least sterically during polymerization.
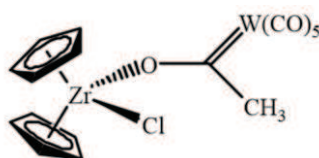
Figure 1.21 [(CO)$_5$W=C(Me)OZr(Cp)$_2$Cl] catalyst.

In 2009, Nomura[105] explored the copolymerization of ethylene with 1-pentene using the catalysts reported in Figure 1.22. The Constrained Geometry Catalyst (4) was reported for comparison.
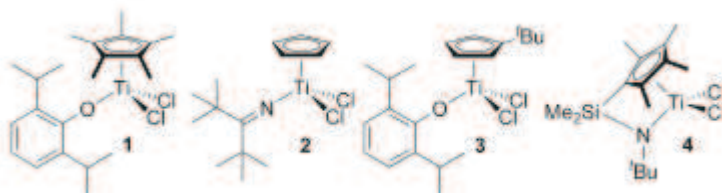
Figure   1.22   (1)   (C$_5$Me$_4$)TiCl$_2$(O-2,6-^{i}Pr$_2$C$_6$H$_3$)   **(2)**   CpTiCl$_2$(N= C^{t}Bu$_2$) **(3)** (C$_5$^{t}Bu)TiCl$_2$(O-2,6-^{i}Pr$_2$C$_6$H$_3$)   **(4)** [Me$_2$Si(C$_5$Me$_4$)(N^{t}Bu)]TiCl$_2$.

All the half-titanocenes were found to give almost alternating copolymer ($r_E r_{Pe}$ <1), whereas the copolymerization by 4 proceeds in a random manner.

Recenly, Leone *et al.* reported on the copolymerization of ethylene with 1-pentene catalyzed by a Ti(IV) diisopropoxy complex bearing a tridentate [O⁻,S,O⁻]-type bis(phenolato) ligand (Figure 1.23) in combination with MAO. With this catalyst, crystalline copolymers with a strong tendency for comonomer alternation were obtained with good comonomer incorporation (about 11.5 mol% for [1-Pentene]/[E] = 8.1).[97]
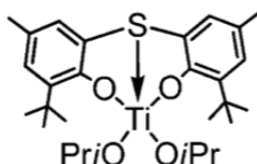
Figure 1.23 Ti(IV) thiobis(phenolate) complex [2,2'-S(4-Me,6-*t*-BuC$_6$H$_2$O)$_2$]Ti(OiPr)$_2$.

1.5.2. Propylene/1-pentene copolymer

The microstructure of propylene/1-pentene copolymers, prepared with the metallocene catalysts *rac*-Et(Ind)$_2$ZrCl$_2$ and *rac*-Me$_2$Si(2-MeBenz-[*e*]Ind)$_2$ZrCl$_2$, was extensively studied by ^{13}C NMR spectroscopy.[68c] Both catalysts lead to the formation of random copolymers although *rac*-Me$_2$Si(2-MeBenz-[*e*]Ind)$_2$ZrCl$_2$ favors a somewhat higher incorporation of 1-pentene than *rac*-Et(Ind)$_2$ZrCl$_2$. Moreover, the presence of 1-pentene has a significant influence on the stereoregularity of the copolymers (Figure 1.24 and 1.25).

Propylene-based copolymers from *rac*-Me$_2$Si(2-MeBenz-[*e*]Ind)$_2$ZrCl$_2$ are characterized by a gradual loss of tacticity which is concurrent with an increase in the amount of all irregular pentads while copolymers from *rac*-Et(Ind)$_2$ZrCl$_2$ retained the isotacticity of polypropylene and featured only the stereoerror pentads *mmmr*, *mmrr* and *mrrm* typical for enantiomorphic site control.
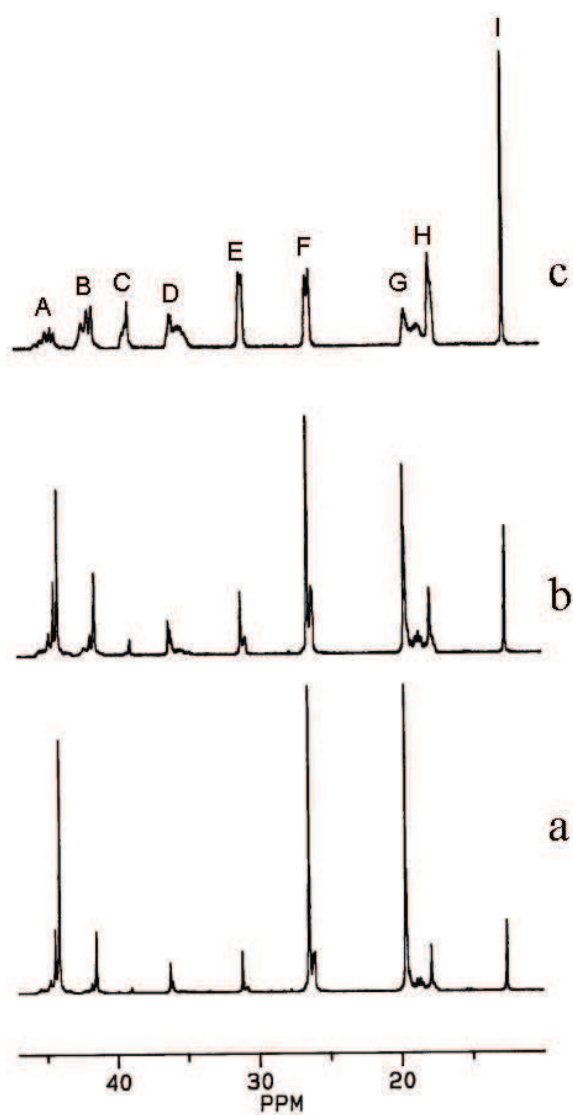
Figure 1.24 ^{13}C NMR spectra of 1-pentene/propylene copolymers prepared with *rac*-Me$_2$Si(2-MeBenz-[*e*]Ind)$_2$ZrCl$_2$ at 1-pentene/propylene feed ratios of 0.2 (a), 0.4 (b) and 1.5 (c).[68c]
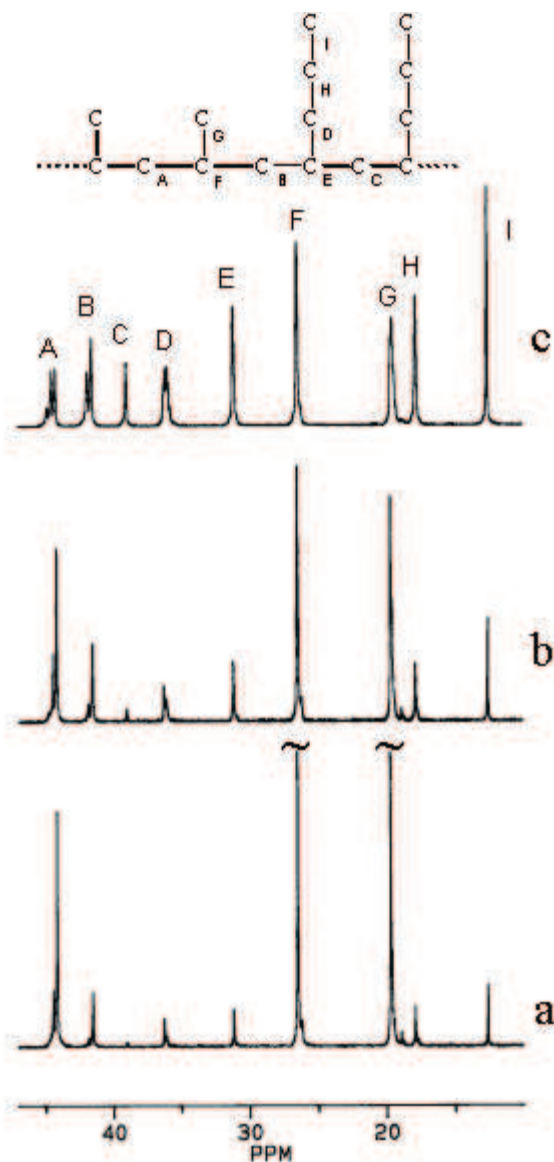
Figure 1.25 ^{13}C NMR spectra of 1-pentene/propylene copolymers prepared with *rac*-Et(Ind)$_2$ZrCl$_2$ at pentene/propylene feed ratios of 0.2 (a), 0.4 (b) and 1.5 (c).[68c]

In Table 1.4 the complete peak assignment for propylene/1-pentene copolymers is reported.

Table 1.4 Peak assignment in ^{13}C NMR spectra of propylene/1-pentene copolymers[a] .[68c]

Region	Carbon	Assignment		δ in ppm
		compositional sequence	Stereosequence	
A	ααCH$_2$	Pe**PP**Pe		44.74
		Pe**PPP**		44.40
		PPPP		44.10
B	ααCH$_2$	Pe**Pe**PPe + P**Pe**PPe		41.79
		Pe**Pe**PP + P**Pe**PP		41.48

C	ααCH$_2$	**PePe**		38.95
D	αCH$_2$	P**PPe**PP		36.22
		Pe**PPe**PP		36.19
		Pe**PPe**PPe		36.16
		P**PePe**PP		36.06
		Pe**PePe**PP		35.98
		P**PePe**PPe		n.d.
		Pe**PePe**PPe		35.82
		PePePe	mmmm	35.72
			mmmr + mmrr + rmmr	35.53
			mmrm + rmrr	35.36
			mrmr + rrrr	35.14
			mrrr	34.99
			mrrm	34.70
E	1-Pentene CH	**Pe**		31.08±31.16
F	Propylene CH	**P**		26.52±26.44
G	Propylene CH$_3$	P**PPP**P	mmmm	19.68
		Pe**PPP**P		19.63
		Pe**PPP**Pe		19.61
		P**PePP**P		19.55
		Pe**PePP**P		19.48
			mmmr	19.40
		P**PePP**Pe		19.41
		Pe**PePP**Pe		19.41
		PePPe		19.33±19.35
			rmmr	19.12
			mmrr	18.87
			mrmm + rmrr	18.62
			rmrm	18.43
			rrrr	18.12
			rrrm	17.95
H	βCH$_2$	**Pe**		17.87
			mrrm	17.62
I	1-Pentene CH$_3$	**Pe**		12.54

[a] Peak positions are given as downfield shifts with respect to the peak of HMDS. P and Pe are abbreviations for propylene and 1-pentene. αα CH$_2$ denotes the backbone methylene carbons, while αCH$_2$, βCH$_2$ and γCH$_2$ identify methylene carbons in the side chain of the 1-pentene units with respect to their CH group.

Thermal and structural properties of abovementioned propylene/1-pentene copolymers were analyzed by differential scanning calorimetry (DSC) and wide angle X-ray diffraction (WAXD):[68e] the thermal behavior of the copolymers was correlated with their microstructural features and a relationship between melting temperatures and average length of the isotactic sequences was established. Furthermore, the influence of the comonomer on the degree and type of crystallinity of the copolymers was investigated. WAXD results demonstrate that only the α-modification is present when crystallization takes place under fast cooling conditions, both in crystallized samples as well as in samples that had been aged for several weeks at room temperature.

Moreover, the melting and crystallization behaviour of isotactic propylene/1-pentene copolymers from *rac*-Et(Ind)$_2$ZrC, with 1-pentene contents up to 50 mol%, were studied by DSC and temperature resolved WAXD/SAXS: in particular, the role of the 1-pentene comonomer in the development of the trigonal modification (δ-form) of *i*-PP was studied: the crystallizing capability of the δ-form, which develops in the composition range between *ca.* 10 and 50mol% of 1-pentene content, only slightly decreases with concentration of 1-pentene. This result has been correlated with the limits imposed to cell expansion by the crystal density. The crystallization kinetics of the trigonal modification is characterized by a composition-dependent induction time followed by a relatively fast development of structural order, the sharp WAXD reflections combined with the SAXS data suggest that, notwithstanding the intrinsic intra-chain structural disorder, thin and wide lamellae characterize the morphology of the δ-form crystallites. De Rosa reported the crystal structure of the trigonal form of isotactic propylene/1-pentene copolymers from *C*$_2$-symmetric metallocene catalyst dimethylsilyl(2,2′-dimethyl-4,4′-diphenylindenyl)ZrCl$_2$ and from *C*$_1$-symmetric metallocene catalyst dimethylsilyl(2,4,7-trimethylindenyl)(dithienocyclopentadienyl)ZrCl$_2$.[101c] The structure of the trigonal form found in the copolymers, similar to the structure of form I of isotactic propylene/1-butene copolymers, demonstrates that the packing of polymer molecules is mainly driven by the crystallographic principles of the maximum entropy and density. Indeed, the copolymers in which the less bulky ethyl lateral group allows a larger incorporation of 1-pentene units in the crystals of the trigonal form represent the best example of the principle of density–entropy driven phase formation in polymers.

1.6 References

1. http://www.marketsandmarkets.com/Market-Reports/polyolefins-market-1235.html

2. V. Busico, *Macromol. Chem. Phys.*, **2007**, *208*, 26.

3. V. Busico, *MRS Bulletin*, **2013**, *38*, 224.

4. M. Gahleitner, L. Resconi, P. Doshev, *MRS Bulletin*, **2013**, *38*, 229.

5. E. W. Faucett, R. O Gibson, *J. Chem. Soc.*, **1934**, 386.

6. K. Ziegler, H. G Gellert, *Ann*, **1950**, *567*, 195.

7. K. Ziegler, H. G. Gellert, *Polymerization of ethylene. US Patent 2*, **1953**, *699*, 457.

8. K. Ziegler, *Brennstoff-Chem.*, **1954**, *35*, 321.

9. K. Ziegler, E. Holzkamp, H. Breil, H. Martin, *Angew. Chem.*, **1955**, *67*, 426.

10. R. Mulhaupt, *Macromol. Chem. Phys.*, **2003**, *204*, 289–327.

11. P. Corradini, *Journal of Polymer Science: Part A: Polymer Chemistry*, **2004**, *42*, 391.

12. P. Corradini, *Macromol. Symp.*, **1995**, *89*, 1.

13. P. Galli, *Macromol. Symp.*, **1995**, *89*, 13.

14. H. Sinn, W. Kaminsky, *Adv. Organomet. Chem.*, **1980**, *18*, 99.

15. W. Kaminsky, Catal. *Today*, **2000**, *62*, 23.

16. G. S. Hlatky, *Chem. Rev.* **2000**, *100*, 1347.

17. G. J. P. Britovsek, V. C. Gibson, D. F. Wass, *Angew. Chem.*, *Int. Ed. Engl.*, **1999**, *38*, 428.

18. V. C. Gibson, S. K. Spitzmesser, *Chem. Rev.*, **2003**, *103*, 283.

19. http://www.plasticseurope.org/documents/document/20151216062943plastics_the_facts_201 5_final_30pages_14122015.pdf

20. P. S. Chum, K. W. Swogger, *Prog. Polym. Sci.*, **2008**, *33*, 797.

21. E. O. Fischer, *Nobel Lectures, Chemistry*, **1973**.

22. G. Wilkinson, *Nobel Lectures, Chemistry*, **1973**.

23. W. Kaminsky, A. Laban, *Appl. Catal. A: General*, **2001**, *222*, 47.

24. F.R.W.P. Wild, L. Zsolnai, G. Huttner, H. H. Britzinger, *J. Organomet. Chem.*, **1982**, *232*, 233.

25. (a) H. Schnutenhaus, H. H. Brintzinger, *Angew. Chem., Int. Ed. Engl.*, **1979**, *18*, 777; (b) F. R. W. P. Wild, L. Zsolnai, G. Huttner, H. H. Brintzinger, *J. Organomet. Chem.,* **1982**, *232*, 233.

26. (a) J. A. Ewen, *J. Am. Chem. Soc.*, **1984**, *106*, 6355; (b) J. A. Ewen, *J. Mol. Cat. A: Chem.,* **1998**, *128*, 103.

27. W. Kaminsky, K. Kuelper, H. H. Brintzinger, F. R. W. P. Wild, *Angew. Chem.,* **1985**, *97*, 507.

28. H. Braunschweig, F.M Breitling, *Coord. Chem. Rew.*, **2006**, *250*, 2691.

29. (a) H. Sinn, W. Kaminsky, H. Hoker, Eds. *Alumoxanes*; Macromolecular Symposia 97; (b) Hüthing & Wepf: Heidelberg, Germany, **1995**; (c) S. Srinivasa Reddy, S. Sivaram, *Prog. Polym. Sci.,* **1995**, *20*, 309; (d) J. Stellbrink, A. Niu, J. Allgaier, D. Richter, B. Koenig, R. Hartmann, G. W. Coates, L. J. Fetters, *Macromolecules,* **2007**, *40*, 4972.

30. W. Kaminsky, H. Sinn, *Adv. Polym. Sci.*, **2013**, *258*, 1–28.

31. L. Resconi, S. Bossi, *Macromolecules*, **1990**, *23*, 4489.

32. (a) F.S. Dyachkovskii, A. K. Shilova, E. A. Shilov, *J. Polym. Sci.*, **1967**, *16*, 2333; (b) W. Kaminsky, *Makromol. Chem. Phys.,* **1996**, *197*, 3907; (c) W. Kaminsky, C. Strubel, *J. Mol. Catal*., **1998**, *128*, 191; (d) I. Tritto, S. X. Li, M. C. Sacchi, P. Locatelli, G. Zannoni, *Macromolecules,* **1995**, *28*, 5358; (e) I. Tritto, S. X. Li, M. C. Sacchi, G. Zannoni, *Macromolecules,* **1993**, *26*, 7111; (f) I. Tritto, R. Donetti, M. C. Sacchi, P. Locatelli, G. Zannoni, *Macromolecules,* **1999**, *32*, 264; (f) C. Sishta, R. M. Halthorn, T. J. Marks, *J. Am. Chem. Soc.*, **1992**, *114*, 1112; (g) R. F. Jordan, W. E. Dasher, S. F. Echols, *J. Am. Chem. Soc.*, **1986**, *108*, 1718; (h) M. Bochmann, *J. Organomet. Chem.*, **2004**, *689*, 3982; (i) H. H. Britzinger, D. Fisher, R. Mulhaupt, B. Rieger, R.M. Waymouth, *Angew. Chem., Int. Ed. Engl.,* **1995**, *34*, 1143.

33. E. Y-X. Chen, T. J. Marks, *Chem. Rev.,* **2000**, *100*, 1391.

34. J. C. W. Chien, R. Sugimoto, *J. Polym. Sci., Polym. Chem. Ed.,* **1991**, *29*, 459.

35. L. Resconi, L. Cavallo, A. Fait, F. Piemontesi, *Chem. Rev.*, **2000**, *100*, 1253.

36. X. Yang, C. L. Stern, T. J. Marks, *Organometallics*, **1991**, *10*, 840.

37. C. Sishta, R. M. Hathorn, T. J. Marks, *J. Am. Chem. Soc.*, **1992**, *114*, 1112.

38. G. G. Hlatky, H. W. Turner, R. R. Eckmann, *J. Am. Chem. Soc.*, **1989**, *111*, 2728.

39. J. C. W. Chien, W. M. Tsai, M. D. Rausch, *J. Am. Chem. Soc.*, **1991**, *113*, 8570.

40. M. Bochmann, S. J. Lancaster, *Organometallics*, **1993**, *12*, 633.

41. A. Zambelli, P. Longo, A. Grassi, *Macromolecules*, **1989**, *22*, 2186.

42. T. Shiono, *Adv. Polym. Sci.,* **2013**, 211.

43. (a) W. Kaminsky, *Makromol. Chem. Phys.,* **1996**, *197*, 3907; (b) W. Kaminsky, C. Strubel, *J. Mol. Catal*., **1998**, *128*, 191; (c) I. Tritto, S. X. Li, M. C. Sacchi, P. Locatelli, G. Zannoni,

Macromolecules, **1995**, *28*, 5358; (d) I. Tritto, S. X. Li, M. C. Sacchi, G. Zannoni, *Macromolecules,* **1993**, *26*, 7111; (e) I. Tritto, R. Donetti, M. C. Sacchi, P. Locatelli, G. Zannoni, *Macromolecules,* **1999**, *32*, 264; (f) C. Sishta, R. M. Halthorn, T. J. Marks, *J. Am. Chem. Soc.*, **1992**, *114*, 1112; (g) R. F. Jordan, W. E. Dasher, S. F. Echols, *J. Am. Chem. Soc.*, **1986**, *108*, 1718; (h) M. Bochmann, *J. Organomet. Chem.*, **2004**, *689*, 3982; (i) H. H. Britzinger, D. Fisher, R. Mulhaupt, B. Rieger, R.M. Waymouth, *Angew. Chem., Int. Ed. Engl.,* **1995**, *34*, 1143.

44. K. P. Bryliakov, E. P. Talsi, *Coord. Chem. Rev.*, **2012**, *256*, 2994.

45. E. Y. X. Chen, T. J. Marks, *Chem. Rev.*, **2000**, *100*, 1391.

46. D. E. Babushkin, H. H. Brintzinger, *J. Am. Chem. Soc.,* **2002**, *124*, 12869.

47. I. Tritto, R. Donetti, M. C. Sacchi, P. Locatelli, G. Zannoni, *Macromolecules*, **1997**, *30*, 1247.

48. D. E. Babushkin, N. V. Semikolenova, V. A. Zakharov, E. P. Talsi, *Macromol. Chem. Phys.*, **2000**, *201*, 558.

49. M. Bochmann, S. J. Lancaster, *Angew. Chem. Int. Ed. Engl.*, **1994**, *33*, 1634.

50. M. Bochmann, *Organometallics*, **2010**, *29*, 4711.

51. C. R. Landis, K. A. Rosaaen, D. R. J. Sillars, *J. Am. Chem. Soc.*, **2003**, *125*, 1710.

52. D. E. Babushkin, H. H. Brintzinger, *J. Am. Chem. Soc.*, **2010**, *132*, 452.

53. J. W. Lauher and R. Hoffmann, *J. Am. Chem. Soc.,* **1976**, *98*, 1729.

54. (a) P. Cossee, *Tethaedron Lett.*, **1960**, *17*, 12; (b) P. Cossee, in "*The Stereochemistry of Macromolecules*", A. D. Ketley, Ed.; Marcel Dekker: New York, 1967; Vol. 1.

55. (a) B. J. Burger, M. E. Thompson, W. D. Cotter, J. E. Bercaw, *J. Am. Chem. Soc.,* **1990**, *112*, 1566; (b) S. Hajela, J. E. Bercaw, *Organometallics,* **1994**, *13*, 1147; (c) Y. W. Alelyunas, Z. Guo, R. E. LaPointe, R. F. Jordan, *Organometallics,* **1993**, *12*, 544; Z. Guo, D. Swenson, R. Jordan, *Organometallics,* **1994**, *13*, 1424; (d) P. L. Watson, D. C. Roe, *J. Am. Chem. Soc.,* **1982**, *104*, 6471; (e) L. Resconi, F. Piemontesi, G. Franciscono, L. Abis, T. Fiorani, *J. Am. Chem. Soc.,* **1992**, *114*, 1025.

56. U. Stehling, J. Diebold, R. Kirsten, W. Roell, H. H. Brintzinger, S. Juengling, R. Muelhaupt, F. Langhauser, *Organometallics,* **1994**, *13*, 964.

57. (a) J. C. W. Chien, C.-I. Kuo, *J. Polym. Sci.: Part A: Polym. Chem.,* **1986**, *24*, 1779; (b) J. C. W. Chien, B. P. Wang, *J. Polym. Sci., A: Polym. Chem.,* **1988**, *26*, 3089; (c) J. C. W. Chien, A. Razavi, *J. Polym. Sci., A: Polym. Chem.,* **1988**, *26*, 2369; (d) J. C. W. Chien, B. P. Wang, *J. Polym. Sci., A: Polym. Chem.,* **1990**, *28*, 15; (e) L. Resconi, S. Bossi, L. Abis, *Macromolecules*, **1990**, *23*, 4489; (f) N. Naga, K. Mizunuma, *Polymer,* **1998**, *39*, 5059; (g) G. J. P. Brtovsek, V. C. Gibson, B. S. Kimberley, P. J. Maddox, S. J. McTavish, G. A. Solan, A. J. P. White, D. Williams, *Chem. Commun.,* **1998**, 849; (h) B. L. Small, M. Brookhart, *J. Am. Chem. Soc.,* **1998**, *120*, 7143.

58. (a) V. Busico, R. Cipullo, P. Corradini, *Makromol. Chem.,* **1993**, *194*, 1079; (b) V. Busico, R. Cipullo, J. C. Chadwick, J. F. Modder, O. Sudmeijer, *Macromolecules*, **1994**, *27*, 7538; (c) S. B. Amin, T. J. Marks, *Angew. Chem. Int. Ed.,* **2008**, *47*, 2006.

59. J. Boor Jr., in "*Ziegler-Natta Catalysts and Polymerization*", Academic Press: New York, **1979**, Cap. 10, 245.

60. W. Kaminsky, R. Steiger, *Polyhedron,* **1988**, *26*, 2375.

61. P. J. Flory, in "*Principles of Polymer Chemistry*", Cornell University Press,: Ithaca, New York, **1953**.

62. A. M. Thayer, *Chemical & Engineering News*, September **1995**, Copyright ACS.

63. M. Galimberti, F. Piemontesi, L. Alagia, S. Losio, L. Boragno, P. Stagnaro, M.C. Sacchi, *J. Polym. Sci.: Polym. Chem.,* **2010**, 48, 2063.

64. Y.V. Kissin, *"Isospecific Polymerization of Olefins",* Springer Verlag, N.Y., **1985**.

65. C. Cosewith, G. VerStrate, *Macromolecules*, **1971**, *4*, 482.

66. C. J. Carman, R. A. Harrington, C. E. Wilkes, *Macromolecules*, **1977**, *10*, 536.

67. G. J. Ray, P. E. Johnson, J. R. Knox, *Macromolecules*, **1977**, *10*, 773.

68. (a) M. Arnold, O. Henschke, J. Knorr, *Macromol. Chem. Phys.,* **1996**, *197*, 563; (b) M. J. Scheineider, R. Mülhaupt, *Macromol. Chem. Phys*., **1997**, *198*, 1121; (c) M. C. Sacchi, F. Forlini, S. Losio, I. Tritto, P. Locatelli, U. M. Wahner, I. Tincul, J. Joubert, E. R. Sadiku, *Macromol. Chem. Phys*., **2003**, *204*, 1643; (d) U. M. Wahner, I. Tincul, F. Forlini, D. J. Joubert, E. R. Sadiku, S. Losio, I. Tritto, M. C. Sacchi, *Macromol. Chem. Phys*., **2003**, *204*, 1738; (e) G. Costa, P. Stagnaro, V. Trefiletti, M. C. Sacchi, F. Forlini, G. C. Alfonso, I. Tincul, U. M. Wahner, *Macromol. Chem. Phys*., **2004,** *205*, 383; (f) R. Quijada, J. L. Guevara, G. B. Galland, F. M. Rabagliati, J. M. Lopez-Majada, *Polymer,* **2005**, *46*, 1567; (g) K. Jeon, H. Palza, R. Quijada, R. G. Alamo, *Polymer,* **2009**, *50*, 832.

69. I. Tincul, D. Joubert, R. Sanderson, *Macromol. Symp*., **2007**, *260*, 58.

70. www.sasol.com

71. I. Tincul, J. Smith, P. van Zyl, *Macromol. Symp*., **2003**, *193*, 13.

72. G. Leone, S. Losio, D. Piovani, A. Sommazzi, G. Ricci, *Polym. Chem.*, **2012**, *3*, 1987.

73. S. Losio, G. Leone, F. Bertini, G. Ricci, M. C. Sacchi, A. C. Boccia, *Polym. Chem.*, **2014**, *5*, 2065.

74. S. Losio, F. Forlini, A. C. Boccia, M. C. Sacchi, *Macromolucules*, **2011**, *44*, 3276.

75. C. J. Carman, C. E. Wilkes, *Rubber Chem. Technol.,* **1971**, *44*, 781.

76. D. E. Dorman, E. P. Otocka, F. A. Bovey, *Macromolecules*, **1972**, *5*, 574.

77. J. C. Randall, *J. Macromol. Sci., Rev. Macromol. Chem. Phys.,* **1989**, *C29* (2&3), 201.

78. A. Carvill, L. Zetta, G. Zannoni, M. C. Sacchi, *Macromolecules*, **1998**, *31*, 3783.

79. A. Carvill, I. Tritto, P. Locatelli, M. C. Sacchi, *Macromolecules*, **1997**, *30*, 7056.

80. In the expanded spectra the less intense peaks assigned to *iso*-butenyl (15.94, 23.67, and 28.48 ppm) and 2-butenyl (10.87 and 32.24 ppm) end groups are also detectable.

81. G. Natta, P. Corradini, W. Bassi, *Rend. Fis. Acc. Lincei,* **1955**, *19*, 404.

82. H. Kusanagi, M. Takase, Y. Chatani, H. Tadokoro, *J. Polym. Sci. Polym. Phys. Ed.,* **1978**, *16*, 131.

83. C. De Rosa, *Macromolecules*, **2003**, *36*, 6087.

84. M. Takayanagi, N. J. Kawasaki, *Macromol. Sci. Phys.,* **1967**, *B1*, 741.

85. J. Ruan, A. Thierry, B. Lotz, *Polymer*, **2006**, *47*, 5478.

86. A. Nakajima, S. Hayashi, T. Taka, *Kolloid. Z. Z. Polym.,* **1969**, *233*, 869.

87. G. Charlet, G. Delmas, F. J. Revol, R. St. J. Manley, *Polymer*, **1984**, *25*, 1613.

88. G. Charlet, G. Delmas, *Polymer*, **1984**, *25*, 1619.

89. C. De Rosa, A. Borriello, V. Venditto, P. Corradini, *Macromolecules,* **1994**, *27*, 3864.

90. C. De Rosa, F. Auriemma, A. Borriello, P. Corradini, *Polymer,* **1995**, *36*, 4723.

91. R. Hasegawa, Y. Tanabe, M. Kobayashi, M. Tadokoro, A. Sawaoka, N. Kawai, *J. Polym. Sci., Polym. Phys. Ed.,* **1970**, *8*, 1073.

92. G. Charlet, G. Delmas, *Polym. Bull.*, **1982**, *6*, 367.

93. C. De Rosa, *Macromolecules,* **1999**, *32*, 935.

94. S. M. Aharoni, G. Charlet, G. Delmas, *Macromolecules,* **1981**, 14, 1390.

95. P. Stagnaro, L. Boragno, S. Losio, M. Canetti, G. C. Alfonso, M. Galimberti, F. Piemontesi, M. C. Sacchi, *Macromolecules*, **2011**, 44, 3712.

96. M. Canetti, G. Leone, G. Ricci, F. Bertini, *European Polymer Journal*, **2015**, *73*, 423.

97. G. Leone, M. Mauri, S. Losio, F. Bertini, G. Ricci, L. Porri, *Polym. Chem.,* **2014**, *5*, 3412.

98. M. C. Sacchi, S. Losio, L. Fantauzzi, P. Stagnaro, R. Utzeri, M. Galimberti, *J. Polym. Sci. Part A*, **2015**, *53*, 2575.

99. (a) S. Losio, I. Tritto, G. Zannoni, M. C. Sacchi, *Macromolecules*, **2006**, *39*, 8920; (b) S. Losio, P. Stagnaro, T. Motta, M. C. Sacchi, F. Piemontesi, M. Galimberti, *Macromolecules*, **2008**, *41*, 1104; (c) S. Losio, A. C. Boccia, M. C. Sacchi, *Macromol. Chem. Phys*., **2008**, *209*, 1115; (d) S. Losio, A. C. Boccia, L. Boggioni, M. C. Sacchi, D. R. Ferro, *Macromolecules*, **2009**, *49*, 6964; (e) I. Suarez, S. Losio, B. Coto, *Europ. Polym. J.,* **2013**, *49,* 3402;

100. M. C. Da Silva, G. B. Galland, *Polymer*, **2008**, *46*, 947.

101. (a) M. C. Sacchi, F. Forlini, S. Losio, I. Tritto, G. Costa, P. Stagnaro, I. Tincul, U. M. Wahner, *Macromol. Symp.,* **2004**, *213*, 57; (b) P. Stagnaro, L. Boragno, M. Canetti, F. Forlini, F. Azzurri, G. C. Alfonso, *Polymer*, **2009**, *50*, 5242; (c) C. De Rosa, O. R. de Ballesteros, F. Auriemma, M. R. Di Caprio, *Macromolecules*, **2012,** *45,* 2749; (d) L. Boragno, P. Stagnaro, F. Forlini, F. Azzurri, G. C. Alfonso, *Polymer*, **2013**, *54*, 1656.

102. P. Stagnaro, G. Costa, V. Trefiletti, M. Canetti, F. Forlini, G. C. Alfonso, *Macromol. Chem. Phys.*, **2004***, 207*, 2128.

103. (a) C. Descour, R. Duchateau, M. R. Mosia, G. J. M. Gruter, J. R. Severn, S. Rastogi, *Polym. Chem.,* **2011**, *2*, 2261; (b) C. Descour, T. Meijer-Vissers, T. Macko, M. Parkinson, D. Cavallo, M. van Drongelen, G. Hubner, H. Goossens, R. Duchateau, *Polymer*, **2012**, *53*, 3096.

104. (a) N. Luruli, L. C. Heinz, V. Grumel, R. Brull, H. Pasch, H. G. Raubenheimer, *Polymer*, **2006**, *47*, 56; (b) N. Luruli, T. Pijpers, R. Brull, V. Grumel, H. Pasch, V. Mathot, *J. Polym. Sci.: Pol. Phys.*, **2007**, *45*, 2956; (c) N. Luruli, V. Grumel, R. Brull, A. Du Toit, H. Pasch, A. J. Van Reenen, H. G. Raubenheimer, *J. Polym. Sci.: Pol.Chem.,* **2004**, *42*, 5121.

105. K. Kakinuki, M. Fujiki, K. Nomura, *Macromolecules*, **2009**, *42*, 4585.

2.

Experimental part

2.1 General remarks

All experiments involving air-sensitive compounds were carried out under nitrogen with rigorous exclusion of oxygen and moisture. Manipulations were performed in flamed or oven-stored Schlenk-type glassware using high-vacuum lines (10^{-6} Torr), standard Schlenk-line and glove-box techniques ($O_2 < 2$ ppm).

2.2 Reagents

Gases - Nitrogen, ethylene (E) and propylene (P), supplied by Air-Liquide, were purified at atmospheric pressure by fluxing through columns of BTS-catalysts, $CaCl_2$, and finally molecular sieves 4 Å 4-8 mesh. Ethylene concentration in toluene was calculated according to Henry's law:

$$C_E = P_E H_0 e^{\frac{\Delta H_L}{RT}} \qquad (1)$$

Where C_E, P_E, H_0, ΔH_L, R, and T are: ethylene concentration (mol L^{-1}), ethylene pressure (atm), Henry coefficient (0.00175 mol L^{-1} atm^{-1}), ethylene solvation enthalpy in toluene (2569 cal mol^{-1}), universal gas constant (1.989 cal mol^{-1} K^{-1}), and temperature (K), respectively.
Obviously, Henry coefficient is different for each kind of gas, and also the enthalpy of solvatation is characteristic for each gas in each solvent.
For what concern propylene we have:

$$C_P = P_P H_0 e^{\frac{\Delta H_L}{RT}} \qquad (2)$$

Where C_P, P_P, H_0, ΔH_L, R, and T are: propylene concentration (mol L^{-1}), propylene pressure (atm), Henry coefficient (0.0072 mol L^{-1} atm^{-1}), propylene solvation enthalpy in toluene (3295.6 cal mol^{-1}), universal gas constant (1.989 cal mol^{-1} K^{-1}), and temperature (K), respectively.

Toluene - (Sigma-Aldrich). Each bottle was first dried with anhydrous $CaCl_2$ and then freshly distilled on sodium under nitrogen atmosphere, in a special apparatus specifically planned for solvent distillation.

1-pentene - (Aldrich, $\geq$ 99% pure) was refluxed over $LiAlH_4$, then distilled trap-to-trap and, finally, stored under nitrogen and kept at 0°C.

4-methyl-1-pentene - (Aldrich, $\geq$ 99% pure) was refluxed over $LiAlH_4$, then distilled trap-to-trap and, finally, stored under nitrogen and kept at 0°C.

Methylaluminoxane (MAO) - (Sigma-Aldrich) was used after removing all volatiles and drying the resulting powder at 60 °C for 3-4 h under reduced pressure (0.1 mmHg), in order to improve its storage stability. After the drying procedure, the powder was stored in the glove-box.

1,2-Dideutero-1,1,2,2-tetrachloroethane - ($C_2D_2Cl_4$) was purchased from Cambridge Isotope Laboratories and used without further purification.

Catalysts - C_2-symmetric metallocenes: *rac*-Et(IndH_4)_2ZrCl_2 (EBTHI) was provided by Basell Polyolefine Italia; *rac*-Me_2Si(2-MeBenzInd)_2ZrCl_2 (MBI) was donated by Targor and *rac*-CH_2(3-*t*BuInd)_2ZrCl_2 (TBI) was kindly donated by L. Resconi.

2.3 General procedures

2.3.1 Tipical polymerization procedure

The copolymerizations were performed at 50 °C, in a 250 mL glass reactor equipped with a magnetic stirrer according to the following general procedure: 100 mL of anhydrous toluene, the proper amounts of comonomer and MAO were added in the said order. After thermal equilibration of the reactor system, ethylene or propylene was continuously added until saturation. The polymerization was typically started by adding 2 μmol of the metallocene to the mixture via syringe. A small amount of MAO (10 wt% of the total) is added to the metallocene to preactivated it. The final Al/Zr molar ratio was in the range between 1200 and 3000, depending on the experiment. The pressure of ethylene or propylene was kept constant at 1.08 bar for all the experiments. The copolymerization was terminated after 15 min by adding a small amount of ethanol and dilute hydrochloric acid, and polymers were precipitated by addition of the whole reaction mixture to ethanol (1000 mL) to which concentrated hydrochloric acid (5 mL) had been added. The copolymer samples were collected by filtration and dried under vacuum at 70 °C.

2.4 Characterizations

The resulting polymers were characterized by means of ^{13}C-NMR to evaluate the monomer content and the comonomer sequences distribution along the polymer chain. Thermal properties (T_g, T_m, T_c, ΔH_m, ΔH_c) were examined by DSC analysis, molar masses (M_w) and molar mass distribution (M_w/M_n) by SEC measurements. Room temperature wide-angle X-ray diffraction (WAXD) measurements were carried out on as polymerized samples. Interactive liquid chromatography (HT-HPLC) was applied to the separation of a series of copolymers according to their chemical compositions.

2.4.1 Nuclear magnetic resonance analysis (NMR)

For ^{13}C NMR, about 100 mg of copolymer was dissolved in $C_2D_2Cl_4$ in a 10 mm tube. HDMS (hexamethyldisiloxane) was used as internal chemical shift reference. The spectra were recorded on a Bruker NMR AVANCE 400 Spectrometer equipped with a SEX 10 mm probe with automatic matching and tuning, operating at 100.58 MHz (^{13}C) in the PFT mode working at 103 °C. The applied conditions were the following: 10 mm probe, 14.30 μs as 90° pulse angle; 64 K data points; acquisition time 5.56 s; relaxation delay 20 s; 3−4 K transient. Proton broad-band decoupling was achieved with a 1D sequence using bi_waltz_16_32 power-gated decoupling. ^{13}C DEPT NMR experiments were performed. In this case, the spectra were measured with composite pulse decoupling using the sequence τ_1-90 °-τ_2-180 °, 90°-τ_2-135 °, 180 °-τ_2-CPD-acquire, with delays τ_1 of 5 s, and τ_2 of 3.8 ms and 90° pulse widths of 14.3 and 28.1 ms for ^{13}C and ^{1}H, respectively.

2.4.2 Differential scanning calorimetry measurements (DSC)

Measurements of the synthesized copolymers was investigated on as-polymerized samples by differential scanning calorimetry (DSC) carried out on a Mettler DSC 821^e instrument. Heating curves were recorded from 0 up to 250 °C at a scanning rate of 10 °C/min, under N_2 (40 mL/min).

2.4.3 Size exclusion chromatography (SEC)

The weight average molar mass (M_w) and the molar mass distribution (M_w/M_n) were obtained by a high temperature Waters GPCV2000 size exclusion chromatography (SEC) system using two online detectors: a differential viscometer and a refractometer. The experimental conditions consisted of three PL Gel Olexis columns, *o*-DCB as the mobile phase, 0.8 mL×min^{-1} flow rate, and 145 °C temperature. The calibration of the SEC system was constructed using eighteen narrow M_w/M_n polystyrene standards with molar masses ranging from 162 to 5.6×10^6 g×mol^{-1}. For SEC analysis, about 12 mg of polymer was dissolved in 5 mL of *o*-DCB with 0.05% of BHT as antioxidant.

2.4.4 Wide-angle X-ray diffraction measurements (WAXD)

WAXD patterns at room temperature of P/Y copolymers were carried out with a Siemens diffractometer model D-500 equipped with a Siemens FK 60-10, 2000 W Cu tube (Cu Kα radiation, $\lambda = 0.154$ nm) and reflections were collected in the 2θ range between 5 and 35°.

2.4.5 High Temperature HPLC (HT-HPLC)

Instrumentation

All measurements were carried out in a high-temperature chromatograph PL-GPC 210 (Polymer Labs, Church Stretton, England) connected to an evaporative light scattering detector (ELSD, model PL-ELS 1,000, Polymer Labs). The following parameters were used at the ELSD: gas flow rate 1.5 L/min, nebulizer temperature 160 °C, evaporator temperature 260 °C. The hot gas coming out of the ELSD, which was composed of air and a solvent in gas phase, was cooled in a cooler. In this way, contamination of atmosphere in laboratory by 1-decanol and 1,2,4-trichlorobenzene (TCB) was eliminated. A quaternary gradient pump (model Agilent 1,200 Series) was used for all measurements. The flow rate of the mobile phase was 0.8 mL/min. The characteristics of the column were as follows: 100-mm length × 4.6-mm i.d. packed with porous graphite particles with a particle diameter of 5 μm, a surface area of 120 m^2/g and a pore size of 250 Å (Hypercarb®, Thermo Scientific, Dreieich, Germany). The column was placed in the column oven and thermostated at 160 °C.

Solvents, mobile phase

1-Decanol, 1-octanol and TCB (VWR, Darmstadt, Germany) were used as the mobile phases and to form a linear gradient 1-decanol/TCB. The composition of the mobile phase was changed in 10 min from 0% to 100% of TCB subsequently; pure TCB was pumped for ten additional minutes. A linear gradient from 100% to 0% of TCB followed in 2 min. Finally, the column was purged for 20 min with pure 1-decanol with the aim of reestablishing adsorption equilibrium between 1-decanol and the sorbent.

Polymer samples

The polymers analysed were first dissolved in 1-decanol at 160 °C at a concentration of about 1–3 mg/mL. The time of dissolution for the samples varied between 60 and 120 min. It was assumed that a polymer sample is completely dissolved when a sample solution is transparent and does not cause a sudden increase of pressure after its injection into the column. Of each sample solution, 13 μL was injected in the column. Linear PE standards with peak molar masses from 2 to 126 kg/mol were obtained from Polymer Standards Service GmbH, Mainz, Germany.

2.5 4-methyl-1-pentene content in propylene based copolymers

To obtain the 4-methyl-1-pentene (Y) content of propylene/4-methyl-1-pentene (P/Y) copolymers from the observed integrals of ^{13}C NMR spectra, a procedure starting from the assignment of the different peaks has been set up.

This procedure is necessary since, in the spectrum, a few sequences belonging to $\alpha\alpha$-methylene of propylene and those of the methylenes of the comonomer branch, falling in the spectral region between 44.48 and 43.89 ppm, partially overlap as well as the signals of the different compositional and stereo-sequences of the methyl of propene in the region between 19.67 and 17.54 ppm.

The analysis of the spectra of the copolymers provides a certain number of peak integrals, each peak corresponding to one or more signals. For each peak, on the basis of the assumption that the area of a signal is proportional to the population of the carbons generating that signal, we wrote a linear equation describing the observed (normalized) integral as a function of the unknown molar fractions. For each copolymer composition, a set of linear equations, whose variables were chosen among the molar fractions, was generated. A number of stoichiometric constraints reduced the number of independent variables.

a) Determination of the set of linear equations

The independent variables v_i are so chosen as to limit the microstructural description at a given level of complexity (e.g. the triad level): the dependent variables do not include independent variables of higher level in their expression.

The variables are listed in the order of growing complexity level and independent variables are in boldface.

- $f(\mathbf{Y}) = \underline{v_1}$
- $f(P) = \underline{1-v_1}$

where $f(Y) + f(P) = 1$

At the dyad level:

- $f(\mathbf{PY}) = v_2$
- $f(YY) = f(Y)- \frac{1}{2} f(\mathbf{PY}) = \underline{v_1-\frac{1}{2}v_2}$
- $f(PP) = 1-f(Y)- \frac{1}{2} f(\mathbf{PY}) = \underline{1-v_1-\frac{1}{2}v_2}$

At the triad level:

- $f(\mathbf{PYP}) = \underline{v_3}$
- $f(\mathbf{YPY}) = \underline{v_4}$
- $f(YPP) = f(YP)- 2f(\mathbf{YPY}) = \underline{v_2-2v_4}$

- $f(PPP) = f(PP) - \frac{1}{2}f(\mathbf{YPP}) = \underline{1 - v_1 - v_{2} + v_4}$

- $f(PYY) = f(PY) - 2f(\mathbf{PYP}) = \underline{v_2 - 2v_3}$

- $f(YYY) = f(YY) - \frac{1}{2}f(\mathbf{YYP}) = \underline{v_1 - v_{2} + v_3}$

At the tetrad level:

- $f(\mathbf{PYYP}) = \underline{v_5}$

- $f(\mathbf{YPYP}) = \underline{v_6}$

- $f(\mathbf{YPPY}) = \underline{v_7}$

- $f(YYYY) = f(YYY) - \frac{1}{2}f(YYYP) = \underline{v_1 - 3/2v_2 + 2v_3 + v_5}$

- $f(YYYP) = f(PYY) - 2f(\mathbf{PYYP}) = \underline{v_2 - 2v_3 - 2v_5}$

- $f(YYPY) = f(PYY) - f(\mathbf{YYPP}) = \underline{2v_4 - v_6}$

- $f(YYPP) = f(\mathbf{PYPY}) + f(PY) - 2f(\mathbf{YPY}) - 2f(\mathbf{PYP}) = \underline{v_2 - 2v_4 - 2v_3 + v_6}$

- $f(PYPP) = f(PPY) - f(YYPP) = \underline{2v_3 - v_6}$

- $f(YPPP) = f(PPY) - 2f(\mathbf{YPPY}) = \underline{v_2 - 2v_4 - 2v_7}$

- $f(PPPP) = f(PPP) - \frac{1}{2}f(\mathbf{YPPP}) = \underline{1 - v_1 - 3/2v_2 + 2v_4 + v_7}$

However, although most tetrads have been safely assigned, only part of the information contained in the spectra can be fully exploited, due to the overlap of several peaks. Thus, according to the above relationships:

At 41.90 ppm, $f(PPYP) + f(PPYY) = 2v_3 - v_6 + v_2 - 2v_4 - 2v_3 + v_6 = \underline{v_2 - 2v_4}$

In the region spanning from 42.49 to 42.28 ppm, $f(PYPY) + f(YYPY) = v_6 + 2v_4 - v_6 = \underline{2v_4}$

In the region spanning from 43.89 to 44.58 ppm, $f(PPPP) + f(PPPY) + f(PYP) + f(PYY) = 1 - v_1 - 3/2v_2 + 2v_4 + v_7 + v_2 - 2v_4 - 2v_7 + v_3 + v_2 - 2v_3 = \underline{1 - v_1 - \frac{1}{2}v_2 - v_7}$

A full description at the triad level is possible along with only a partial description at the tetrad level since the two pairs of tetrads P$\underline{YY}$X (X means P or Y) and Y$\underline{PY}$X cannot be distinguished. This explain the absence of the YY and PY centred tetrads whose linear equations are strictly connected to the P$\underline{YY}$P and Y$\underline{PY}$P molar fractions, (see v_5 and v_6 variables).

The comonomer content (v_1) is obtained by the least-squares fitting of the set of equations.

It is worth noting that, although most tetrads have been safely assigned, only part of the information contained in the spectra can be fully exploited, due to the overlap of several peaks. Indeed, the fact that the two pairs of tetrads PYYX and YPYX cannot be distinguished explains the absence of the YY and PY centred tetrads whose linear equations are strictly connected to the PYYP and YPYP molar fractions. This fact results in a limited estimate of the compositional tetrads.

2.6 Statistical approach for the determination of reactivity ratio

The triad level microstructure of the P/Y copolymers were analyzed according to the first- order and the second-order Markov statistical models by means of the procedure below described.

First-order Markov

It is known that the Markovian probabilities $P(M_1/Mt-M_2)$ (probability of monomer M_1 insertion in a metal-monomer M_2 bond) and $P(M_2/Mt-M_1)$ (probability of M_2 insertion in a metal-M_1 bond) depend on the copolymerization bath composition f (mole ratio between M_1 and M_2) and on the reactivity ratios according to the following equations:

$$p(M_2/Mt - M_1) = \frac{1}{r_1 f + 1}$$

$$p(M_1/Mt - M_2) = \frac{f}{f + r_2}$$

The combination of these two probability parameters generates the theoretical Markovian expressions for comonomer sequences (diads, triads or longer ones).

The two probability parameters depend only on the polymerization bath composition, as the reactivity ratios r_1 and r_2 are expected to be constant with a given catalytic system and given polymerization conditions (e.g. temperature, solvent, and total monomer pressure). Therefore, the reactivity ratios r_1 and r_2 can be treated as the parameters to be optimized through the fitting of the experimental diad or triad distributions.

The fitting procedure can be described as follows.
(1) For each copolymerization bath composition f_i, two probability parameters $P(M_1/Mt-M_2)_i$ e $P(M_2/Mt-M_1)_i$ are evaluated using two initial values for r_1 and r_2
(2) The related diad or triad distributions are then calculated from the following expressions using the starting parameters $p(M_1/Mt-M_2)_i$ e $p(M_2/Mt-M_1)_i$ for a sake of simplicity M_1=E and M_2=P.

$PPP_{calc} = NP(P/M\text{-}E)[1 - P(E/M\text{-}P)]^2$
$PPE_{calc} = 2NP(P/M\text{-}E)P(E/M\text{-}P)[1 - P(E/M\text{-}P)]$
$EPE_{calc} = NP(P/M\text{-}E)P(E/M\text{-}P)^2$
$PEP_{calc} = NP(P/M\text{-}E)^2P(E/M\text{-}P)$
$PEE_{calc}= 2NP(P/M\text{-}E)P(E/M\text{-}P)[1 - P(P/M\text{-}E)]$

$$\text{EEE}_{\text{calc}} = NP(\text{E/M-P})[1 - P(\text{P/M-E})]^2$$
with $N = 1/[P(\text{P/M-E}) + P(\text{E/M-P})]$

(3) The sum of the squares of the deviations between experimental and calculated distribution (triads, for example) for each copolymer sample is evaluated as

$$\text{LS}_i = (\text{PPP}_{\text{exp}} - \text{PPP}_{\text{calc}})^2 + (\text{PPE}_{\text{exp}} - \text{PPE}_{\text{calc}})^2 + (\text{EPE}_{\text{exp}} - \text{EPE}_{\text{calc}})^2 + (\text{PEP}_{\text{exp}} - \text{PEP}_{\text{calc}})^2 + (\text{PEE}_{\text{exp}} - \text{PEE}_{\text{calc}})^2 + (\text{EEE}_{\text{exp}} - \text{EEE}_{\text{calc}})^2$$

(4) All the values of LS*i* are collected in the summation over all copolymer samples, as follows:

$$\text{LS}_{\text{tot}} = \sum\nolimits_i \text{LS}_i$$

(5) LS_{tot} is minimized by changing the values of r_1 and r_2.
This calculation was done in the present work using the Solver macro in the MS Excel program

Second-order Markov

The second-order Markovian model describes a copolymerization when the insertion of a comonomer is influenced by both the two last inserted units (penultimate effect). As a consequence of the adoption of the second-order Markovian model, the following reactivity ratios can be derived:

$r_{11} = k_{111}/k_{112}$
$r_{21} = k_{211}/k_{212}$
$r_{22} = k_{222}/k_{221}$
$r_{12} = k_{122}/k_{121}$

Probability parameters for the insertion of a comonomer (either M_1 or M_2) into a growing chain described taking into account the two last inserted comonomer units (i.e. either Mt-M_1M_1 or Mt-M_1M_2 or Mt-M_2M_1 or Mt-M_2M_2) were calculated from the experimental reactivity ratios (r_{11}, r_{12}, r_{21} and r_{22}) and from the polymerization bath composition f, using the following expressions, where for simplicity M_1=E and M_2= P

$a = p(\text{P|Mt-EE}) = 1 / (r_{11} \cdot f + 1)$
$(1-a) = p(\text{E|Mt-EE}) = r_{11} \cdot f / (r_{11} \cdot f + 1)$
$b = p(\text{E|Mt PE}) = f / (r_{12} + f)$
$(1-b) = p(\text{P|Mt-PE}) = r_{12} / (r_{12} + f)$
$c = p(\text{P|Mt-EP}) = 1 / (r_{21} \cdot f + 1)$
$(1-c) = p(\text{E|Mt-EP}) = r_{21} \cdot f / (r_{21} \cdot f + 1)$
$d = p(\text{E|Mt-PP}) = f / (r_{22} + f)$
$(1-d) = p(\text{P|Mt-PP}) = r_{22} / (r_{22} + f)$
It should be noted that only four parameters are independent.

The diad compositions (diad probabilities) were evaluated from the probability parameters:

$p(EE) = [p(E|Mt\text{-}PP)]\cdot[p(E|Mt\text{-}EP)]/S$

$p(PE) = [p(P|Mt\text{-}EE)]\cdot[p(E|Mt\text{-}PP)]/S$

$p(EP) = [p(P|Mt\text{-}EE)]\cdot[p(E|Mt\text{-}PP)]/S$

$p(PP) = [p(P|Mt\text{ -}EE)]\cdot[p(P|Mt\text{-}PE)]/S$

where S is a normalization factor defined as:

$S = [p(E|Mt\text{-}PP)]\cdot[p(E|Mt\text{-}EP)]+2\cdot[p(P|Mt\text{-}EE)]\cdot[p(E|Mt\text{-}PP)]+[p(P|Mt\text{-}PE)]\cdot[p(P|Mt\text{-}EE)]$

The triad composition was evaluated according to the following equations:

$PPP_{calc} = p(PP)\cdot(1\text{-}d)$

$PPE_{calc} = p(PP)\cdot d + p(PE)\cdot(1\text{-}b)$

$EPE_{calc} = p(PE)\cdot b$

$PEP_{calc} = p(EP)\cdot c$

$PEE_{calc} = p(EE)\cdot a+p(EP)\cdot(1\text{-}c)$

$EEE_{calc} = p(EE)\cdot(1\text{-}a)$

(3) The sum of the squares of the deviations between experimental and calculated distribution (triads, for example) for each copolymer sample is evaluated as

$LS_i = (PPP_{exp} \text{ - } PPP_{calc})^2 + (PPE_{exp} \text{ - } PPE_{calc})^2 + (EPE_{exp} \text{ - } EPE_{calc})^2 + (PEP_{exp} \text{ - } PEP_{calc})^2 +(PEE_{exp} \text{ - } PEE_{calc})^2 + (EEE_{exp} \text{ - } EEE_{calc})^2$

(4) All the values of LS_i are collected in the summation over all copolymer samples, as follows:

$$LS_{tot} =\sum_i LS_i$$

(5) LS_{tot} is minimized by changing the values of the four reactivity ratio $r_{11,}$ $r_{12,}$ r_{21} and r_{22}. This calculation was done in the present work using the Solver macro in the MS Excel program.

3.

Results

## 3.1 Ethylene/1-pentene copolymers

Ethylene/1-pentene (E/Pe) copolymers have been synthetized in a wide compositional range with two homogeneous metallocenes, *rac*-ethylenebis(tetrahydroindenyl)zirconium dichloride, *rac*-Et(IndH$_4$)$_2$ZrCl$_2$ (EBTHI) and *rac*-methylenebis(3-tert-butylindenyl)zirconium dichloride, *rac*-H$_2$C-(3-^{t}BuInd)$_2$ZrCl$_2$ (TBI) with MAO as cocatalyst and toluene as solvent. EBTHI is the prototypical moderately isospecific metallocene used to prepare the first prevailingly isotactic polypropylene (mmmm = 91.5%) from a single center catalyst.[1] EBTHI promotes ethylene/propylene copolymerizations with a relatively low reactivity ratio product ($r_1r_2 = 0.49$).[2] TBI is able to prepare a highly regio- and stereoregular polypropylene,[3] and promotes ethylene/propylene copolymerization with a high reactivity ratio product ($r_1r_2 = 1.8$).

A complete microstructural characterization has been conducted by ^{13}C NMR in order to check chemical shifts previously assigned and to accomplish all possible new sequence assignments.

3.1.1 Synthesis of ethylene/1-pentene copolymers

The copolymerizations were carried out at 45°C with the organometallic complexes shown in Figure 3.1.1, in combination with methylalumoxane (MAO), in toluene at an atmospheric pressure of ethylene (Table 3.1.1).

Different feedstock comonomers composition, *i.e.*, [Pe]/[E] from 0.8 to 13.7, (Pe = 1-pentene; E = ethylene) were investigated.
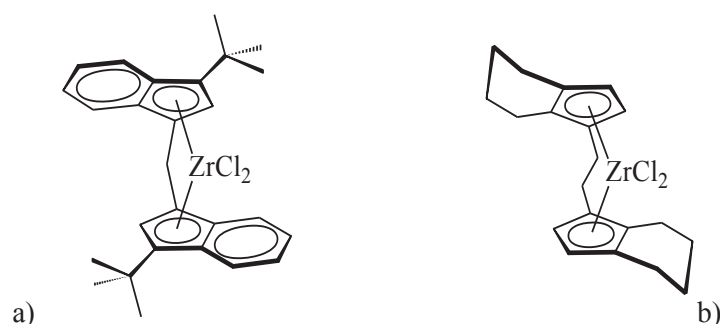
Figure 3.1.1 C$_2$ symmetric metallocenes under investigation: (a) *rac*-H$_2$C-(3 ^{t}BuInd)$_2$ZrCl$_2$ (TBI) (b) *rac*-Et(IndH$_4$)$_2$ZrCl$_2$ (EBTHI).

In Table 3.1.1, data on E/Pe copolymerizations and on the obtained copolymers are reported. The wide range of E/Pe ratios in the polymerization bath allows the preparation of copolymers with a 1-pentene content ranging from about 5 to about 55 mol %. Mw/Mn values close to 2 were determined for samples prepared with any of the catalytic system and for different chemical compositions, as clear indication of the single center nature of the catalytic systems.

Table 3.1.1 Ethylene/1-pentene copolymerization with different metallocenes and MAO as the catalytic system[a]

Catalyst	Run	Pe/E[b] (mol/mol)	t (min)	[catalyst] μmol	Al/Zr (mol/mol)	Yield (g)	Activity[c]	Pe %[d] (mol)	Conversion %	Mw[e] (x10^3)	Mw/Mn[e]
TBI	1	0.8	4	1.0	3000	0.461	6915	4.27	9.5	213	2.3
	2	1.5	5	1.0	3000	0.373	4476	9.33	7.0	95	2.2
	3	2.2	5	2.0	3000	0.476	2856	15.02	9.4	44	2.3
	4	4.0	15	1.0	3000	0.137	548	25.04	2.2	41	2.2
	5	5.9	20	1.0	3000	0.203	609	27.08	2.4	47	2.3
	6	8.7	8	1.0	3000	0.481	3608	33.47	4.4	40	2.1
	7	13.7	30	1.0	3000	0.637	1274	51.71	4.8	29	2.0
EBTHI	8	0.8	3	1.0	3000	0.461	4920	6.96	7.3	127	3.0
	9	1.5	3	1.0	3000	0.327	6540	13.07	8.5	88	2.6
	10	2.2	3	1.0	3000	0.262	5240	22.65	7.4	59	2.2
	11	4.0	5	2.0	3000	0.503	3018	36.20	10.5	17	2.3
	12	5.9	5	1.0	3000	0.543	6516	39.38	8.1	20	2.2
	13	8.7	15	1.0	3000	0.256	1024	47.89	2.9	21	2.0
	14	13.7	10	1.0	3000	0.675	4050	54.51	5.3	27	2.2

[a] Polymerization conditions: total volume = 100 mL, T = 45 °C, P = 1.08 atm, Al/Zr = 3000 (mol/mol). [b] Pe/E feed ratio in liquid phase. [c] mg$_{pol}$/(mmol$_{Zr}$ h). [d] From ^{13}C NMR analysis. [e] Molar mass and polydispersity index from SEC analysis.

Copolymerization conditions were optimized to obtain copolymer samples with homogeneous comonomer composition, suitable for microstructure investigation. This implies that rigorous comments on catalytic activities can not be possible, as the polymerization conditions were not exactly reproduced.

To maintain nearly constant the comonomer concentration in solution throughout the whole course of the reaction, conversion of both comonomers was kept in most cases below 2% and had

a maximum value of 10%, following an experimental approach already reported.[2c] It is worth underlining that the use of a good solvent as toluene, the low monomer conversion, and the consequent low polymer concentration in the polymerization medium allowed us to assume that a homogeneous polymerization solution was obtained and that the comonomer concentration on the catalytic center was reasonably constant.

The general structure and carbon labelling of an ethylene/1-pentene copolymer chain are sketched in Figure 3.1.2.
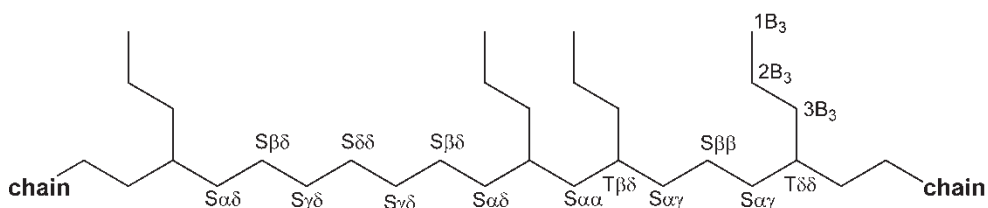
Figure 3.1.2 General structure and carbon labelling of an ethylene/1-pentene copolymer.

The carbons were labelled according to the nomenclature first defined by Carman and modified by Dorman and Randall, where P, S, and T refer to the primary (methyl), secondary (methylene), and tertiary (methine) carbons of the main chain, respectively.[4-6] Methylene carbons along the backbone were identified by a pair of Greek letters to indicate the distance to branches in either directions. Methyl and methylene carbons in the side chain were designated by the symbols $1B_3$, $2B_3$, and $3B_3$ according to Galland.[7] In the following, ''E'' and ''P'' indicate the ethylene and 1-pentene comonomer units, respectively, in the descriptions of monomer sequence distributions. The extreme sensitivity of ^{13}C NMR chemical shifts to variations in microstructural environment of the copolymer backbone is demonstrated by comparing the spectra obtained at 103 °C of ethylene/1-pentene copolymers with four different comonomer contents (Figure 3.1.3).
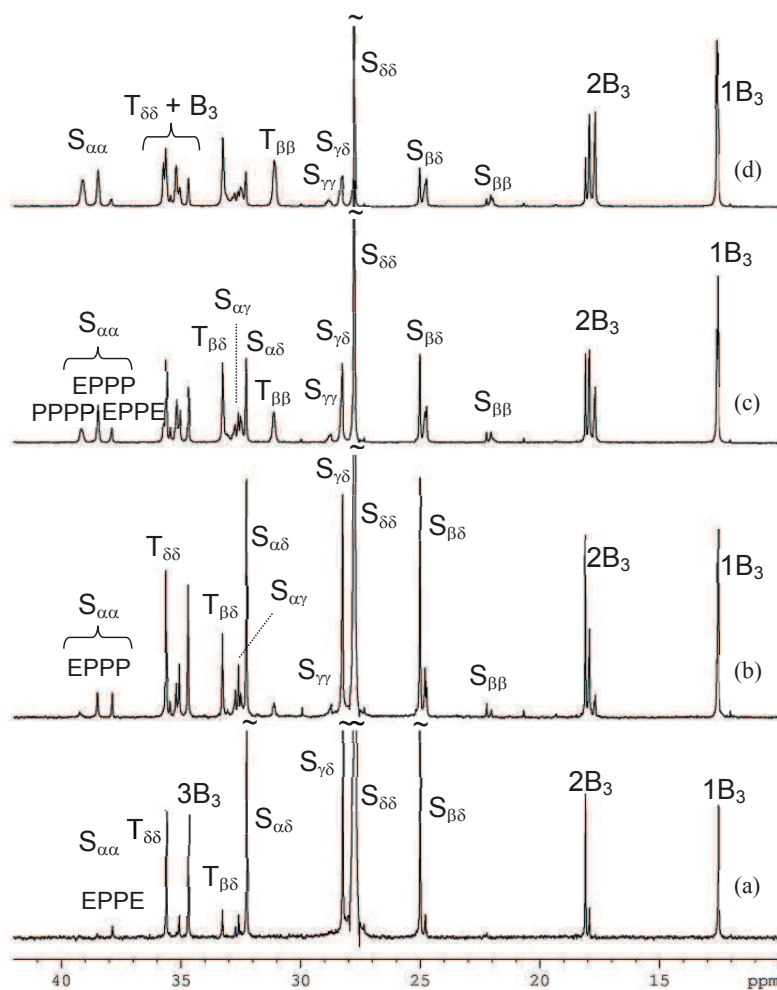
Figure 3.1.3 ^{13}C NMR spectra of E/Pe copolymers from *rac*-H₂C-(3-ᵗBuInd)₂ZrCl₂ with different comonomer content: (a) 4.27 mol% (run 1 in Table 3.1.1), (b) 15.02 mol% (run 3 in Table 3.1.1), (c) 33.47 mol% (run 6 in Table 3.1.1), (d) 51.71 mol% (run 7 in Table 3.1.1).

The ^{13}C NMR spectra of Figure 3.1.3 show many new features in terms of well-resolved resonances compared to previously reported low field data.[8] The better resolution and dispersion will provide evidence on the presence of higher *n*-ad sequences such as tetrad, pentad, hexad, etc. Most of the observed resonances in the ^{13}C NMR spectra are those from methylene carbons; however, the DEPT experiment helps to identify the resonances from the few unique methine and methyl carbons (Figure 3.1.4)
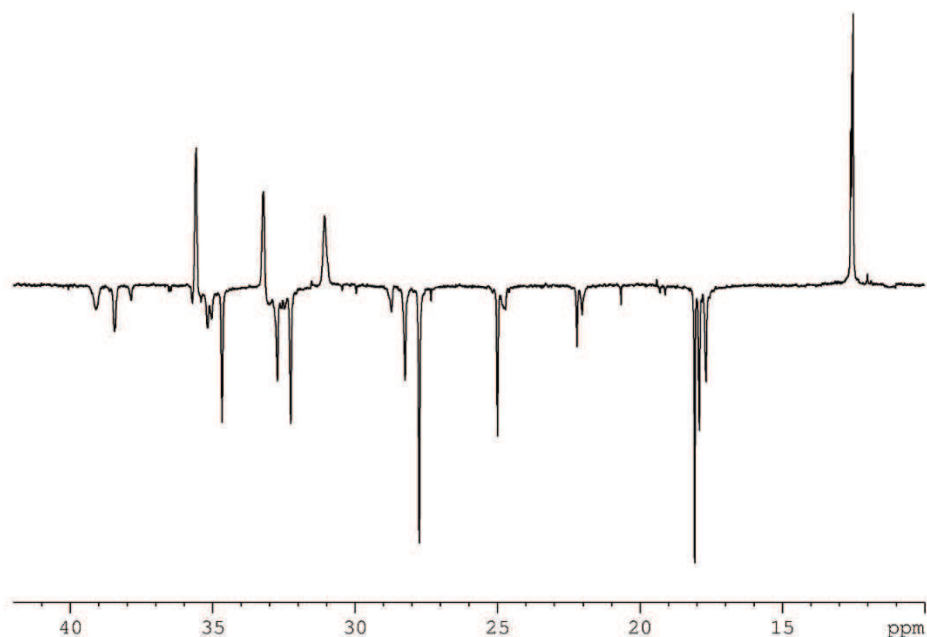
Figure 3.1.4 ^{13}C NMR DEPT spectrum of E/Pe copolymer with 33.47 mol% (run 6 in Table 3.1.1).

**Main chain region.** In the ^{13}C NMR spectra, CH and CH_2 carbons from both the main chain and from the branch are found in the 17.0-40.0 ppm range, while the resonances of CH_3 group appear at 12.51 ppm. The low intensity resonances at 12.02, 20.68, and 29.90 ppm from saturated chain ends are observed in copolymers from EBTHI, however, these signals are not detected in the spectra of copolymer from TBI.[9]

In the spectrum of Figure 3.1.3a, the main chain resonances related to isolated 1-pentene sequences appear at the following chemical shifts: $S_{\beta\delta}$ at 24.99 ppm, $S_{\gamma\delta}$ at 28.22 ppm, $S_{\alpha\delta}$ at 32.35 ppm, and $T_{\delta\delta}$ at 35.62 ppm.

When this spectrum is compared to those of copolymers at higher 1-pentene content, many new resonances are clearly observed. Neighbouring monomer units produce a large number of additional possible structures, due to the higher probability of forming triad monomer sequences containing two and three 1-pentene units.

In the 37.50-40.00 ppm region of Figure 3.1.3b, 3.1.3c and 3.1.3d, several methylene resonances from long 1-pentene sequences (e.g. $\alpha\alpha_{PPPP}$, $\alpha\alpha_{PPPE}$, and $\alpha\alpha_{EPPE}$ methylenes) can be evidently pointed out. In the ^{13}C NMR spectrum of Figure 3.1.3a, only a single $\alpha\alpha$-methylene resonance at 37.85 ppm is observed and assigned to EPPE sequence, due to the low comonomer content (4.98 mol%). It is worth noting that, as already observed for ethylene/4-methyl-1-pentene copolymers, *rac*-H_2C-(3-[t]BuInd)$_2$ZrCl$_2$ catalyst favours the formation of comonomer centred tetrad with a 1-pentene content as low as 4.98 mol%.[2c,10a-c] The capability of this catalyst of giving comonomer dyads is confirmed by the presence of a narrow signal assigned to the $T_{\beta\delta}$ methine carbon which is well detectable at 33.25 ppm.

The methylene resonances of ββ carbons are expected to fall in the range 21.50-22.50 ppm. These signals are detected for EPEPE, EPEPP, and PPEPP sequences, respectively, as well as observed for ethylene/higher 1-olefins copolymers, such as 1-hexene and 1-octene.[11] The three centred PEP pentads are assigned although only EPEPE pentad can be easily evaluated due to the partial overlapping of PPEPE and PPEPP pentads (Figure 3.1.5c).
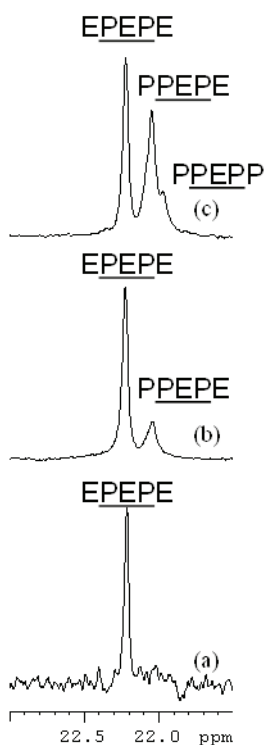
Figure 3.1.5 Expanded plot of ββ methylene region of ethylene/1-pentene copolymers from EBTHI with different comonomer content: (a) 7.08 mol% (run 8 in Table 3.1.1), (b) 13.08 mol% (run 9 in Table 3.1.1), (c) 55.21 mol% (run 14 in Table 3.1.1).

Figure 3.1.6 shows the expanded regions of $S_{\beta\delta}$ and $S_{\alpha\delta}$ resonances of methylene carbon atoms at increasing comonomer content. At low comonomer content, the isolated resonances belonging to $\alpha\delta^+$ and $\beta\delta^+$ methylene carbons appear at 32.25 and 24.99 ppm, respectively. At higher field (24.75 ppm), the presence of a small resonances, that was assigned to the EPEEPE sequence, can be observed. Actually, EPEEPE and EPEEPP sequences are indistinguishable, thus we indicate them as EPEEPZ. From now on, Z means ethylene or 1-pentene in all pair of sequences which are indistinguishable. In the corresponding spectrum of the region spanning from 32 to 34 ppm the peak at 32.58 pm is safely assigned to the same sequence by comparison with the areas of the signals. The peak at 32.71 ppm is assigned to αγ methylene carbons. In Figure 3.1.6b, two other resonances appear at 32.49 and 24.67 ppm respectively, becoming more intense at increasing comonomer content. Therefore, both resonances should be related to PPEEPZ sequence.
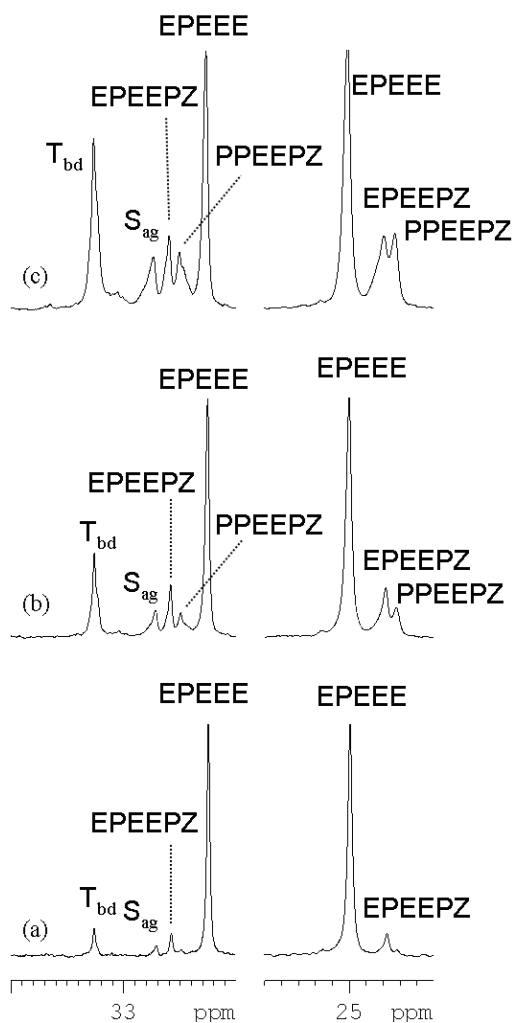
Figure 3.1.6 Expanded plot of βδ and αδ methylene region of ethylene/1-pentene copolymers from *rac*-H₂C-(3-*t*BuInd)₂ZrCl₂ with different comonomer content: (a) 4.98 mol% (run 1 in Table 3.1.1), (b) 15.34 mol% (run 3 in Table 3.1.1), and (c) 27.08 mol% (run 5 in Table 3.1.1). Z means E or P in all pair of sequences where are indistinguishable.

Side chain region. Figure 3.1.7 shows the expanded plots of the spectral regions of methylene 2B$_3$ and 3B$_3$ and of methyl 1B$_3$ carbons of the side chain at increasing comonomer content.

In the methylene region spanning from 17 to 19 ppm, at least three resonances (2B$_{EPE}$, 2B$_{PPE,}$ and 2B$_{PPP}$) are resolved in Figure 3.1.5c, while only 2B$_{EPE}$ and 2B$_{PPE}$ are observed in Figure 3.1.7a with lower 1-pentene content. The three centred triads PPP, PPE, and EPE are definitively assigned and very easily evaluated.

Similarly, resonances such as those previously attributed to 2B$_3$ can be observed for 1B$_3$. As it is apparent by inspecting the spectra of Figure 3.1.3, the methyl region is less resolved than the methylene one and consequently is less suitable for quantitative evaluation of 1-pentene centred sequences. However, by analysis of the intensity peak among the copolymers with increasing comonomer content and especially by comparison with the intensities of the more resolved signals of the corresponding 2B$_3$ region, it is possible to unequivocally assign the three resonances, as shown in Figure 3.1.7 and listed in Table 3.1.2.
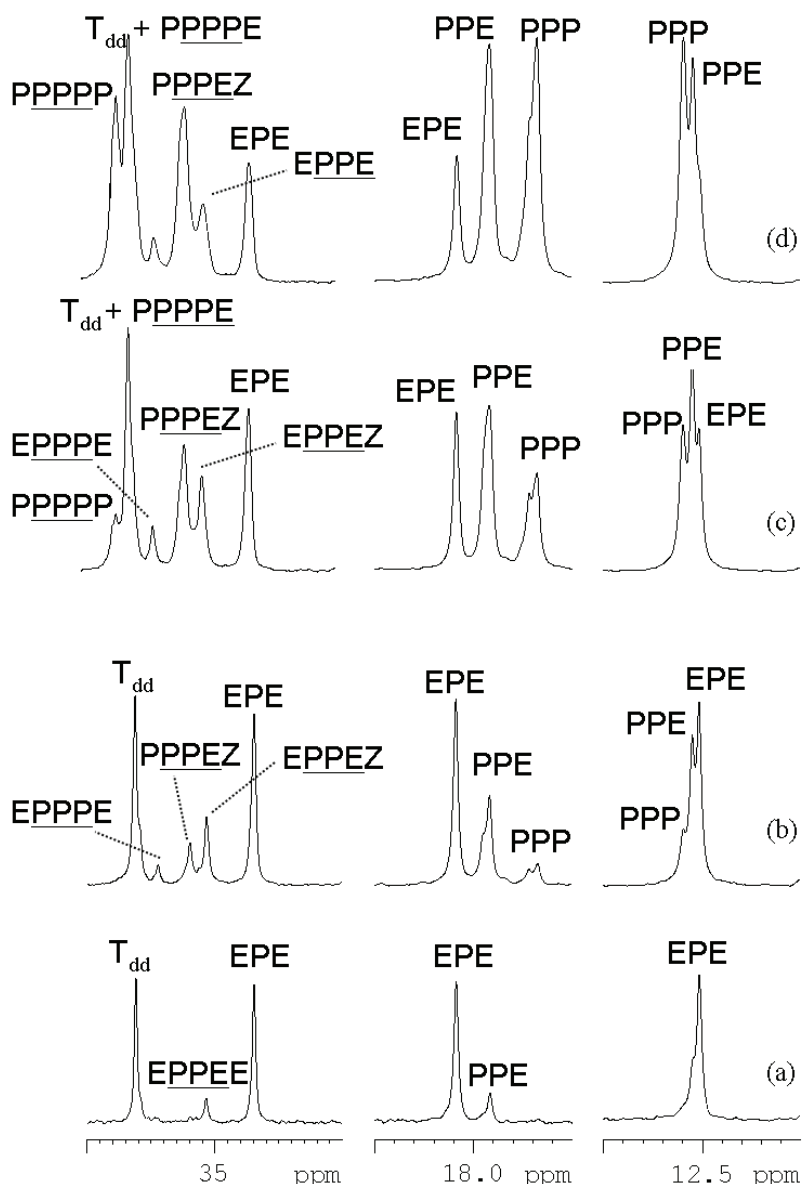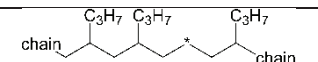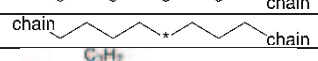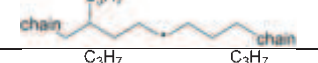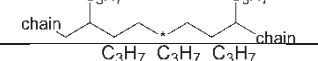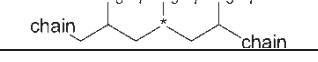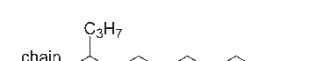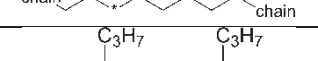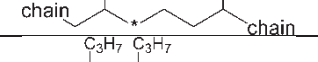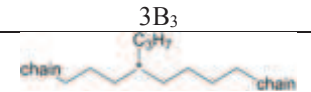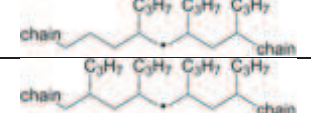
Figure 3.1.7 Expanded plot of the methylene, 3B₃ (left) and 2B₃ (middle), and of 1B₃ (right) methyl side chain region of ethylene/1-pentene copolymers with different comonomer content: (a) 4.98 mol% (run 11 in Table 3.1.1), (b) 15.34 mol% (run 3 in Table 3.1.1), (c) 33.47 mol% (run 6 in Table 3.1.1), (d) 51.71 mol% (run 7 in Table 3.1.1). Z means E or P in all pair of sequences where are indistinguishable.

The analysis of 3B₃ region is difficult due to the overlap of the Tδδ and 3B₃ resonances as detected in DEPT spectrum (Figure 3.1.4) at 35.62 ppm. Here the comparison with the corresponding spectral region relative to 2B₃ is fundamental for the assignment. At low comonomer content, three signals are visible: it is easy to locate Tδδ at 35.62 ppm and EPE triad at 34.69 ppm. The signal at 35.07 ppm cannot but be assigned to PPE triad. In particular, due to the low comonomer content, this resonances is assigned to the PPE centred pentad richest in ethylene EPPEE. Because the introduction of E on one side decreases or cancels the effect of further substitution on the same side, indeed the EPE sequence is always observed as a narrow single peak, EPPEE and EPPEP pentads are actually indistinguishable, thus we indicate them as EPPEZ. At increasing comonomer content, two other resonances appear at lower field with respect EPE triad, at 35.19

and 35.44 ppm, respectively (Figure 3.1.7b). In the corresponding spectrum of 2B$_3$ region, besides EPE resonances, two signals are detected, unequivocally assigned to PPE and PPP triad. The integrated peak area of the signal at 17.91 ppm is about the sum of the areas of resonances at 35.06 and 35.19 ppm. Therefore, both the resonances should be related to PPE sequences, thus the PPPEZ sequence is assigned at 35.19 ppm. The resonance at 35.45 ppm of similar intensity of the resonance at 17.67 ppm is assigned to EPPPE pentad. At increasing comonomer content, one new resonance appears at 35.72 ppm. At the same time, the integral of the δδ methine peak appears surprisingly higher than the necessary connected peak at 34.69 ppm, as belonging to the same EPE sequence. The higher the content, the more evident the effect. In addition, by observing the resonance intensity variation at increasing 1-pentene content in the spectra, we assign the PPPPP pentad at 35.72 ppm and the EPPPP pentad at 35.63 ppm. The complete ^{13}C chemical shift assignments are listed in Table 3.1.2. These detailed resonance assignments permit more straightforward quantitative determination of the structural details in this polymer.

Table 3.1.2 Chemical shift assignments for ethylene/1-pentene copolymers.

Chemical Structure	Carbon		Compositional Sequence	Chemical Shift (ppm)
1B$_3$	methyl	EPE		12.51
		PPE		12.55
		PPP		12.58
2B$_3$	methylene	PPP	PPP	17.67
			PPPPZ	17.72
		PPE		17.91
		EPE		18.08
	S$_{\beta\beta}$	PEP	PPEPP	21.97
			PPEPE	22.04
			EPEPE	22.22
	S$_{\beta\delta}$	PEE	PPEEPZ	24.67
			EPEEPZ	24.75
	S$_{\beta\delta}{}^+$		PEEE	24.99
	S$_{\delta\delta}$	EEE		27.73
	S$_{\gamma\delta}$	PEEE		28.22
	S$_{\gamma\gamma}$	PEEP		28.69
	T$_{\beta\beta}$	PPP		31.08
	S$_{\alpha\delta}{}^+$	PEE	PEEE	32.25
	S$_{\alpha\delta}$	PEE	PPEEPZ	32.49
			EPEEPZ	32.58
	S$_{\alpha\gamma}$	PEP		32.71–33.09
	T$_{\beta\delta}$	PPE		33.25
		EPE		34.69
		PPE	EPPEZ	35.07
			PPPEZ	35.19

			EPPPE	35.45
		PPP	EPPPP	35.58
			PPPPP	35.73
3B₃	methylene			
[structure: chain with C₃H₇]	Tδδ	EPE		35.62
[structure: chain with C₃H₇ C₃H₇]			EPPE	37.85
[structure: chain with C₃H₇ C₃H₇ C₃H₇]	Sαα	PP	EPPP	38.46
[structure: chain with C₃H₇ C₃H₇ C₃H₇ C₃H₇]			PPPP	38.97-39.13

E = ethylene, P = 1-pentene, Z means ethylene or 1-pentene in all pair of sequences which are indistinguishable.

Due to the partial overlapping of the signals coming from $T_{\delta\delta}$ and $3B_3$ carbon atoms, for the determination of the 1-pentene centred triads, the $2B_3$ side chain methylene resonances were profitably used. In particular, it permits a correct determination of dyad and triad copolymer composition and of comonomer content and distribution as shown in Table 3.1.3.

Table 3.1.3 ^{13}C NMR characterization of ethylene/1-pentene copolymers prepared with different metallocene catalysts and MAO as the catalytic system.

Run [a]	Pe/E (mol/mol)	1-Pe (mol%)[b]	PPP	PPE	EPE	PEP	PEE	EEE	PP	PE	EE	n(E)[c]	n(P)[d]
1	0.8	4.27	0.00	0.88	3.69	0.00	8.19	87.24	0.75	8.37	90.87	23.30	1.12
2	1.5	9.33	0.66	2.79	5.88	0.60	13.12	76.95	1.61	14.05	84.33	12.70	1.28
3	2.2	15.02	1.64	6.19	7.19	1.15	17.28	66.56	4.41	20.44	75.14	8.68	1.46
4	4.0	25.04	5.77	10.88	8.40	2.75	21.84	50.36	10.35	27.19	62.46	5.48	1.64
5	5.9	27.08	6.93	11.16	8.98	3.25	22.35	47.33	11.97	29.19	58.84	5.06	1.64
6	8.7	33.47	10.10	14.59	8.79	4.00	23.54	38.99	16.94	31.36	51.70	4.22	2.04
7	13.7	51.71	23.58	19.55	8.27	6.20	21.15	20.95	36.19	29.67	34.14	2.87	2.84
8	0.8	6.96	0.12	0.74	6.10	0.57	11.83	80.64	0.26	13.32	86.42	14.35	1.06
9	1.5	13.07	0.48	1.70	10.88	1.94	19.13	65.87	1.00	23.61	75.40	7.56	1.11
10	2.2	22.65	2.05	5.19	15.41	5.03	24.73	47.59	3.78	35.50	60.72	4.45	1.25
11	4.0	36.20	6.01	11.45	18.73	10.36	27.63	25.80	13.10	47.60	39.30	2.63	1.52
12	5.9	39.38	7.41	12.09	19.88	11.41	27.47	21.68	13.46	50.64	35.90	2.40	1.52
13	8.7	47.89	13.64	14.95	19.29	12.99	24.16	14.96	21.30	50.79	27.90	2.07	1.79
14	13.7	54.51	20.11	18.41	16.00	14.66	20.72	10.11	29.74	49.62	20.64	1.81	2.16

[a] The numbers of the samples are those of the corresponding runs. [b] From triad distribution as P% = (PPP + PPE + EPE). [c] n(E) = E/(PEP + 0.5PEE) where E = EEE+EEP+PEP. [d] n(P)= P/(EPE + 0.5EPP) where P = PPP+PPE+EPE.

Triad distribution collected in Table 3.1.3, derived from ^{13}C NMR data, indicates that E/Pe copolymers from TBI with respect to those from EBTHI are characterized by relatively long homosequences of both comonomer units, with only a minor presence of alternate comonomer units. For TBI the sum of P and E homotriads and homodiads was found to be greater than at least 43% and 70% (run 7 in Table 3.1.3). By comparing the diad distribution, it appear that for EBTHI

(run 11-14 in Table 3.1.3) the heterodiad PE is higher or at least comparable to the sum of the two homodiads. A comparative analysis of the relative abundance of ethylene-rich and comonomer-rich triads leads to the following comments: i) the EEE/E ratio appears to be higher for copolymers from TBI than from those from EBTHI: for example, run 7 with 51.71 mol% of Pe content has a EEE content of 20.95 mol%, whereas run 14 with 54.41 mol% of Pe has a EEE content of 10.11 mol%; ii) the PPP/P ratio appears to be higher for copolymers from TBI, with 23.58 mol% of PPP (run 7 in Table 3.1.3) *vs* a percentage of PPP of 20.11 mol% of run 14 in Table 3.1.3; iii) as far as the alternate triads are concerned, it is worth noticing that the amount of EPE triad is higher than PEP triad; iv) taking again into consideration run 7 and run 14 in Table 3.1.3, it appears that PEP triad is 6.20 mol% in run 7 and 14.66% in run 14, while PE dyad is 29.67 mol% in run 7 and 49.62 mol% in run 14, thus indicationg a tendency to give alternating sequences with EBTHI.

A clear picture of the copolymers appears thus from the copolymer triad distribution. For TBI both comonomers tend to preferentially form homosequences and in the case of Pe, the homosequences are, to minor extent, interrupted by single ethylene units.

3.1.2 Statistical analysis of copolymerization data

Triad molar fractions, reported in Table 3.1.3, were analysed and the copolymerization reactivity ratios as well as their product were determined. r_1 and r_2 reactivity ratios, with their confidence intervals, and the product of reactivity ratios r_1r_2 are reported in Table 3.1.4, and compared with those reported in literature for ethylene/4-methyl-1-pentene copolymers prepared with the same catalysts.

Table 3.1.4 Reactivity ratios calculated with a 1st order Markov model for ethylene/1-pentene copolymerizations from isospecific organometallic complexes.

Catalyst	Comonomers	$r_1\pm\delta\, r_1$	$r_2\pm\delta\, r_2$	$r_1r_2\pm\delta\, r_1r_2$	Ref.
EBTHI	E/Pe	8.60 ±0.74	0.08±0.02	0.7±0.2	-
	E/4M1P	91.2±16.1	0.11±0.05	9.8±6.2	12
TBI	E/Pe	21.12±1.89	0.13±0.03	2.8±0.9	-
	E/4M1P	93.9±15.6	0.18±0.05	17.2±8.1	12

For any of the catalysts, r_1 and r_2 are respectively higher and lower than 1, thus indicating a preferred insertion of ethylene regardless of the last inserted unit. In line with the results obtained with E/4M1P copolymerizations and the observation of triad distribution in Table 3.1.3, the E/Pe copolymerization from TBI is characterized by a reactivity ratio higher than 1, thus confirming that this metallocene favours the presence along the same macromolecular chain of homosequences of both ethylene and 1-pentene. Contrary to the results obtained with E/4M1P copolymers from EBTHI, such a metallocene promotes E/Pe copolymerizations characterized by r_1r_2 products lower than 1. For these copolymerizations, the r_1 and r_2 values are very similar to

those previously reported in literature for ethylene/propylene copolymers prepared with the same metallocene: r_1 moves from 10.6 to 8.6, r_2 from 0.07 to 0.08, and r_1r_2 from 0.8 to 0.7.[13]

To better elucidate the correlation between catalytic system and copolymer microstructure copolymerization data were elaborated with the 2nd order Markovian model, that takes into account also the penultimate effect.

Values for r_{ij} reactivity ratios as well as for comonomer distribution index (CDI) for ethylene/1-pentene and for ethylene/4-methyl-1-pentene copolymerizations from the two isospecific metallocenes are reported in Table 3.1.5.

Table 3.1.5 r_{ij} reactivity ratios and comonomer distribution index (CDI), calculated with a 2nd order Markov model for ethylene/1-pentene and ethylene/4-methyl-1-pentene copolymerizations from isospecific organometallic complexes.

|	Comonomers	r_{11}	r_{21}	r_{12}	r_{22}	CDI^a
EBTHI	E/Pe	8.95 ±0.62	7.23 ±1.10	0.05±0.01	0.16±0.03	0.91±0.25
	E/4M1P^b	134.1±13.7	19.6±3.7	0.03±0.01	0.094±0.008	4.5±1.2
TBI	E/Pe	20.15±1.55	28.50±3.57	0.11±0.03	0.16±0.03	3.19±0.99
	E/4M1P^c	109.7±25.4	7.0±30	0.12±0.06	0.096±0.013	4.5±2.6

^{a} Comonomer distribution index calculated according to the formula $CDI = \sqrt[3]{r_{11}^2 r_{22}^2 r_{12} r_{21}}$; ^{b} Data from reference 14; ^{c} Data from reference 10a.

Dwelling upon the CDI values in Table 3.1.5, it appears that longer sequences of comonomers are present in E/Pe copolymer chains obtained with TBI rather than with EBTHI, analogously to what reported by elaborating data with the first-order Markovian model. Otherwise, *blocky* copolymers were prepared with both metallocenes when 4M1P is the comonomer, as shown by the CDI values, higher than 1. As shown above, in the case of 1-pentene as the 1-olefin, sequential copolymers were obtained with only the highly isospecific metallocenes TBI. It can be commented that catalyst precursor such as EBTHI is not isospecific enough to promote long 1-pentene sequences in E/Pe copolymers, whereas it increases its stereospecific ability thanks to a bulkier 1-olefin such as 4-methyl-1-pentene as the comonomer.

More interesting hints on copolymerization mechanism obviously arise from the examination of reactivity ratios. The two metallocenes give rise to almost the same r_{22} value to indicate that an isospecific site with a growing chain with two 1-pentene units as the last inserted ones has the same comonomer relative reactivity, that is, the same stereospecific ability regardless of the geometric features of the catalytic precursors. As already reported,[15,16] the selectivity of a catalytic site is made by the cooperation between the catalyst precursor and the growing chain and is further enhanced by a bulky 1-olefin. In the 1-olefin hydro(deuterium) oligomerization promoted by metallocene-based catalytic systems, it was observed that the highest enantioselectivity of 1-pentene insertion was determined for the deuterio-oligomerization reaction, that is, in the presence of the growing chain, and that the regioselectivity of the 1-olefin insertion promoted by the same metallocenes (EBTHI) was found to be higher for 1-pentene with respect to propylene. The 1-olefin thus seems to play a key role.

To help the interpretation of data of Table 3.1.5, the relative reactivity of E with respect to 1-pentene is shown in the bar chart of Figure 3.6 as a function of chain end sequences, i.e. when the last inserted units are EE-Zr, PE-Zr, EP-Zr and PP-Zr, respectively. This type of representation was selected as a mark of the sequential nature of an E/1-olefin copolymer.[2c]
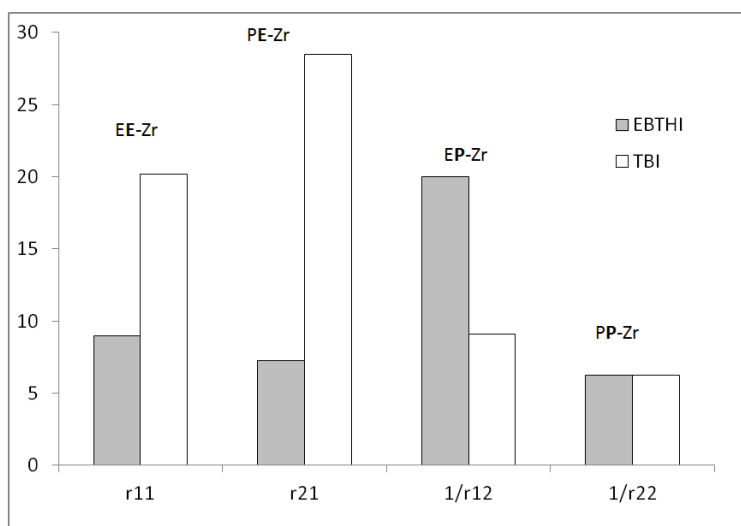
Figure 3.1.6 E/Pe relative reactivity (r_1, $r_{1'}$, $1/r_2$, and $1/r_{2'}$) obtained from second-order ($r_1{\neq}r_{1'}$ and $r_2{\neq}r_{2'}$) reactivity ratios for copolymerizations promoted by *rac*-(EBTHI)ZrCl$_2$ and *rac*-H$_2$C-(3-*t*BuInd)$_2$ZrCl$_2$.

Indeed, for E/Pe copolymerization promoted by TBI, the ethylene reactivity was found to decrease in the following order: PE-Zr, EE-Zr, EP-Zr and PP-Zr, as shown in Figure 3.1.6: 1-pentene as the last inserted unit favours the insertion of further 1-olefin units. However this trend was not observed for copolymers from EBTHI. These data confirms what previously commented: the enantioselectivity of the catalytic site is made by the cooperation of the organometallic complex and of the growing chain. By examining data arising from EBTHI, it can be commented that the isospecificity level is not high enough to bring about a *blocky* E/Pe copolymer, as shown in particular by the high value of $1/r_{12}$ value, that is, of E/Pe relative reactivity when Pe is the last inserted unit. With the slightly more isospecific EBTHI, a PP chain end caused a $1/r_{22}$ value lower than r_{11} and r_{21} values, thus indicating that a more isospecific site, brought about by the presence of two last inserted PP units, favours a further P insertion. Bar char referring to copolymer from TBI allows to identify that lower $1/r_{12}$ and $1/r_{22}$ are the fingerprint for an ethylene copolymer with relatively long sequences of the 1-olefin.

To provide a sort of fingerprint of the microstructure of such copolymers, the probabilities of having sequences composed of n E units, [P(E)$_n$P], or of n P units, [E(P)$_n$E] were calculated for run 7 and 14 in table 3.1.1. The calculations were performed using the experimental values of reactivity ratios given in Table 3.1.5, for bath composition $f = 13.7$.
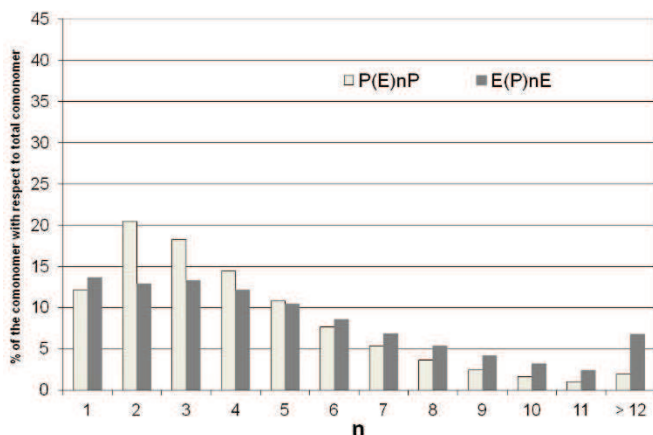
Figure 3.1.7 Probability of sequences of n comonomer units for run 7 in Table 3.1.1 (Pe = 51.71 mol%).
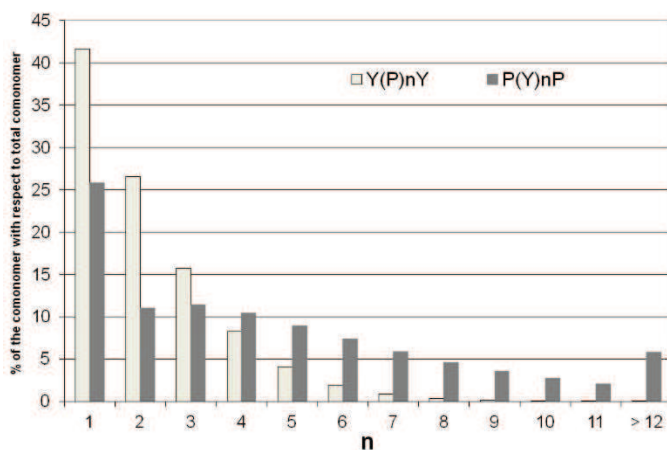
Figure 3.1.8 Probability of sequences of n comonomer units for run 14 in Table 3.1.1 (Pe = 55.21 mol%).

In copolymer from EBTHI (Figure 3.1.8) both comonomers are prevailingly present along the polymer chain as isolated units (n=1) or short sequences (n=2-4) of E. Copolymers from TBI shows as well short E sequences as shown in Figure 3.1.7. Isolated or short (n=2-4) ethylene units are about 92 mol% and 65 mol% for EBTHI and TBI, respectively.

3.1.3 DSC thermal analysis

The thermal behavior of the synthesized ethylene/1-pentene copolymers was investigated by differential scanning calorimetry (DSC). The values of glass transition, crystallization and melting temperatures (T_g, T_c, and T_m, respectively) and those of the corresponding crystallization and melting enthalpies (ΔH_c and ΔH_m) are listed in Table 3.1.6.

E/Pe copolymers from TBI and EBTHI become completely amorphous above 30 mol% of 1-pentene co-units.

Upon cooling from the melt, the copolymers, close to equimolar composition, practically do not show any appreciable endothermic signals. This is in line with the results shown in Figure 3.1.7

and 3.1.8, where for both catalytic systems, the amount of 1-pentene homosequences containing at least 12 units is about 5 mol%.

Table 3.1.6 DSC thermal characterization of ethylene/1-pentene copolymers.

Catalyst	Run	1-Pe[c] (mol%)	I heating[a]		cooling		II heating[b]		
			T_m (°C)	ΔH_m (J/g)	T_c (°C)	ΔH_c (J/g)	T_g (°C)	T_m (°C)	ΔH_m (J/g)
TBI	1	4.27	108	127	90	109	n.d.[d]	104	108
	2	9.33	84	84	78	80	n.d.[d]	90	84
	3	15.02	78	53	60	55	n.d.[d]	66	47
	4	25.04	45	n.d.[d]	-.	17	n.d.[d]	43[e]	21
	5	27.08	43	n.d.[d]	-	13	n.d.[d]	35[e]	19
	6	33.47	42	n.d.[d]	-	-	-57	-	-
	7	51.71	-	-	-	-	-54	-	-
EBTHI	8	6.96	105	116	87	97	n.d.[d]	101	108
	9	13.07	81	54	72	57	n.d.[d]	89	59
	10	22.65	77	18	55	21	n.d.[d]	74	19
	11	36.20	-	-	-	-	n.d.[d]	-	-
	12	39.38	-	-	-	-	-61	-	-
	13	47.89	-	-	-	-	-63	-	-
	14	54.51	-	-	-	-	-58	-	-

[a] 1st heating run on as-polymerized samples (crystallized from solution). [b] 2nd heating run on samples crystallized from the melt. [c] From ^{13}C NMR analysis. [d] n.d. = not detectable. [e] broad melting endotherms.

3.1.4 Separation of ethylene/1-pentene copolymers by High Temperature HPLC (HT-HPLC)

Ethylene/1-pentene copolymers from TBI catalyst were analyzed by means of high temperature HPLC at German Institute for Polymers in Darmstadt by the group of Prof. Tibor Macko.

Prof. Macko introduced a new separation principle among the analytical characterizations of polyolefins.[17,18] According to this technique, polyolefins can be selectively separated via high-performance liquid chromatography on the basis of their adsorption/desorption behaviours at temperatures as high as 160 °C. A Hypercarb® column packed with porous graphite was chosen.[19,20] The mobile phase consisted of a mixture of 1-decanol and 1,2,4-trichlorobenzene. This chromatographic system was applied to the separation of ethylene/1-olefins copolymers, showing that the elution volumes of the samples correlate linearly with the average chemical composition of samples.

For ethylene based copolymers, the elution volume is indirectly proportional to the concentration of branches. Indeed, branching shortens the length of continuous methylene sequences of the

polymer backbone, thus decreasing the probability of orientation of a methylene sequence in a flat conformation on the graphite surface, which enables the most intensive van der Waals interactions between the methylene backbone and the carbon surface.[21]

The ethylene/1-pentene copolymers from TBI catalyst, described in Table 3.1.1, were dissolved in 1-decanol, as the mobile phase and injected into the Hypercarb column. After the injection, a part or whole sample either eluted from the column or not at all. When a sample is strongly adsorbed on the column packing, *i.e.* no peak appears on the chromatogram after the injection and flushing the column with pure 1-decanol, the adsorbed sample is desorbed by the action of 1,2,4-trichlorobenzene (TCB) in a linear gradient starting from 1-decanol and ending with pure TCB. The chromatograms for ethylene/1-pentene copolymers are shown in the Figure 3.1.9a together with the correlations between the elution volume and the average chemical composition of samples (Figure 3.1.9b). All these copolymers eluted exclusively in the gradient.
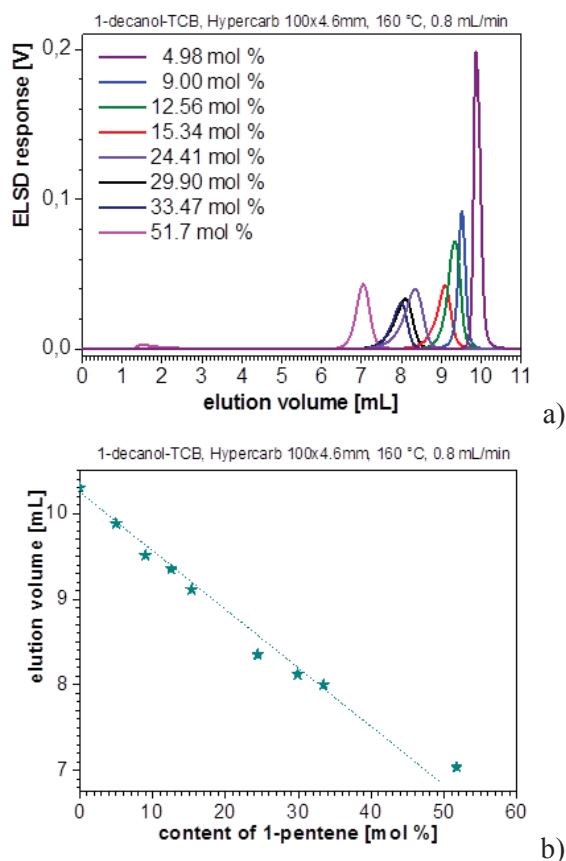
Fig. 3.1.9 Overlay of chromatograms (a) and dependence of the elution volume on the average comonomer composition (b) for ethylene/1-pentene copolymers.

On the other hand, by comparing the result of ethylene/1-pentene with those reported in literature for ethylene/4-methyl-1-pentene copolymers, it is possible to observe that with 4-methyl-1-pentene as comonomer, copolymers elute either isocratically (*i.e.* in 1-decanol) or in the gradient or in both mobile phases (Figure 3.1.10).[21]
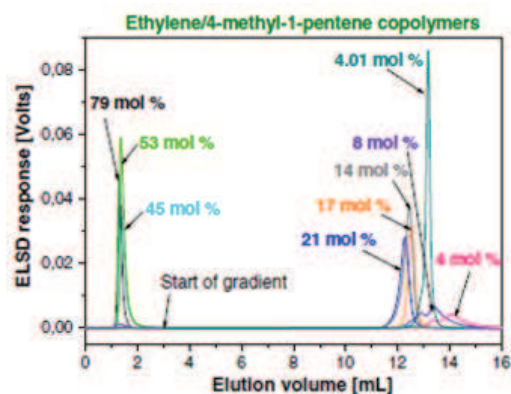
Fig. 3.1.10 Overlay of chromatograms for ethylene/4-methyl-1-pentene copolymers.

The elution volumes of copolymers decreased with the increase of the concentration of the branching in the ethylene/1-olefins copolymers; this trend seems also valid for ethylene/4-methyl-1-pentene copolymers (Figure 3.1.10) even if, with the more sterically hindered comonomer, these copolymers were not adsorbed and eluted before the start of the gradient with a branches concentration is high (above ~40 mol% 4M1P).

3.1.5 References

1. W. Kaminsky, K. Kuulper, H. H. Brintzinger, F. R. W. P Wild, *Angew. Chem. Int. Ed.*, **1985**, *24*, 507.

2. (a) M. Galimberti, F. Piemontesi, O. Fusco, I. Camurati, M. Destro, *Macromolecules*, **1998**, *31*, 3409; (b) M. Galimberti, F. Piemontesi, O. Fusco, I. Camurati, M. Destro, *Macromolecules*, **1999**, *32*, 7968; (c) S. Losio, F. Piemontesi, F. Forlini, M. C. Sacchi, I. Tritto, P. Stagnaro, G. Zecchi, M. Galimberti, *Macromolecules*, **2006**, *39*, 8223.

3. L. Resconi, A. Fait, L. Cavallo, F. Piemontesi, *Chem. Rev.*, **2000**, *100*, 1253.

4. C. J. Carman, R. A. Harrington, C. E. Wilkes, *Macromolecules*, **1977** *10*, 536.

5. J. C. Randall, *J Macromol Sci Rev Macromol. Chem. Phys.*, **1989**, *C29*, 201.

6. D. E. Dorman, E. P. Otocka, F. A. Bovey, *Macromolecules*, **1972**, *5*, 574.

7. G. B. Galland, R. F. de Souza, R. Santos Mauler, F. F. Nunes, *Macromolecules*, **1999**, *32*, 1620.

8. M. C. Da Silva, G. B. Galland, *Polymer*, **2008**, *46*, 947.

9. (a) A. Carvill, A, Zetta, G. Zannoni, M. C. Sacchi, *Macromolecules*, **1998**, *31*, 3783; (b) A. Carvill, I. Tritto, P. Locatelli, M. C. Sacchi, *Macromolecules*, **1997**, *30*, 7056.

10. (a) M. Galimberti, F. Piemontesi, L. Alagia, S. Losio, L. Boragno, P. Stagnaro, M. C. Sacchi, *J. Polym. Sci.: Polym. Chem.*, **2010**, *48*, 2063; (b) S. Losio, A. C. Boccia, L. Boggioni, M. C. Sacchi, D. R. Ferro, *Macromolecules*, **2009**, *49*, 6964; (c) S. Losio, P. Stagnaro, T. Motta, M. C. Sacchi, F. Piemontesi, M. Galimberti, *Macromolecules*, **2008**, *41*, 1104.

11. (a) J. C. Randall, *Macromol. Sci., Rev. Macromol. Chem. Phys.*, **1989**, *C29*, 420; (b) W. Liu, P. L. Rinaldi, L. H. McIntosh, R. P. Quirk, *Macromolecules*, **2001**, *34*, 4757.

12. (a) M. C. Sacchi, F. Forlini, S. Losio, I. Tritto, U. M. Wahner, I. Tincul, D. J. Joubert, E. R. Sadiku, *Macromol. Chem. Phys.*, **2003**, *204*, 1643; (b) G. Costa, P. Stagnaro, V. Trefiletti, M. C. Sacchi, F. Forlini, G. C. Alfonso, I. Tincul, U. M. Wahner, *Macromol. Chem. Phys.*, **2004**, *205*, 383; (c) M. C. Sacchi, F. Forlini, S. Losio, I. Tritto, G. Costa, P. Stagnaro, I. Tincul, U. M. Wahner, *Macromol. Symp.*, **2004**, *213*, 57; (d) P. Stagnaro, L. Boragno, M. Canetti, F. Forlini, F. Azzurri, G. C. Alfonso, *Polymer*, **2009**, *50*, 5242; (e) C. De Rosa, O. R. de Ballesteros, F. Auriemma, M. R. Di Caprio, *Macromolecules*, **2012,** *45,* 2749; (f) L. Boragno, P. Stagnaro, F. Forlini, F. Azzurri, G. C. Alfonso, *Polymer*, **2013**, *54*, 1656.

13. M. Galimberti, F. Piemontesi, N. Mascellani, I. Camurati, O. Fusco, M. Destro, *Macromolecules*, **1999**, *32*, 7968.

14. P. Stagnaro, L. Boragno, S. Losio, M. Canetti, G. C. Alfonso, M. Galimberti, F. Piemontesi, M. C. Sacchi, *Macromolecules*, **2011**, *44*, 3712.

15. (a) M. C. Sacchi, P. Locatelli, I. Tritto, *Makromol. Chem.*, **1989**, *190*, 139; (b) A. Zambelli, P. Locatelli, M. C. Sacchi, I. Tritto, *Macromolecules*, **1982**, *15* , 831.

16. (a) A. Zambelli, A. Grassi, M. Galimberti, R. Mazzocchi, F. Piemontesi, *Makromol. Chem. Rapid. Commun.*, **1991**, *12*, 523; (b) P. Pino, P. Prada, M. Galimberti, In Frontier of Macromolecular Science; T. Saegusa, T. Higashimura, A. Abe, Eds.; Blackwell Scientific Publications: Oxford, **1989**, 43.

17. T. Macko, H. Pasch, *Macromolecules*, **2009**, *42*, 6063.

18. T. Macko, R. Brüll, Y. Zhu, Y. Wang, *J. Sep. Sci.,* **2010**, *33*, 3446.

19. M. Gilbert, J. Knox, B. Kaur, *Chromatographia*, **1982**, *16*, 138.

20. L. Pereira, *J. Liq. Chromatogr.*, **2008**, *31*, 687.

21. T. Macko, R. Brüll, R. G. Alamo, F. J. Stadler, S. Losio, *Anal. Bioanal. Chem.*, **2011**, *399*, 1547.

3.2 Propylene/4-methyl-1-pentene copolymers

Three series of propylene/4-methyl-1-pentene (P/Y) copolymers, promoted by three metallocenes characterized by different enantioselective ability in propylene homopolymerization, have been synthetized. Copolymers were prepared in solution, over a wide range of chemical composition, determining their molar mass by size exclusion chromatography (SEC) and the comonomer sequences, at the triad level, through ^{13}C NMR analysis.[1] A statistical elaboration of copolymerization data was performed by applying 1st and 2nd order Markovian models in order to calculate the reactivity ratios of the copolymerizations.

3.2.1 Synthesis of propylene/4-methyl-1-pentene copolymers

The metallocene complexes used are shown in Figure 3.2.1. *rac*-Et(IndH₄)₂ZrCl₂ (EBTHI), *rac*-Me₂Si(2-MeBenzInd)₂ZrCl₂ (MBI), and *rac*-CH₂(3-*t*BuInd)₂ZrCl₂ (TBI) belong to the class of C_2-symmetric metallocenes and were selected as they are endowed with different stereospecificity, that increases from the moderately isospecific EBTHI, to the more isospecific MBI and up to the highly isospecific TBI.
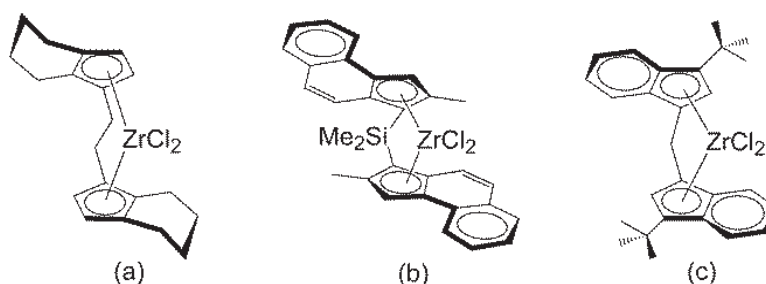
FIGURE 3.2.1 C_2 symmetric metallocenes under investigation: (a) *rac*-Et(IndH₄)₂ZrCl₂, EBTHI, (b) *rac*-Me₂Si(2-Me-BenzInd)₂ZrCl₂, MBI, and (c) *rac*-CH₂(3-*t*BuInd)₂ZrCl₂, TBI.

Data available in the literature on microstructure of polypropylene (PP) prepared with such metallocenes are reported in Table 3.2.1. Both stereo- and regiospecificity decrease in the order TBI > MBI > EBTHI.[2-6]

Table 3.2.1 Microstructure of polypropylene (PP) obtained with the three different metallocene complexes and MAO as the cocatalyst.

Catalyst	I.I.[a] (mmmm%)	Regiomistakes (%)	Ref.
EBTHI	91.5	1.0	7
MBI	93.0	0.3	2
TBI	97.0	0.0	7

[a] I.I.: isotactic index

Copolymerization and molecular characterization data are shown in Table 3.2.2.

Table 3.2.2 Copolymerization data for P/Y system with different metallocene catalysts.[a]

Catalyst	Run	Y/P^b (mol/mol)	t (min)	[catalyst] μmol	Al/Zr (mol/mol)	Activity^c	Y^d (mol%)	Conversion %	M_w^e (x10^3)	M_w/M_n^e
EBTHI	E1	0.04	10	1.1	3000	2406	1.88	2.9	20	2.1
	E2	0.08	10	1.1	3000	2345	3.57	2.5	16	1.9
	E3	0.12	10	2.5	3000	2213	5.70	5.8	10	1.8
	E4	0.22	10	2.6	3000	503	9.92	1.3	10	1.8
	E5	0.33	15	6.0	3000	754	15.74	5.8	7	1.8
	E6	0.42	15	4.1	3000	1202	18.72	5.9	8	1.8
	E7	0.86	15	3.5	3000	1166	35.88	3.6	11	1.9
	E8	1.21	30	3.0	3000	388	43.00	2.0	7	1.8
	E9	1.75	45	3.4	3000	562	53.27	4.2	7	1.8
	E10	1.84	45	3.3	3000	146	60.75	1.1	6	1.9
	E11	2.43	90	7.0	3000	136	67.21	2.9	10	2.1
	E12	3.00	60	5.0	3000	506	85.81	5.4	43	2.1
MBI	M1	0.03	15	2.0	3000	1246	3.00	7.6	133	2.5
	M2	0.05	15	1.1	3000	1286	5.27	6.5	130	2.1
	M3	0.06	15	2.2	3000	1195	8.79	9.7	69	2.3
	M4	0.07	15	2.2	3000	1019	10.10	8.2	66	2.3
	M5	0.17	15	1.6	3000	586	14.86	3.7	62	1.9
	M6	0.30	15	2.6	3000	173	22.82	1.4	40	2.1
	M7	0.46	30	3.9	3000	90	29.72	1.8	25	2.0
	M8	0.60	90	10.0	1200	82	51.95	13.6	20	2.2
	M9	1.19	60	10.0	1200	46	62.77	2.9	47	3.9
	M10	1.74	90	10.0	1200	70	73.53	5.0	44	3.2
	M11	1.84	120	10.0	1200	111	76.94	10.4	18	2.6
	M12	2.43	90	10.0	1200	70	81.06	3.8	24	2.9
	M13	3.00	60	10.0	1200	130	88.70	4.0	15	1.9
TBI	T1	0.03	10	2.0	3000	2493	2.95	15.0	12	1.5
	T2	0.05	25	2.0	3000	936	4.99	13.2	19	2.3
	T3	0.11	12	5.0	1200	1436	10.60	14.2	10	1.8
	T4	0.17	10	2.0	3000	927	15.10	4.5	15	2.1
	T5	0.30	12	5.0	1200	390	22.72	5.8	12	1.8
	T6	0.46	18	5.0	1200	786	32.32	12.1	12	2.1
	T7	0.86	15	5.0	1200	482	43.88	4.4	12	1.8
	T8	1.19	30	5.0	1200	861	59.57	13.2	13	1.9
	T9	1.74	18	5.0	1200	923	68.39	6.3	18	1.8
	T10	2.43	15	5.0	1200	531	82.58	2.4	10	1.7
	T11	3.00	15	5.0	1200	446	90.81	1.7	38	2.1

[a] Polymerization conditions: total volume = 100 mL, T = 50 °C, P = 1.08 atm, Al/Zr = 3000-1200 (mol/mol), EBTHI: T= 30°C, Al/Zr = 3000. [b] Y/P feed ratio in liquid phase. [c] $mg_{pol}/(mmol_{Zr}$ h). [d] From ^{13}C NMR analysis. [e] Molar mass and polydispersity index from SEC analysis.

[Y]/[P] feed ratio varied from 0.03 to 3.00 mol/mol and allowed the preparation of copolymers in wide ranges of chemical composition, from about 3 to about 90 as Y mol%. To maintain nearly constant the comonomer concentration in solution throughout the reaction course, low Y conversion was adopted (up to about 15%).[7] Catalyst concentrations and polymerization times were thus adjusted in order to obtain reasonable copolymer yields. In particular, with MBI, catalyst amounts up to 10 μmol were used and polymerization times up to 2 h were adopted. As for ethylene/1-pentene copolymers, rigorous comments on catalytic activities are not conceivable, as the polymerization conditions were not exactly reproduced. It is nevertheless possible to observe the decrease of the catalytic activity as the Y content in the polymerization bath increases for copolymerizations promoted by all of the three metallocenes and, in particular, by MBI. Indeed with a Y/P higher than 0.46, 10 μmol of catalyst have been used to obtain sufficient amount of copolymers necessary for all the required characterization analysis.

Figure 3.2.2 shows the Y content in the copolymer as a function of the P/Y molar ratio in the polymerization bath. Hence, to prepare P/Y copolymers with a given comonomer content, larger Y concentration in the polymerization bath has to be used in the case of EBTHI with respect to MBI and TBI.
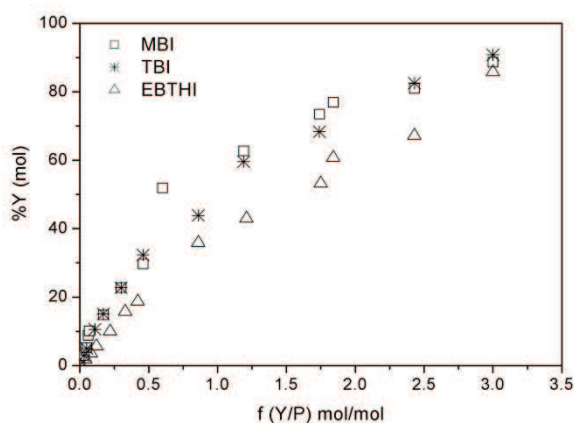
FIGURE 3.2.2 Y molar content in propylene/4-methyl-1-pentene copolymer as a function of Y/P molar ratio in the polymerization bath.

GPC characterization evidenced that all samples exhibit polydispersity around 2 indicative of the single site nature of the metallocene catalytic systems used. MBI leads to fairly high molar mass values, while samples produced from TBI and EBTHI exhibit lower molar masses. Moreover, it can be noticed that with MBI, the copolymer molar mass decreases as the Y content increases.

3.2.2 ^{13}C NMR analysis

Comonomer content and microstructure of the copolymers were determined by means of ^{13}C NMR spectroscopy.[3] The general structure of P/Y copolymer is shown in Scheme 3.2.1.
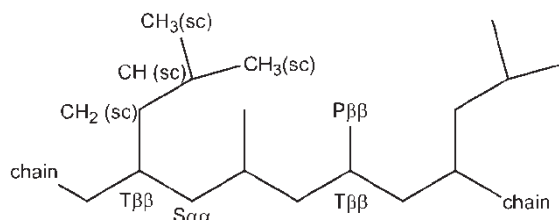
Scheme 3.2.1 Structure and carbon labelling of P/Y copolymer.

Figure 3.2.3 shows the ^{13}C NMR spectra of P/Y copolymers with similar comonomer content (about 15 mol%) from EBTHI, MBI and TBI catalysts. Because of the low molar masses, several sma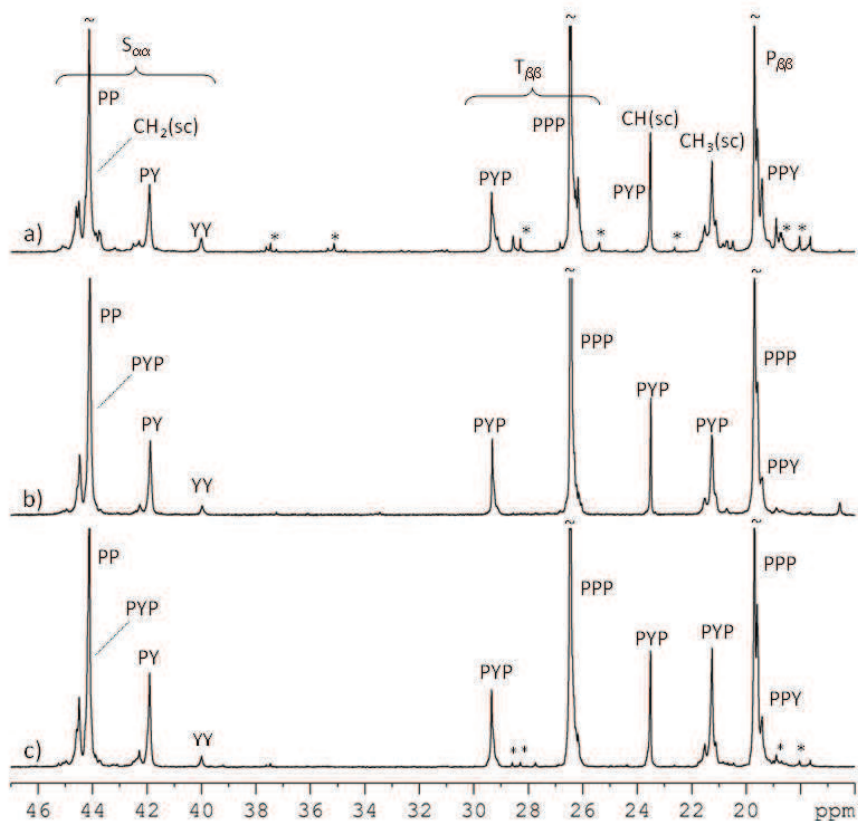ll signals are detected in the spectra of the copolymers obtained with EBTHI and TBI as catalyst precursors, that are assigned to a variety of chain end groups (starred signals in spectra 3.2.3a and 3.2.3c).[1] Figure 3.2.4 shows the expanded methylene regions of copolymers having higher Y content (about 60 mol%).

Figure 3.2.3 ^{13}C NMR spectra of P/Y copolymers with similar comonomer content: a) 15.74 mol% content prepared with *rac*-Et(IndH$_4$)$_2$ZrCl$_2$ (run E5 in Table 3.2.2), b) 14.86 mol% content prepared with *rac*-Me$_2$Si(2-MeBenzInd)$_2$ZrCl$_2$ (run M5 in Table 3.2.2), and c) 15.10 mol% content prepared with *rac*-CH$_2$(3-^{t}BuInd)$_2$ZrCl$_2$ (run T4 in Table 3.2.2).

The spectrum allows some qualitative comments on the comonomer distributions obtained with the three different catalyst precursors. While copolymers at low Y content have apparently similar ^{13}C NMR spectra, as shown in Figure 3.2.3, clear differences become detectable by increasing comonomer content, as revealed by the inspection of the expanded region of Y side chain methylene carbon (Figure 3.2.4). In fact, the relative intensity of the signal due to CH$_2$(sc) of YYYYY pentad (43.65 ppm) with respect to that of the signal due to CH$_2$(sc) of PYYYZ pentad (Z means P or Y) is higher in copolymers from MBI and EBTHI compared to copolymers from TBI.
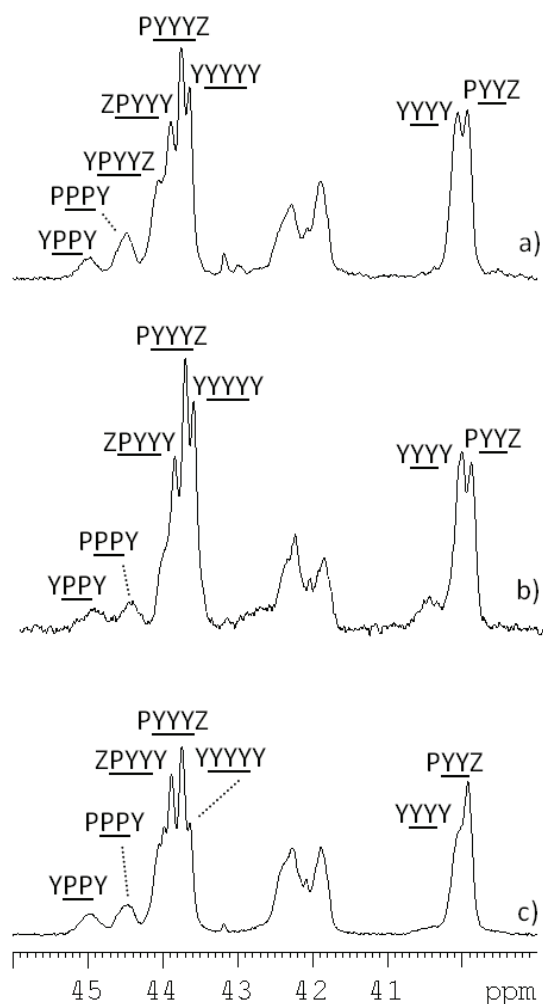
Figure 3.2.4 ^{13}C NMR spectra of P/Y copolymers with similar comonomer content: a) 59.57 mol% content prepared with *rac*-CH$_2$(3-^{t}BuInd)$_2$ZrCl$_2$ (run T8 in Table 3.2.2), b) 62.77 mol% content prepared with *rac*-Me$_2$Si(2-MeBenzInd)$_2$ZrCl$_2$ (run M9 in Table 3.2.2), and c) 60.75 mol% content prepared with *rac*-Et(IndH$_4$)$_2$ZrCl$_2$ (run E10 in Table 3.2.2). Z means P or Y.

Analogously, the relative intensity of the signal due to the centred αα-methylene of YYYY tetrad at 40.05 ppm with respect to the signal of the PYYZ tetrad at 39.90 ppm is lower in copolymers from TBI. Thus, EBTHI and MBI seem to reveal a higher ability to form Y homosequences with respect to TBI. Triad molar fractions for copolymers from EBTHI, MBI, and TBI up to about 70% in comonomer content are reported in Table 3.2.3.[9] These values were obtained from ^{13}C

NMR spectra, applying a best fitting procedure.[1a] The analysis of the data of Table 3.2.3 shows that, in general, the relative content of YYY triad is higher in copolymers prepared with MBI and EBTHI rather than in copolymers from TBI. In fact, by examining, as an example, data of copolymers with about 60% by moles as Y content, whose ^{13}C NMR spectra are shown in Figure 3.2.4, it appears that copolymer from TBI with 59.57 mol% as Y content (Run T8) has 21.6 mol% as YYY triad, whereas copolymers from MBI with 62.77 mol% as Y content (Run M9) and from EBTHI with 60.75 mol% as Y content (Run E10) have 30.2 mol% and 33.7 mol% as YYY triad content, respectively.

TABLE 3.2.3 Triad molar fractions from ^{13}C NMR spectra of P/Y copolymers prepared with EBTHI, MBI, and TBI as catalyst precursors.

Run	Y/P	Y (mol%)[a]	$R^{2\,b}$	Triad					
				PPP	PPY	YPY	PYP	PYY	YYY
E3	0.12	5.70	99.68	0.847	0.088	0.008	0.049	0.006	0.002
E4	0.22	9.92	99.92	0.739	0.139	0.016	0.067	0.037	0.004
E5	0.33	15.74	99.75	0.629	0.177	0.028	0.091	0.052	0.022
E7	0.86	35.88	99.84	0.312	0.244	0.072	0.078	0.232	0.062
E8	1.21	43.00	99.79	0.198	0.265	0.077	0.120	0.179	0.160
E9	1.75	53.27	99.74	0.108	0.241	0.089	0.126	0.168	0.267
E10	1.84	60.75	99.86	0.095	0.219	0.091	0.142	0.116	0.337
E11	2.43	67.21	99.93	0.042	0.172	0.098	0.133	0.102	0.451
M1	0.03	3.00	99.59	0.907	0.062	0.000	0.030	0.001	0.000
M2	0.05	5.27	99.86	0.856	0.086	0.005	0.045	0.006	0.001
M3	0.06	8.79	99.84	0.770	0.130	0.012	0.072	0.010	0.005
M4	0.07	10.03	99.68	0.732	0.154	0.013	0.087	0.007	0.007
M5	0.17	14.86	99.85	0.612	0.210	0.029	0.125	0.018	0.005
M6	0.30	22.82	99.41	0.479	0.256	0.036	0.135	0.059	0.034
M7	0.46	29.72	99.82	0.428	0.198	0.077	0.100	0.151	0.046
M8	0.60	51.95	99.87	0.136	0.237	0.108	0.020	0.313	0.187
M9	1.19	62.77	99.44	0.121	0.122	0.130	0.057	0.268	0.302
M10	1.74	73.53	99.83	0.046	0.080	0.139	0.031	0.296	0.408
T1	0.03	2.95	99.65	0.917	0.051	0.002	0.025	0.005	0.000
T2	0.05	4.99	99.87	0.868	0.075	0.008	0.043	0.005	0.003
T3	0.11	10.60	99.84	0.742	0.134	0.018	0.071	0.028	0.007
T4	0.17	15.10	99.40	0.573	0.236	0.023	0.116	0.051	0.001
T5	0.30	22.72	99.78	0.490	0.238	0.045	0.133	0.062	0.032
T6	0.46	32.32	99.86	0.313	0.248	0.084	0.131	0.159	0.064
T7	0.86	47.88	99.90	0.143	0.250	0.129	0.188	0.133	0.157
T8	1.19	59.57	99.81	0.031	0.163	0.175	0.096	0.320	0.216
T9	1.74	68.39	99.78	0.085	0.091	0.139	0.053	0.265	0.367

[a] From diad distribution, [b] Total discrepancy function.[8a]

3.2.3 Statistical analysis of copolymerization data

Triad molar fractions, reported in Table 3.2.3, were analyzed and the copolymerization reactivity ratios, r_1 and r_2, as well as the product of reactivity ratios $r_1 r_2$, were determined. Said values and the respective confidence intervals are reported in Table 3.2.4.

TABLE 3.2.4 Reactivity ratios and their products for P/Y copolymerizations with different metallocene catalysts.

Catalyst	r_1	r_2	$r_1 r_2$
EBTHI	2.20±0.28	1.33±0.38	2.93±1.12
MBI	1.13±0.11	1.97±0.23	2.25±0.48
TBI	0.96±0.10	1.27±0.17	1.22±0.29

Copolymerizations from TBI revealed a product of reactivity ratios $r_1 r_2$ not far from 1 and the lowest value of r_1 and r_2. The most random distribution of the comonomers appears thus to be obtained with the most isospecific metallocene.

EBTHI, the least isospecific metallocene, gave the highest value of $r_1 r_2$ product with a high value of r_1. It is worth observing that the value of r_2 is larger than 1 for copolymerizations from all of the three metallocenes and is larger than the r_1 value for copolymerizations from MBI and TBI. In the literature, r_2 value higher than 1 has not been reported for E/P copolymerizations.[10] Moreover, the r_2 values appear higher than those reported for metallocene-catalyzed copolymerizations of propylene with higher 1-olefins,[11] suggesting a particularly easy formation of Y homosequences. The r_2 value appears also higher than that observed in the literature for the same pair of comonomers in the presence of *rac*-Me$_2$Si(4-Ph-2MeInd)$_2$ZrCl$_2$ where the comonomer content was very low (up to 7 mol%). To better elucidate the correlation between catalytic system and copolymer microstructure copolymerization data were elaborated with the 2nd order Markovian model, which takes into account also the penultimate effect.

Values for r_{ij} reactivity ratios as well as for comonomer distribution index (CDI) are reported in Table 3.2.5.

Table 3.2.5 R parameter, r_{ij} reactivity ratios and comonomer distribution index (CDI), calculated with a 2nd order Markovian model for P/Y copolymerizations from isospecific organometallic complexes.

	r_{11}	r_{21}	r_{12}	r_{22}	CDI^a	R^b
EBTHI	2.029±0.199	2.034±0.511	0.445±0.111	2.012±0.307	2.47±0.82	4.40
MBI	1.198±0.139	0.705±0.170	1.364±0.343	1.923±0.233	1.72±0.55	0.76
TBI	1.014±0.075	0.681±0.108	0.968±0.163	1.548±0.183	1.18±0.28	0.86

Comonomer distribution index calculated according to the formula $CDI = \sqrt[3]{r_{11}^2 r_{22}^2 r_{12} r_{21}}$; ^{b}R= (P/Y)$_{copolymer}$/(P/Y)$_{feed}$.

Data reported in Table 3.2.5 confirm that, in the P/Y copolymerization promoted by TBI, the comonomer distribution is close to the *random* one, as indicated by the value of the comonomer

distribution index (CDI ~ 1). The larger CDI values, observed for MBI and EBTHI, confirm that copolymers with prevailingly sequential enchainment of comonomers are obtained with metallocenes with lower isospecificity, in particular with EBTHI. Data in Table 3.2.5 allow to investigate the relative reactivity of P with respect to Y, as a function of chain end sequences *i.e.,* when the chain end sequences are PP-Zr, YP-Zr, PY-Zr and YY-Zr. To better analyze data of Table 3.2.5, the relative reactivity of P with respect to Y is shown in the bar chart of Figure 3.3.5. This type of representation was selected as a fingerprint of the sequential nature of a propylene/1-olefin copolymer.
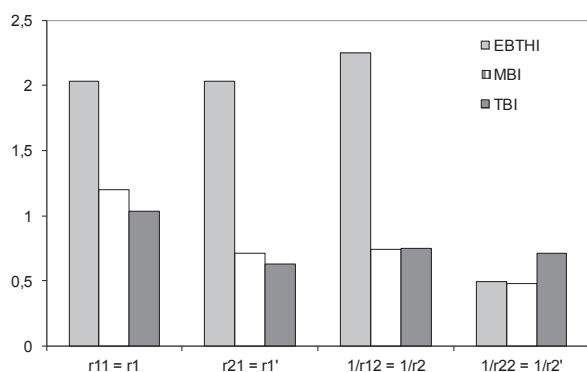
Figure 3.2.5 P/Y relative reactivity (r_1, $r_{1'}$, $1/r_2$, and $1/r_{2'}$) obtained from second-order ($r_1 \neq r_{1'}$ and $r_2 \neq r_{2'}$) reactivity ratios for copolymerizations promoted by MBI, TBI, and EBTHI.

With TBI as the catalyst precursor: i) r_{11} value is about 1, this means that P and Y have almost the same reactivity when PP is the sequence on the Zr atom; ii) r_{21} as well as $1/r_{12}$ and $1/r_{22}$ values are not so far from 1 and are rather close to each other, the Y reactivity increases when at least one of the two last inserted units is Y. It appears that two comonomers, such as P and Y, though endowed with different steric encumbrance, have very similar reactivity towards a catalytic site based on a highly isospecific metallocene.

Similar findings are observed with MBI as the catalyst precursor where: i) the P/Y reactivity ratios is higher than 1 when PP are the two last inserted comonomer units, and ii) the Y reactivity becomes prevailing when Y is one of the two last inserted units and, in particular, when YY is the sequence on the Zr atom.

With the least isospecific metallocene, EBTHI, different behaviour can be observed: indeed, the P/Y relative reactivity is much higher when P is one of the two last inserted units and only the homo YY sequence promotes a higher Y reactivity.

According to literature, highly isospecific metallocenes were found able to promote ethylene/propylene (E/P) copolymerizations with high r_1r_2 product,[7,10,12,13] and also moderately isospecific metallocenes such as EBTHI and EBI were demonstrated able to give rise to ethylene copolymerization with high r_1r_2 product, when 4-methyl-1-pentene was the comonomer. This latter result was explained with the enhanced isoselectivity of the catalytic system, thanks to the cooperation between the organometallic complex and the growing chain containing the bulky comonomer.[14]

It can be hypothesized that in propylene/4-methyl-1-pentene copolymerization, in the case of the metallocene with the lowest isospecificity, EBTHI, the different bulkiness of P and Y favours the

formation of P sequences. The tendency to form Y sequences could be explained with the insertion of Y unit(s) that causes the enhancement of the isospecificity of the catalytic site. In the case of EBTHI, two Y units are required to observe the increase of probability of a further Y insertion. To explain why Y insertion, in the polymer chain growing on the EBTHI catalytic site, occurs to such an extent to justify sequences formation, the P/Y relative reactivity towards the catalytic centre can be taken into consideration. This reactivity is indicated by the R parameter, given by the following expression:

$$R = (P/Y)_{copolymer}/(P/Y)_{feed}$$

By examining the R values shown in Table 3.2.5, it is clear that EBTHI has much higher reactivity for P, whereas MBI and TBI show slightly higher reactivity for Y. The formation of long sequences of both P and Y, in P/Y copolymers from EBTHI, could be thus explained with the preferential reactivity of EBTHI for P and the increase of Y relative reactivity after Y insertions, that occurs as a consequence of the larger Y concentration in the polymerization bath (see also Figure 3.2.2).

An appreciably lower value of the CDI index was calculated for P/Y copolymers from MBI. Taking into account the similar isospecificity of MBI and EBTHI, this finding could be firstly ascribed to the much closer reactivity of P and Y for MBI, revealed by the R parameter and, as a consequence, to the more similar concentration of P and Y in the polymerization bath.

P/Y copolymers from TBI are characterized by an almost random distribution of comonomers. In particular, it is worth observing the very similar values of r_{11} and r_{12} reactivity ratios: P and Y have almost the same probability to be inserted in the polymer chain, when either P or Y are the last inserted units and Y is in the penultimate position. The only reactivity ratio appreciably larger than 1 is r_{22}: two Y as the last inserted units make further Y insertion more probable than the P insertion. These findings are in line with what observed in the case of E/Y copolymerizations:[14,15] Y insertion has higher probability when Y is one or both of the last inserted units. In the light of the similar R values of MBI and TBI, results obtained with the latter metallocene could be ascribed to its higher isospecificity.

3.2.4 DSC thermal analysis

The study of the microstructural and statistical features of the P/Y copolymers has risen the interest in understanding their influence on the final properties finalized to the possible applications of these materials.

Thus, the thermal behavior of the synthesized P/Y copolymers, as well as of the reference homopolymers, was investigated by differential scanning calorimetry (DSC). The values of glass transition, crystallization and melting temperatures (T_g, T_c, and T_m, respectively) and those of the corresponding crystallization and melting enthalpies (ΔH_c and ΔH_m) are listed in Table 3.2.6. Melting behaviour was recorded both during the first DSC heating run on as-polymerized samples, that is on samples precipitated from solution, and during the second DSC heating run, that is immediately after cooling from the molten state at a rate of -10 °C/min.

Table 3.2.6 DSC thermal characterization of P/Y copolymers and of the reference homopolymers.

Catalyst	Run	$Y\%^c$ (mol)	I heating[a] T_m (°C)	ΔH_m (J/g)	cooling T_c (°C)	ΔH_c (J/g)	II heating[b] T_g (°C)	T_m (°C)	ΔH_m (J/g)
EBTHI	E0	0	122	81	93	76	-17	120	73
	E1	1.88	118	79	89	70	-19	116	76
	E2	3.57	(52) 100	(6.5) 48	68	48	-15	100	54
	E3	5.70	(56) 86	(25) 47	47	48	-19	86	45
	E4	9.92	(44) 78	(13) 1	-	-	-25	57	2
	E5	15.74	44	8	-	-	-19	-	-
	E6	18.72	46	12	-	-	-17	-	-
	E7	35.88	-	-	-	-	-6	-	-
	E8	43.00	-	-	-	-	-7	-	-
	E9	53.27	-	-	-	-	-3	-	-
	E10	60.75	-	-	-	-	-1.5	-	-
	E11	67.21	(55) 80	(9) 10	-	-	0	-	-
	E12	85.81	161	29	139	19	3	157	22
	E13	100	208	40	191	49	26[d]	208	49
MBI	M0	0	143	84	106	81	-2[d]	139	92
	M1	3.00	121	80	84	64	-8	121	64
	M2	5.27	106	47	68	45	-9	105	49
	M3	8.79	(50) 87	(7) 39	11	9	-11	85[e]	26[e]
	M4	10.10	(50) 75	(17.5) 2			-12	-	-
	M5	14.86	(50) 75	(17.5) 2	-	-	-10	-	-
	M6	22.82	(46) 72	(2.5) 1	-	-	-7	-	-
	M7	29.72	-	-	-	-	-5.5	-	-
	M8	34.6	-	-	-	-	-4	-	-
	M9	51.95	-	-	-	-	4	-	-
	M10	62.77	81	10.5	-	-	12	-	-
	M11	73.53	81	19.7	-	-	12	-	-
	M12	76.94	(48) 82	(4) 16	-	-	12	-	-
	M13	81.06	(50) 141	(1) 20	115	10	12	137	12
	M14	88.70	n.d.[f]	n.d.[f]	168	20	13	168	20
	M15	100	212	25	198	25	22[d]	215	25
TBI	T0	0	146	101	109	100	n.d[f]	140	102
	T1	2.95	(49)121	(5.5)68	88	71	-13	117	72
	T2	4.99	(46)110	(6.3)47	78	55	-11	107	55
	T3	10.86	(50)90	(11.7)7.4	-	-	-13	75[g]	15[g]
	T4	15.10	45	16	-	-	-13	-	-
	T5	22.72	-	-	-	-	-7.5	-	-
	T6	32.32	-	-	-	-	-6	-	-
	T7	43.88	-	-	-	-	0	-	-
	T8	59.57	-	-	-	-	7	-	-
	T9	68.39	82	5.9	-	-	13	-	-
	T10	82.58	114	16.1	83	10	18	115	10
	T11	90.81	181	18.5	160	26	20	179	32
	T12	100	229	51	211	52	51[d]	229	52

[a] 1st heating run on as-polymerized samples (crystallized from solution). [b] 2nd heating run on samples crystallized from the melt. [c] From ^{13}C NMR analysis. [d] After quenching in liquid nitrogen. [e] Cold crystallization on 2nd heating: T_{cc} = 11°C, ΔH_{cc} = 16 J/g. [f] n.d. = not detectable. [g] Cold crystallization on 2nd heating: T_{cc} = 14°C, ΔH_{cc} = 11 J/g.

Some DSC traces of the investigated copolymers recorded during the second heating run are shown in Figures 3.2.6a, 3.2.6b, 3.26c where the DSC traces of the reference homopolymers are also reported for sake of comparison.
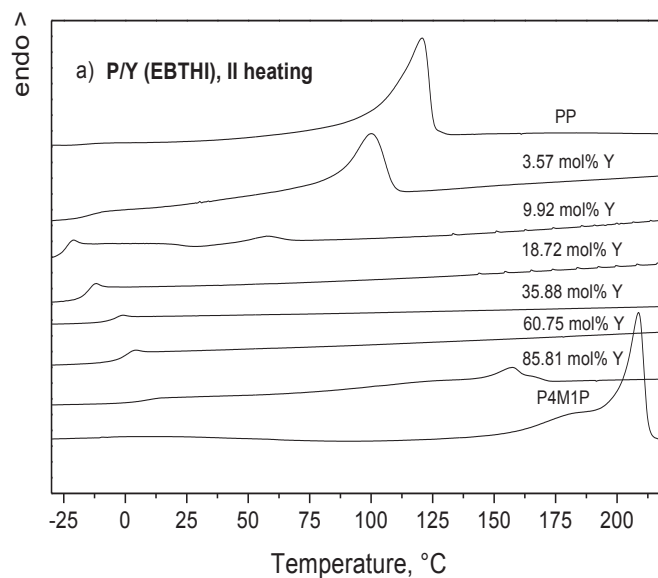
Figure 3.2.6 (a) DSC heating profiles for P/Y copolymers from EBTHI obtained after cooling from the melt at -10 °C/min; corresponding curves of polypropylene and poly(4-methyl-1-pentene) homopolymers are also reported as references.
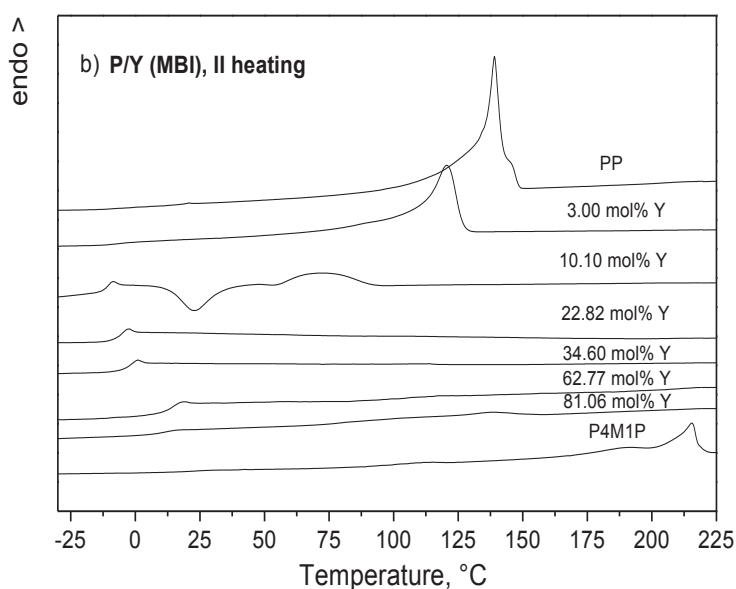

Figure 3.2.6 (b) DSC heating profiles for P/Y copolymers from MBI obtained after cooling from the melt at -10 °C/min; corresponding curves of polypropylene and poly(4-methyl-1-pentene) homopolymers are also reported as references.
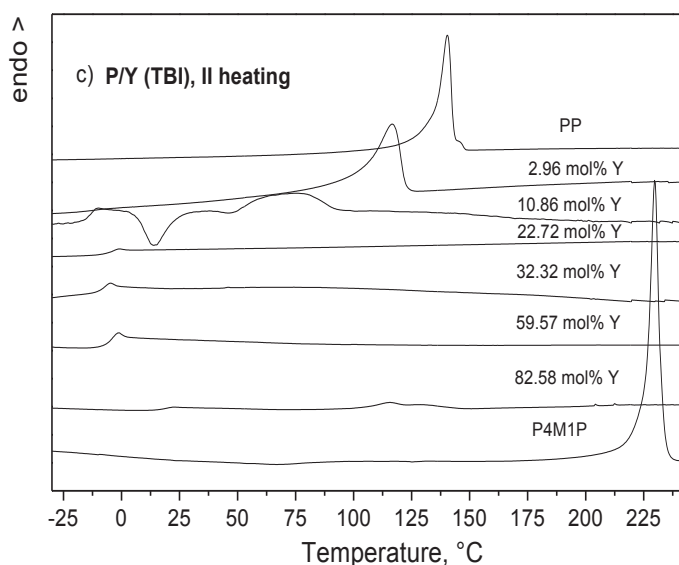
Figure 3.2.6 (c) DSC heating profiles for P/Y copolymers from TBI obtained after cooling from the melt at -10 °C/min; corresponding curves of polypropylene and poly(4-methyl-1-pentene) homopolymers are also reported as references.

The evolution of T_g values versus Y molar content for all the investigated samples are plotted in Figure 3.2.7. On the whole, the glass transition temperature of the copolymers increases with Y content, passing from temperatures below 0°C for the PP homopolymers to ambient or higher temperatures for the poly(4-methyl-1-pentene) homopolymers. In the literature, thermal behaviour of an analogous P/Y copolymer series obtained from MAO-activated MBI catalyst was reported.[16] Values of T_g shown and their trend against composition are in line with the findings of this work.

More in detail, the curves fitting the experimental T_g values of the three copolymer series present a negative deviation with respect to the Fox-Flory linear prediction for random copolymers.[17] By a closer inspection of the T_g *vs.* composition plots, one can observe that for compositions which range from about 60 up to Y content of about 85 mol% the glass transition tends to increase very slowly. This phenomenon is more evident for the copolymers from EBTHI and MBI, in comparison with the copolymers from TBI. Indeed, from the statistical analysis of the NMR microstructural data, EBTHI and MBI catalysts resulted to have a more pronounced capability of producing longer Y homosequences, thus at high Y contents more and more homosequences of the bulky comonomer become long enough to be engaged in the crystalline lamellae, while the amorphous phase enriches in the low T_g component.
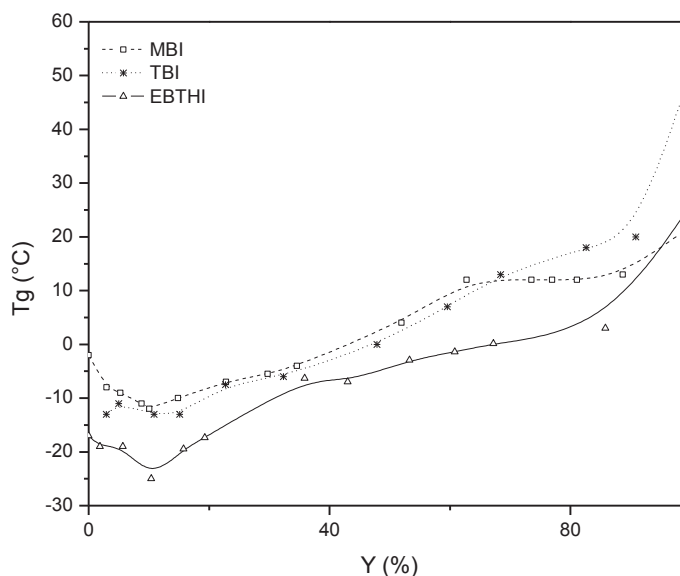
Figure 3.2.7 Glass transition temperatures of P/Y copolymers of Table 3.2.6 *vs* Y molar content.

Furthermore, copolymers from EBTHI exhibit the lowest values of glass transition temperature, this could be ascribed to the fact that this catalyst produces polymer chains with the highest content of defects, that likely lead to high free volume and, in turns, high chain mobility.

The DSC data reported in Table 3.2.6 show that the values of crystallization and melting temperatures and those of the related enthalpies for both the homopolymers are in line with those reported in the literature for polypropylene (PP)[16,18,19] and poly(4-methyl-1-pentene)[8a,16,20] homopolymeric samples obtained using the same (MBI) or other isoselective metallocene complexes in similar polymerization conditions. Furthermore, the values of crystallization and melting temperatures for both the homopolymers synthesized from MBI and TBI catalysts, that is from catalysts with similar and high iso- and regioselectivity, are comparable; whereas, both homopolymer samples prepared by the less isoselective and less regioregular EBTHI complex exhibit lower crystallization and melting temperatures. As regards PP homopolymers, the measured enthalpy values are comparable for the samples prepared by the more stereoregular MBI and TBI catalysts and higher in comparison with those of the less stereoregular PP obtained EBTHI metallocene. Instead, in the case of poly(4-methyl-1-pentene) the samples synthesized from TBI and EBTHI in the adopted conditions formed a larger amount of crystalline material probably because their low molecular weights increased chain motion capability.

Differences observed in the crystallization and melting temperatures as well as in the related enthalpies of the homopolymers listed in Table 3.2.6 can be explained taking into account: i) the different stereo- and regioregularity of the polymer chains produced from the three investigated metallocenes (see Table 3.2.1), and ii) the different chain motion capability of samples with quite dissimilar molecular masses (see Table 3.2.6). Deeper insights on these aspects are out of the scope of the present work.

Table 3.2.6 also evidenced that, irrespective of the catalyst used, for propylene-rich copolymers crystallized from the melt, as generally observed for random copolymers of propylene with higher linear 1-olefins,[18-19] the melting endotherm progressively shifts towards lower temperatures on increasing the content of the bulky Y comonomer up to about 8 mol%. For copolymers containing 10-12 mol% of Y crystallization on cooling from the melt at a rate of -10°C/min becomes difficult and cold crystallization phenomena are observable in the subsequent DSC heating traces (Figure 3.2.6). Correspondingly, the related enthalpy values consistently reduce with respect to the PP homopolymers because of the penalty effect on crystallization brought about by the presence of the bulky branched comonomer. Higher contents of Y co-units completely hamper crystallization in the adopted experimental conditions and, consequently, only the signal corresponding to the glass transition temperature is detected in the successive heating run.

On the other hand and remarkably, when the copolymers are moderately rich in 4-methyl-1-pentene co-units crystallization upon cooling from the melt can take place. An analogous melting behaviour was already observed for E/Y copolymers synthesized from EBTHI, where the presence of crystallinity was detectable even in the range of equimolar compositions.[15]

More specifically, for the P/Y series from MBI, when the Y units content is about 60 mol%, the presence of a melting endotherm ascribable to the fusion of defective crystals constituted by Y homosequences was observed in the DSC heating trace of the as-polymerized sample. Whereas, for TBI and EBTHI catalysts analogous phenomena appeared at 4M1P contents of about 70% and are characterized by proportionally lower enthalpy values. It is worth observing that the chemical composition range in which P/Y copolymers from TBI are amorphous is the largest one.

The different behaviour of the three metallocenic catalysts is also displayed in Figure 3.2.8 where the melting enthalpy values of the three investigated copolymer series recorded during the first heating run are plotted as a function of copolymer composition.
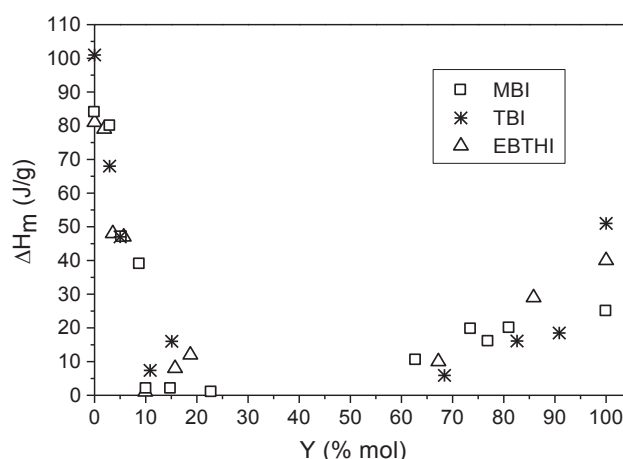
Figure 3.2.8 Melting enthalpy of melt crystallized P/Y copolymers vs. Y molar content for the three series obtained from MBI, TBI and EBTHI catalysts.

By examining the right portion of Figure 3.2.8, one can notice that, even though TBI is the catalyst which produces the highest stereoregularity in poly(4-methyl-1-pentene), up to Y content higher

than 80 mol% copolymers from MBI and EBTHI present larger amounts of crystalline material. This suggests for EBTHI a stronger tendency to blockiness which leads to higher amounts of Y homosequences long enough to be capable of crystallizing (n ≥ 12). A minimum crystallizable sequence length of n = 12 regular repeating units appears to be reliable taking into account literature findings[21] and previous results on E/Y blocky copolymers.[15]

The different capability of the three catalyst to form homosequences is described in the bar charts of Figure 3.2.9, Figure 3.2.10, and Figure 3.2.11, showing the relative contents of comonomer sequences made by n units, with n ranging from 1 to values ≥ 12, for copolymers from EBTHI, TBI, and MBI, and having Y content around 60% by moles. [P(Y)$_n$P] sequences with more than 12 Y units are more than 20 % of the total Y amount in the copolymer from EBTHI (Figure 3.2.9), and about 10% in the sample from MBI (Figure 3.2.10). *Viceversa,* copolymer from TBI show prevailing short Y sequences: only less than 5% of Y form homosequences equal or longer than 12 units. Isolated unit (n = 1) and short sequences (n = 2-5) of P are present in all of the three P/Y copolymers but, in particular, in the sample from TBI (Figure 3.2.12). Isolated P units are about 40%, 35%, and 20% by moles in copolymers from TBI, MBI, and EBTHI, respectively.
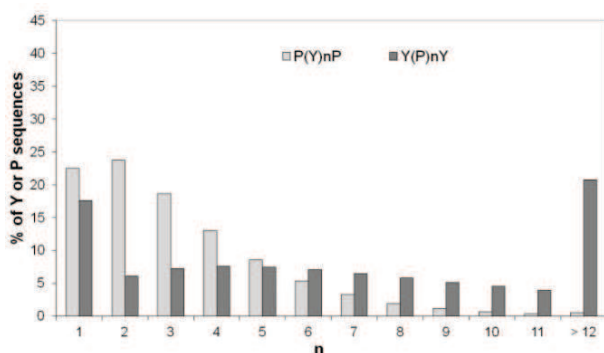

Figure 3.2.9 Probabilities of sequences of n comonomer units for run E10 in Table 3.2.6 (Y = 60.75 mol %).
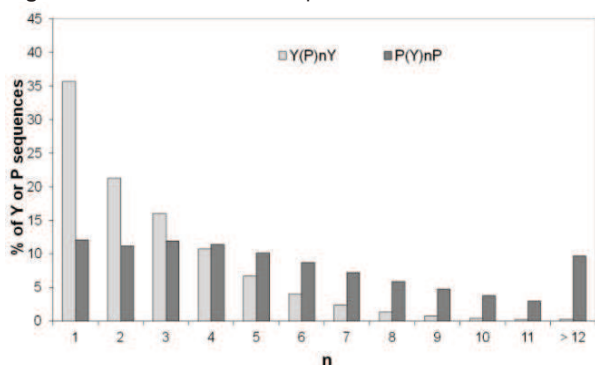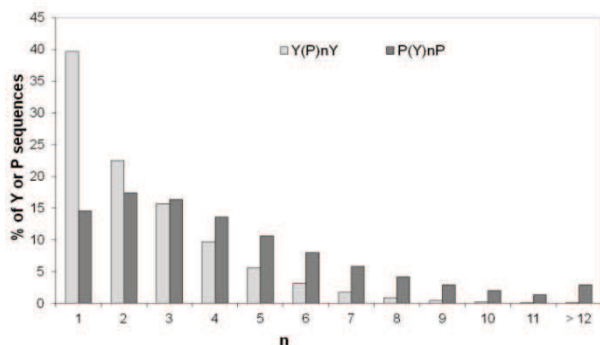

Figure 3.2.10 Probabilities of sequences of n comonomer units for run M10 in Table 3.2.6 (Y = 62.77 mol %).

Figure 3.2.11 Probabilities of sequences of n comonomer units for run T8 in Table 3.2.6 (Y = 59.57 mol %).

DSC results are in perfect agreement and corroborate this statistical analysis, in particular the differences in the tendency of the three metallocene catalysts to form homosequences are better evidenced when data from melting behaviour of the copolymers are correlated with the comonomer distribution in the copolymer chain. In Figure 3.2.12, the melting enthalpy values of as-polymerized P/Y copolymers rich in 4-methyl-1-pentene were plotted versus the Y molar content.
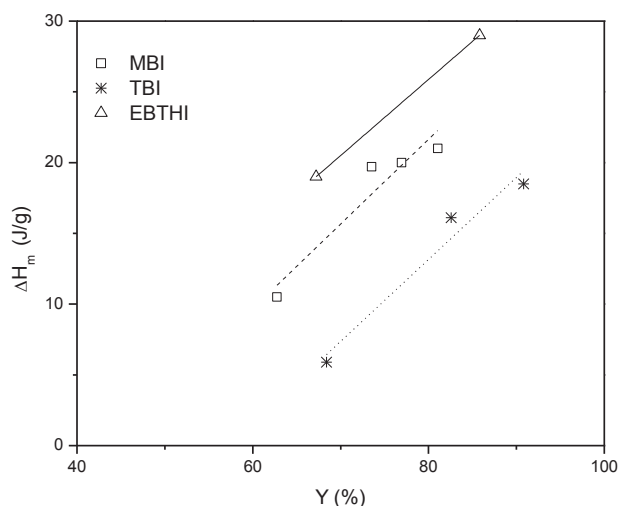
Figure 3.2.12 Melting enthalpy of as-polymerized P/Y copolymers *vs* (a) Y molar content.

By examining Figure 3.2.12, one can notice that, even though TBI is the catalyst which produces the highest stereoregularity in 4-methyl-1-pentene homopolymer, up to Y content of about 90 mol% copolymers from MBI and EBTHI present larger amounts of crystalline material. This is in good agreement with the microstructural data showing for MBI and EBTHI a stronger tendency to form Y blocks, which leads to higher amounts of crystallizable Y homosequences.

3.2.5 X-ray Diffraction Characterization

Wide angle X-ray diffraction experiments were performed on as-polymerized P/Y copolymers. In Figure 3.2.13, Figure 3.2.14 and Figure 3.2.15, WAXD patterns on as-polymerized propylene-rich P/Y copolymers from the three metallocene complexes are shown. For the homopolymers

(PP) and the copolymers (PY) with 4-methyl-1-pentene contents up to 6 mol% the characteristic reflections of the α-form at 2θ = 14.2, 16.9 and 18.6°, corresponding to planes (110), (040) and (130), respectively, dominate the patterns; however, a small signal at 2θ = 20.1°, indicative of the presence of γ-form, is also detectable. As expected, crystallinity rapidly drops on increasing the comonomer content in this composition range.
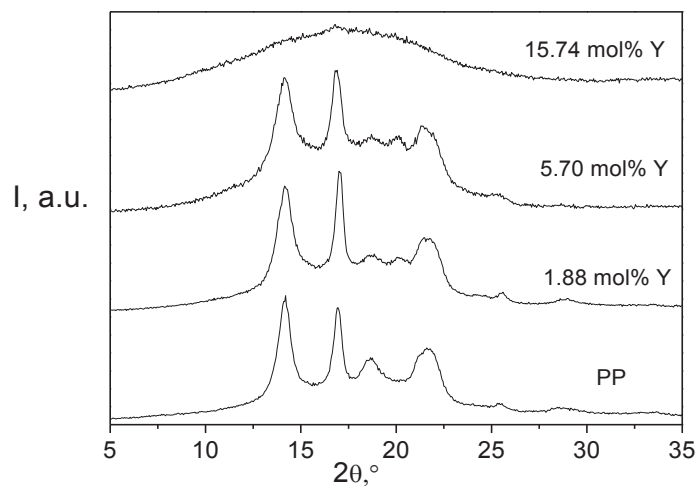

Figure 3.2.13 WAXD patterns on as-polymerized propylene-rich P/Y copolymers from EBTHI catalyst.
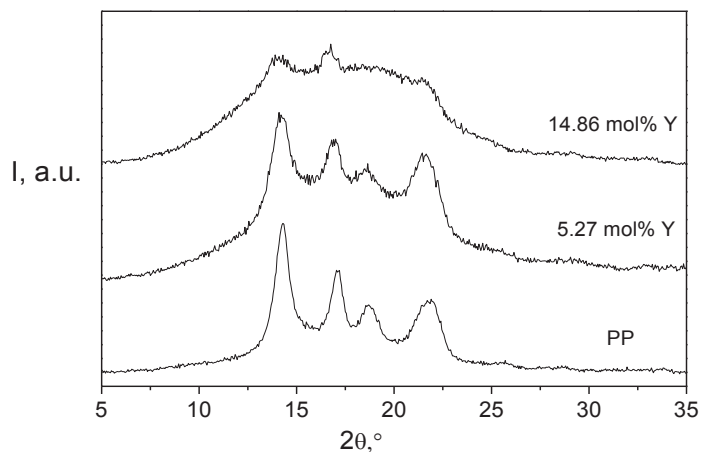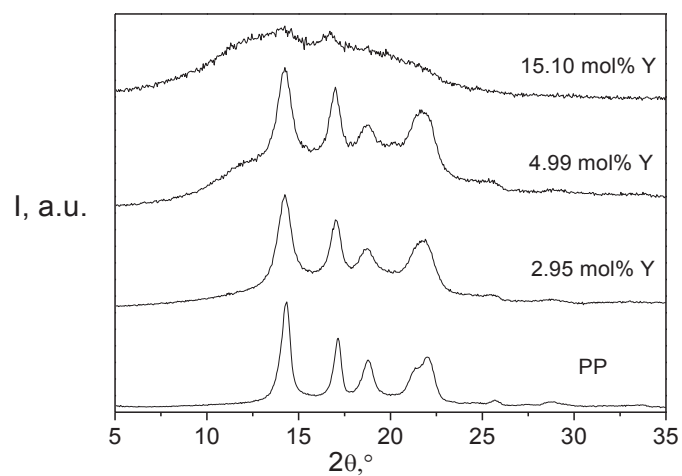

Figure 3.2.14 WAXD patterns on as-polymerized propylene-rich P/Y copolymers from MBI catalyst.
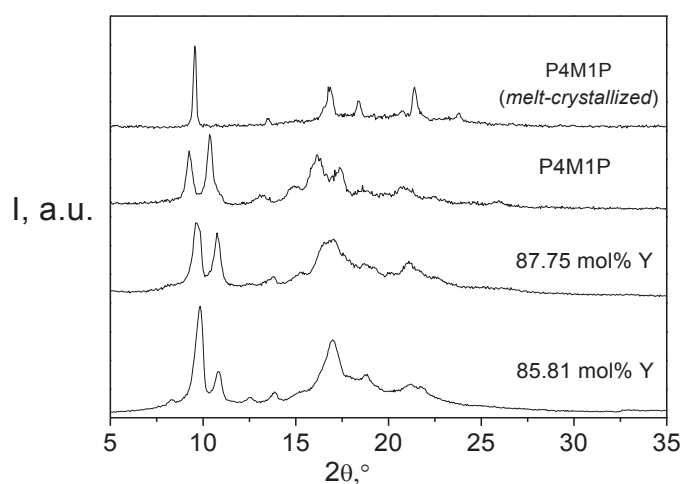
Figure 3.2.15 WAXD patterns on as-polymerized propylene-rich P/Y copolymers from TBI catalyst.

WAXD analysis on as-polymerized 4M1P-rich copolymers (Figure 3.2.16, Figure 3.2.17, Figure 3.2.18) reveale the crystalline reflections featured those of Form I, II and IV of poly(4M1P), whereas the melt-crystallized samples presented the reflections typical of Form I crystals.

Poly(4M1P) from TBI catalyst crystallizes in Form I, it can be recognized thanks to the characteristic sharp peak at about 9.8° 2θ. For P/Y copolymers synthesized from EBTHI and TBI catalysts, at increasing of propylene content, two faint reflections at 2θ = 8.0° and 12.2° can be detect, typical of Form IV crystals.

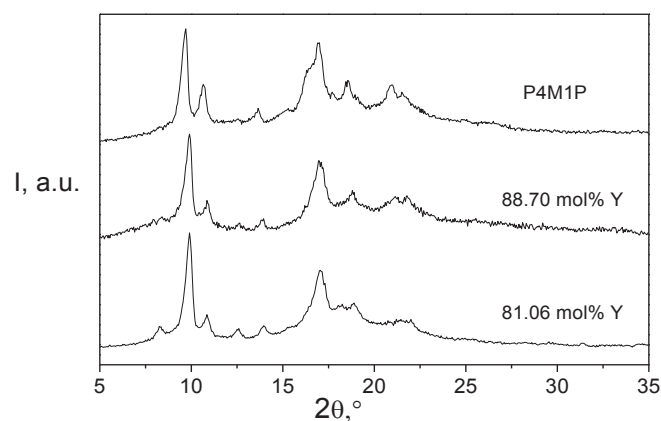**Figure 3.2.16** WAXD patterns on as-polymerized 4M1P-rich P/Y copolymers from EBTHI catalyst.

Figure 3.2.17 WAXD patterns on as-polymerized 4M1P-rich P/Y copolymers from MBI catalyst.
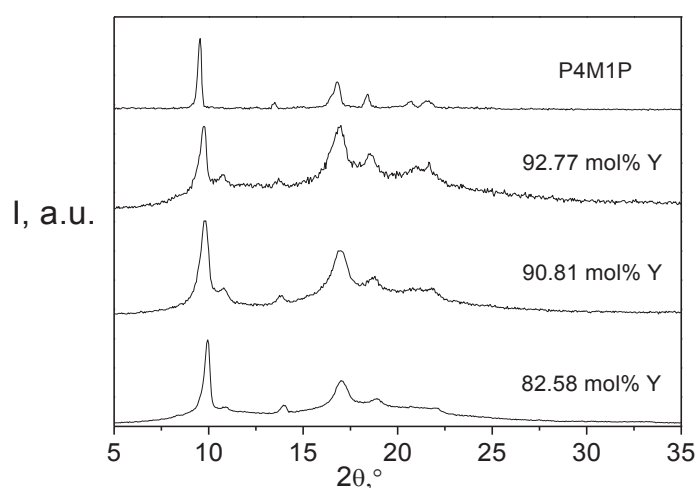
Figure 3.2.18 WAXD patterns on as-polymerized 4M1P-rich P/Y copolymers from TBI catalyst.

3.2.6 References

1. M. C. Sacchi, S. Losio, L. Fantauzzi, P. Stagnaro, R. Utzeri, M. Galimberti, *J. Polym. Sci. Polym Chem.*, **2015**, *53*, 2575.

2. L. Resconi, L. Cavallo, A. Fait, F. Piemontesi, *Chem. Rev.* **2000**, *100*, 1235.

3. L. Resconi, A. Fait, F. Piemontesi, M. Colonnesi, H. Rychlicki, R. Zeigler, *Macromolecules*, **1995**, *28*, 6667.

4. M. C. Leclerc, H.-H. Brintzinger, *JACS*, **1995**, *117*, 1651.

5. V. Busico, R. Cipullo, *JACS*, **1994**, *116*, 9329.

6. V. Busico, R. Cipullo, *Macromol. Symp.*, **1995**, *89*, 277.

7. M. Galimberti, F. Piemontesi, L. Alagia, S. Losio, L. Boragno, P. Stagnaro, M. C. Sacchi, *J. Polym. Sci. Polym. Chem.*, **2010**, *48*, 2063.

8. (a) S. Losio, F. Forlini, A. C. Boccia, M. C. Sacchi, *Macromolecules*, **2011**, *44*, 3276; (b) U. M. Wahner, I. Tincul, D. J. Joubert, E. R. Sadiku, F. Forlini, S. Losio, I. Tritto, M. C. Sacchi, *Macromol. Chem. Phys.*, **2003**, *204*, 1738; (c) M. C. Sacchi, F. Forlini, S. Losio, I. Tritto, G. Costa, P. Stagnaro, I. Tincul, U. M. Wahner, *Macromol. Symp.*, **2004**, *213*, 57.

9. In copolymers with high comonomer content, the overlap of the resonances related to αα-methylene of propylene sequences with the resonances of α-methylene of the comonomer branch does not allow correct quantitative evaluation of the triad distributions neither by applying the least-squares fitting of the ^{13}C NMR signals as reported in reference 8a. Thus, the triad distributions of the copolymers with Y content higher than 74 mol% were not included in Table 3.2.3. The same data were not taken into consideration in the statistical elaboration for obtaining the reactivity ratios and their products.

10. M. Galimberti, F. Piemontesi, O. Fusco, I. Camurati, M. Destro, *Macromolecules*, **1999**, *32,* 7968.

11. (a) M. J. Schneider, R. Mulhaupt, *Macromol. Chem. Phys.*, **1997**, *198*, 1121; (b) P. M. Nedorezova, A. V. Chapurina, A. A. Koval'chuk, A. N. Klyamkina, A. M. Aladyshev, V. A. Optov, B. F. Shklyaruk, *Polym. Sci. Ser. B*, **2010**, *52*, 15; (c) A. A. Koval'chuk, A. N. Klyamkina, A. M. Aladyshev, P. M. Nedorezova, E. M. Antipov *Polym. Bull.*, **2006**, *56*, 145; (d) M. Arnolds, S. Bornemann, F. Koller, T. J. Menke, J. Kressler *Macromol. Chem. Phys.*, **1998***, 199,* 2647; (e) M. Arnolds, S. Bornemann, B. Schade, O. Henschke *KGK-Kautsch. Gummi Kunstst.*, **2001**, *54*, 300.

12. M. Galimberti, F. Piemontesi, O. Fusco, I. Camurati, M. Destro, *Macromolecules*, **1998**, *31*, 3409.

13. S. Losio, F. Piemontesi, F. Forlini, M. C. Sacchi, I. Tritto, P. Stagnaro, G. Zecchi, M. Galimberti *Macromolecules*, **2006**, *39*, 8223.

14. S. Losio, P. Stagnaro, T. Motta, M. C. Sacchi, F. Piemontesi, M. Galimberti *Macromolecules*, **2008**, *41*, 1104.

15. P. Stagnaro, L. Boragno, S. Losio, M. Canetti, G. C. Alfonso, M. Galimberti, F. Piemontesi, M. C. Sacchi *Macromolecules*, **2011**, *44*, 3712.

16. M. Arnold, S. Bornemann, F. Köller, T. J. Menke, J. Kressler, *Macromol. Chem. Phys.*, **1998**, *199*, 2647-2633.

17. (a) T. G. Fox, P. J. Flory, *J. Appl. Phys.*, **1950**, *21*, 581; (b) T. G. Fox, P. J. Flory, *J. Polym. Sci.*, **1954**, *14*, 315; (c) T. G. Fox, P. J. Flory, *J. Phys. Chem.*, **1951**, *55*, 221.

18. A. J. Van Reenen, *Macromol. Symp.*, **2003**, *193,* 57.

19. P. Stagnaro, G. Costa, V. Trefiletti, M. Canetti, F. Forlini, G. C. Alfonso, *Macromol. Chem. Phys.*, **2006**, *207*, 2128.

20. (a) F. Forlini, I. Tritto, P. Locatelli, M. C. Sacchi, F. Piemontesi, *Macromol. Chem. Phys.*, **2000**, *201*, 401; (b) F. Forlini, E. Princi, M. C. Sacchi, F. Piemontesi, *Macromol. Chem. Phys.*, **2002**, *203*, 645.

21. (a) H. Luo, Q. Chen, G. Yang, *Polymer*, **2001**, *42*, 8285; (b) T. M. Madkour, J. E. Mark, *J. Polym. Sci. Polym Phys.*, **2002**, *40*, 840.

3.3 Conclusions

A complete microstructural characterization of two series of ethylene/1-pentene copolymers prepared with different metallocene catalysts at increasing isospecificity, EBTHI and TBI, has been conducted by ^{13}C NMR. The proposed assignments for the full description of the copolymers at the triad level. The statistical analysis showed that the most isospecific catalyst, TBI, gives rise to a *blocky* copolymers whereas a random comonomer distribution is obtained with the metallocene with the minor isospecificity, EBTHI. Moreover, TBI gives rise to a somewhat different copolymer microstructure, with respect to EBTHI: a lower amount of PPEPP sequences (higher r_{21} value) is observed. Furthermore, TBI favours an easier ethylene insertion (high r_{11} and r_{21} values), probably as a consequence of a higher steric hindrance. These results, joint with those reported in literature for ethylene/4-methyl-1-pentene copolymers, confirm: i) the key-role played by the olefin, namely its steric hindrance, in copolymerization and ii) the selectivity of a catalytic site made by the cooperation between the catalyst precursor and the growing chain, that is further enhanced when a bulky 1-olefin is used. Indeed when a comonomer as 1-pentene (not encumbered) is used in ethylene copolymerization, a moderate isospecific catalyst such as EBTHI is not able to give a *blocky* copolymer.

Ethylene/1-pentene copolymers from TBI catalyst were analyzed by means of high temperature HPLC: all these copolymers eluted exclusively in the gradient and the elution volume is indirectly proportional to the concentration of branches.

Copolymers of propylene with 4-methyl-1-pentene (P/Y) have been prepared with several metallocene based catalytic systems at increasing isospecificity. TBI catalyst endowed with a very high isospecificity, prepares copolymers with almost random distribution of P and Y, whereas sequences of both comonomers are obtained with metallocenes with minor enantioselectivity, such as MBI and, in particular, EBTHI. The synthesis of a random copolymer of propylene and 4-methyl-1-pentene, with a highly isospecific catalytic system is, unforeseen, on the basis of literature results on ethylene/4-methyl-1-pentene and ethylene/1-pentene copolymerizations. Here, for propylene-based copolymers, the *random* distribution of the comonomers seems to be due to the easy propagation of both comonomers, thanks to the high enantioselectivity of TBI, and to the similar reactivity of P and Y towards TBI.

DSC analysis revealed that, even though TBI gives the highest stereoregularity in poly(4M1P) homopolymer, up to 4M1P content of *ca.* 90 mol% copolymers from MBI and EBTHI presented larger amounts of crystalline material, in good agreement with the microstructural data. WAXD analysis on as-polymerized 4M1P-rich copolymers revealed the crystalline reflections featured those of Form I, II and IV of poly(4M1P), whereas the melt-crystallized samples presented the reflections typical of Form I crystals.

The obtained results can open the way for the preparation on a large scale of random propylene based copolymers by playing on the stereospecificity of the metallocene and on the steric hindrance of the comonomer.

Publications

- M. C. Sacchi, S. Losio, **L. Fantauzzi**, P. Stagnaro, R. Utzeri, M. Galimberti, Random Propene/4-Methyl-1-pentene copolymers Synthesized with C_2 Symmetric Highly Isospecific Metallocenes, *Journal of Polymer Science, Part A*: *Polymer Chemistry*, 2015, *53*, 2575-2585.

- **L. Fantauzzi**, S. Losio, M.C. Sacchi, F. Bertini, M. Canetti, M. Zoccola, A. Montarsolo, "Esterificazione di micro e nanofibrille di lino mediante microonde e preparazione di compositi a base di polietilene", Atti del XXI Convegno Italiano di Scienza e Tecnologia delle Macromolecole, 183-186, 14-17 Settembre 2014, Torino, ISBN: 978-88-6812-369-7, DOI: 10.4458/3697-040.

- P. Stagnaro, S. Losio, **L. Fantauzzi**, R. Utzeri, G.C. Alfonso, M. Galimberti, M.C. Sacchi, "Nuovi copolimeri a base di 4-metil-1-pentene da catalizzatori metallocenici: correlazione struttura-proprietà", Atti del XXI Convegno Italiano di Scienza e Tecnologia delle Macromolecole, 183-185, 14-17 Settembre 2014, Torino, ISBN: 978-88-6812-369-7, DOI: 10.4458/3697-015.

- A. Montarsolo, F. Bertini, M. Canetti, P. Stagnaro, F. Giunco, S. Losio, **L. Fantauzzi**, C. Tonin, "Produzione di fibrille di lino e canapa e loro utilizzo come rinforzo in compositi", in "Progetto VeLiCa: da antiche colture materiali e prodotti per il futuro", M. Terreni (ed.), Eliocenter s.n.c., Milano, 125-136, 2014, ISBN: 978-88-907569-1-7.

Scientific Contributions

➢ Random propene/4-methyl-1-pentene copolymers from C_2 symmetric highly isospecific metallocenes: correlation between microstructure and properties.

L. Fantauzzi

AIM "Macrogiovani 2015", Bologna, 6 Luglio 2015 (*Oral presentation*).

➢ Fourth International Symposium Frontiers in Polymer Science, "On the structural and thermal features of novel 4-methyl-1-pentene copolymers with uncommon microstructures by C_2 symmetric metallocenes".

P. Stagnaro, S. Losio, **L. Fantauzzi**, R. Utzeri, M. Galimberti, M. C. Sacchi, D. Cavallo, G. C. Alfonso

Riva del Garda, 20-22 Maggio 2015 (*Poster presentation*).

➢ ISMAC workshop 2014 on "Catalytic Olefin Polymerization and High Performance Materials", "Do C_2 symmetric isospecific metallocenes prepare random propene/4-methyl-1-pentene copolymers?".

L. Fantauzzi, S. Losio, M. C. Sacchi, P. Stagnaro, R. Utzeri

Milano, 11 December 2014 (*Poster presentation*).

➢ International workshop on "Catalytic Olefin Polymerization & High Performance Polyolefins", "Do C_2 symmetric isospecific metallocenes prepare random propene/4-methyl-1-pentene copolymers?".

S. Losio, **L. Fantauzzi**, M. C. Sacchi, P. Stagnaro, R. Utzeri

Shanghai, 22-25 October 2014 (*Poster presentation*).

➢ Esterificazione di micro e nanofibrille di lino mediante microonde e preparazione di compositi a base di polietilene".

L. Fantauzzi

XXI Convegno Italiano di Scienza e Tecnologia delle Macromolecole, Torino, 14-17 Settembre 2014 (*Oral Presentation).*

- Evento conclusivo Progetto VeLiCa - "Esterificazione di micro e nano fibrille di lino mediante microonde e preparazione di compositi a base di polietilene".
  L. Fantauzzi, M. Canetti, F. Bertini, S. Losio, A. Montarsolo, M. C. Sacchi, M. Zoccola
  Evento conclusivo Progetto VeLiCa, Milano, 3 febbraio 2014 (*Poster presentation*).

- Design and synthesis of propylene/4-methyl-1-pentene copolymers for food packaging applications, AIM "Macrogiovani 2013".
  L. Fantauzzi
  Politecnico Milano, 11 Febbraio 2013 (*Oral presentation*).

Attendance to Schools and Seminars

- Convegno-Scuola AIM "Mario Farina" su "Caratterizzazione di materiali polimerici: tecniche per polimeri in soluzione", Gargnano (BS), 19-23 Maggio 2014.

- Giornata tecnologica "Polimeri e lo sviluppo sostenibile. Fonti naturali e innovazioni tecnologiche", AIM-Federchimica/Plastic Europe, Milano, 19 Aprile 2014.

- Summer School in High Energy Processing Ultrasound & Microwave Technologies, Università di Torino, 3-7 Giugno 2013, DSTF.

- ISMAC workshop 2012, "Self-Assembled functional nanostructures: material tailoring for electronics and bio-electronics", Milano, 15 Novembre 2012.

- Giornata tecnologica "La ricerca italiana sugli imballaggi attivi, con particolare focus all'utilizzo di nanomateriali", Federchimica, Fiera di Rho (MI), 9 maggio 2012.

Internships

- Study of melt crystallization and morphological features of novel propylene/4-methyl-1-pentene copolymers obtained from various C_2 symmetric single site metallocene catalyst, European Synchrotron Radiation Facility (ESFR), Grenoble (France), May 2015.

- Development of new formulations of PVC plasticized and *scale-up* on pilot plant for rotational moulding assisted by microwave, Sigre s.r.l., Buccinasco (MI), January-July 2014.

Patent proposal

- Nuova formulazione di plastisol per stampaggio rotazionale (rotomoulding) con riscaldamento indotto dalle microonde.
  Inventori: **L. Fantauzzi**, S. Losio, P. Stagnaro, R. Utzeri, I. Tritto, P. Porta, M. Sala, G. Porta, G. Colonna Romano.

Manuscripts in preparation

- **L. Fantauzzi**, F. Bertini, M. Canetti, A. Cacciamani, M. Zoccola, A. Montarsolo, A. Patrucco, S. Losio, Microwave-assisted heterogeneous esterification of flax nanofibrillated cellulose by a long chain fatty acid derivative, *Carbohydrate Polymer*, manuscript submitted.

- S. Losio, **L. Fantauzzi**, M.C. Sacchi, Improved Peak Assignment of ^{13}C NMR Spectra of Ethylene/1-Pentene Copolymers by Metallocene-Based Catalysts, manuscript in preparation

Honors and Awards

- **Best oral presentation**, "Macrogiovani 2015", Bologna, 6 Luglio 2015 (*800 EUR*)

- **Scholarship**: Convegno-Scuola AIM "Mario Farina" su "Caratterizzazione di materiali polimerici:tecniche per polimeri in soluzione", Gargnano (BS), 19-23 Maggio 2014
  (*500 EUR*)